OSTEOCYTE APOPTOSIS INITIATION OF TARGETED BONE REMODELING AFTER ESTROGEN WITHDRAWAL

by

KELLY BROOK EMERTON

A dissertation submitted to the Graduate Faculty in Biomedical Engineering in partial fulfillment of the requirements for the degree of Doctor of Philosophy,
The City University of New York

2009

This manuscript has been read and accepted for the
Graduate Faculty in Engineering in satisfaction of the
dissertation requirement for the degree of Doctor of Philosophy.

Dr. Mitchell B. Schaffler

Date — Chair of Examining Committee

Dr. Mumtaz Kassir

Date — Executive Officer

Dr. Susannah Fritton

Dr. John Tarbell

Dr. Luis Cardoso

Dr. Shoshanna Yakar

Supervision Committee

THE CITY UNIVERSITY OF NEW YORK

ABSTRACT

OSTEOCYTE APOPTOSIS INITIATION OF TARGETED BONE REMODELING AFTER ESTROGEN WITHDRAWAL

by

Kelly Brook Emerton

Adviser: Dr. Mitchell B. Schaffler

Osteocytes play a crucial role in the maintenance and integrity of bone. They are the most abundant bone cell type in bone, and participate in signaling mechanisms that initiate targeted bone remodeling. Bone remodeling is defined as the sequential resorption and replacement of bone tissue at a defined site. Many recent studies have confirmed that osteocyte apoptosis has been linked to bone resorption resulting from estrogen depletion and other resorptive stimuli; however, precise spatial and temporal relationships between the two events have not been clearly established. Estrogen in bone health is of critical importance since osteoporosis, a low bone mass disease associated with an increased fracture risk, is the most prevalent degenerative disease worldwide amongst postmenopausal women. Although bone is clearly a target tissue with respect to estrogen, the mechanisms by which estrogen exerts its effects on bone remodeling remain unclear. We set out to characterize the spatial and temporal relationship between estrogen withdrawal, osteocyte apoptosis, pro-osteoclastogenic signaling and bone resorption. A well-characterized murine model was used to show activation of cortical and cancellous bone resorption in highly consistent patterns. Our studies revealed that osteocyte apoptosis is significantly elevated following estrogen loss, and that the apoptosis occurs

regionally, rather than uniformly throughout the cortex. Moreover, we found that apoptotic osteocytes were overwhelmingly localized within the area where subsequent endocortical resorption is known to occur after ovariectomy in B6 mice. This led us to hypothesize that osteocyte apoptosis plays a comparable controlling role in the activation or targeting of osteoclastic resorption. We tested this by pharmacologically inhibiting osteocyte apoptosis post-ovariectomy and assessed subsequent bone resorption activity. Osteoclastic resorption was elevated only in ovariectomized animals that did not receive treatment, demonstrating that osteocyte apoptosis is a necessary and controlling step in the activation of bone remodeling. Assessment of microenviromental and biological differences in the regions containing elevated osteocyte apoptosis revealed reduced solute transport and increased oxidative damage account for the pattern of exhibited apoptosis post-ovariectomy. Together, these results have clinical significance because they provide increased understanding of factors that initiate remodeling, which is fundamental towards understanding women's bone health and disease.

ACKNOWLEDGMENTS

I would like to take this moment to express my sincere thanks to everyone who made my graduate school years, and life in New York City, the best experience anyone could imagine.

First and foremost, I would like to give thanks to my advisor **Mitch Schaffler** for his exceptional mentorship over the past 3 years. He has been a constant source of encouragement, ideas and many laughs, as well as immeasurable support and guidance every step of the way. It was an honor to learn from him and I am grateful beyond words for his mentorship, as well as his friendship over the years.

To my doctoral committee **Susannah Fritton, Shoshanna Yakar, Luis Cardoso**, and **John Tarbell** who provided valuable input and feedback regarding the project. Special thanks to committee member Shoshanna Yakar, who is a big inspiration to me as a female scientist and 'do-it-all' mom, all while being an exceptional mentor on the LID-OVX project. And to **Dean Kassir**, who has always been very helpful and supportive through the years. To **Sheldon Weinbaum**, whose class was extremely invaluable to my scientific thought process, and who also directed me to Mitch when I needed a PhD advisor. To **Ted Cape**, who opened my eyes to opportunities for scientists other than the research bench, and has been a career path and running coach ever since.

Special thanks to **"Dr. Bob" (Robert Majeska)** for his many lessons on biochemistry, on how to become a better writer, and all of the time and energy he spent on me when I first came to the lab. To **Karl Jepson** for the many "whiteboarding" sessions, snickerdoodles and cupcakes, always appreciating my shoes, and teaching me to think outside the box. Thanks to **Karl Terranova** for his expertise in statistical analysis, and giving me a beautiful case of my own surgical instruments that were used for every surgery I performed. To **Chaoyang Li** who originally taught me OVX and histomorphometry.

To my second family in the Orthopaedic Research Laboratory at Mount Sinai School of Medicine for their expertise, knowledge, and friendship. Thanks to **Damien**

Laudier, one of the most amazing artists and histologists for teaching me bone processing techniques and helping me on histology for every project I was a part of here at MSSM. Very special thanks to **Chris Price, Hayden Courtland, Steve Tommasini, Nimesh Pandey, Joel Williams, Bin Hu, David Fung, Adrian Woo, Cesare Ciani, Rich Able, Makonnen Payne, Yilin Wang, Jean Shine, Eddie Vazquez, Harry Salinas, Brad Herman and Sidd Bhola**. I cannot fit all of the good times we had in print. Thanks for all of your help over the years, for being my second family, for always making me laugh, for helping with my mouse-phobia (blue glove) and for making me look forward to going into lab every day.

To my summer students who contributed to the work presented in this dissertation including **Alex Sinofsky, Marissa Steinberg** and **Joe Pinero**. Also special thanks to **John Salig**, who spent much time and energy into getting me 'mouse' ready, and to **Marvin Lin** who assisted with tail vein injections on the Tracer study.

To **Savvas Xanthos**, who has been one of the most influential people in my life thus far. I am incredibly grateful for the infinite help on my various projects throughout the years, and for being my 'go-to' in so many aspects of my life, both personally and professionally. To **Erik Attia** at Hospital for Special Surgery, who initially taught me mammalian cell culture techniques; many thanks for his continued advice and friendship over the years.

To my inner circle of friends: **Chryssy Pelekanos, Mel Murphy (Chard), Courtney Hartman, Holly Lehto, Kate Liberman, Sarah Grant, Mechelle Ackley, Steph Calkins, Susan Spelios, Colleen and Courtney McAloon, Sarah Katz,** and **Steph Cho.** You are the 'closest to my heart' inner circle of women who inspire me with your strength, beauty, and compassion.

This dissertation is dedicated : 1) to the memory of **Mary Russell** (1961-1996), who was my inspiration for starting into medical engineering, and taken from my life too soon, and 2) my parents, **Daniel Emerton** and **Connie Gannon-Piacentini**, who have always nurtured my love of math and science, and to the rest of my family: **Anne, Daniel, Dave, Vincent, Rosemary, Eli**. You are my harbor in a storm, my heart of hearts, and my everything always. I love you and appreciate your support through the years.

TABLE OF CONTENTS

LIST OF TABLES

LIST OF FIGURES

CHAPTER 1

INTRODUCTION

The molecular pathways controlling bone remodeling in either normal individuals or in disease states are not well understood. This question is of critical importance since osteoporosis, a metabolic bone disease associated with an increased risk of fracture, is the most prevalent degenerative disease worldwide [55; 136]. Osteoporosis caused by estrogen deficiency from menopause or hysterectomy is currently one of the major health problems affecting women in developed countries. In America alone, there are 10 million Americans affected, with 1.5 million fractures annually and costs soaring above $18 million in caring for osteoporosis [109]. Of increasing alarm is the growing notion that current diagnostic tools to assess changes in bone quality caused by metabolic bone disease such as post-menopausal osteoporosis are inaccurate and therefore not accurately diagnosing osteoporosis cases [82]. The current view is that standard bone density modalities (DXA) used to diagnose osteoporosis is inaccurate to asses bone strength (architecture, size, shape and connectivity of bone) independent of mass.

There are two basic types of osteoporosis; Type I (high turnover bone remodeling) and Type II (low turnover state). Type I, or high turnover, osteoporosis occurs in some women between the ages of 50 and 75 because of the sudden postmenopausal decrease in estrogen levels, which results in a rapid depletion of calcium from the skeleton. It is associated with increased amounts of fractures that occur when the vertebrae compress together causing a collapse of the spine and fractures of the hip, wrist, or forearm caused by falls or minor impact accidents [86]. On a cellular level, osteoporosis is generally characterized by a relative decrease in bone formation (bone-forming cells called osteoblasts) vs. bone resorption (bone-eating cells called osteoclasts).

Postmenopausal osteoporosis is therefore a powerful illustration of the importance of estrogen to bone health.

The objective of this chapter is to provide the reader with insight into three basic questions of skeletal functionality and bone remodeling and how it ties to the clinical significance of osteoporosis. First, we will examine how estrogen influences the body and bone remodeling. Second, we will explore the role of the osteocyte and its response to estrogen during bone remodeling. Lastly, a background of mechanisms that contribute to our understanding of why osteocytes undergo apoptosis after estrogen is removed. This approach is important to understanding the factors that attribute to bone loss via estrogen withdrawal and is fundamental to understanding women's bone health and disease.

WHAT IS AN OSTEOCYTE?

In order to answer the question of what an osteocyte is, it is imperative to define the skeletal system that it resides in. The skeletal system is composed of bone and connective tissue that joins them. Bone is the main constituent of the system, and is composed of inorganic salts situated within the matrix of collagen fibers and mineral [54]. The rigidity of bone enables the skeleton to maintain the shape of the body, and to protect the body's organs and soft tissues. The mineral content of bone serves as a reservoir for ions such as calcium. In addition, bone is a self-repairing structural material that adapts to changes in the body and the body's needs. There are two main types of bone within the skeleton; cortical and cancellous bone [*Figure 1.1*]. Cortical bone is dense, solid material that composes 80% of the skeletal mass, and has supportive and

protective function of the skeleton. Cancellous bone is a lattice of plates and rods known as trabecular, and found on the inner portion of bone. The distributions of these two bone types vary greatly between individual bones, and in addition they differ in their development, architecture, function and proximity to marrow and blood supply.

Figure 1.1: The two main types of bone.

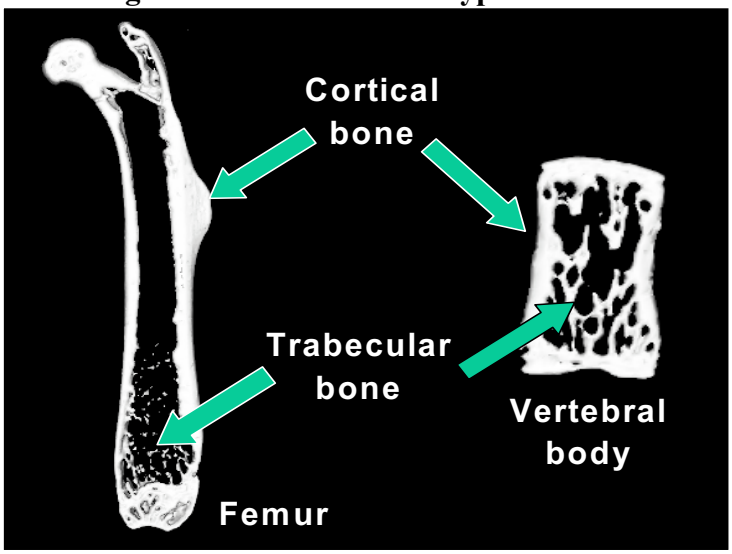

There are four main types of bone cells within the skeleton; osteoblasts (bone building), osteoclasts (bone removal), quiescent bone-lining cells and osteocytes. Osteocytes are terminally differentiated osteoblasts and exist embedded in a mineralized matrix, residing individual in caves called lacunae [120]. Osteocytes are stellate-shaped that communicate with each other and with osteoblasts and lining cells via their prominent cell processes within tunnels called canaliculi, thereby forming a network throughout the skeleton *[Figure 1.2*] [70]. Moreover, they are the most abundant cell type in bone, constituting 90% of all bone cells, yet are more sparsely distributed than in other organs (osteocyte cell density is 15,000 cells/mm^3 compared with 120,000

cells/mm^3 in heart) [48]. Although osteocytes represent the most abundant cell type in bone, their unique location and inaccessibility within the mineralized matrix make them difficult to study outside of *in vivo* models [8]. Furthermore, even if available, isolated osteocytes may not behave the same as they do within their physiological three-dimensional environment. Therefore, an *in vivo* model is optimal (and used for our studies as well) in order to elucidate the physiological function of osteocytes in bone remodeling.

Osteocytes are believed to be the mechanosensors of bone, and regulate activities and communication between other osteocytes and bone cell types. Osteocytes produce many different molecules associated with mineralization regulation (DMP1 and osteocalcin), and local signaling to other bone cell types (sclerostin and TGF-B3) [8; 46; 47; 61; 99]. Osteocytes contain molecules associated with cell to cell communication such as connexin 43 [122]. Osteocytes also express receptors for circulating hormones that control skeletal homeostasis including receptors for estrogen. Most of the effects of estrogen are exerted via the two known estrogen receptors (ERs), ERα and ERβ. ER-knockout studies have shown that these receptors are responsible for mediating trabecular bone mineral density, thymic atrophy, fat composition, and uterine weight [46]. Their molecular interactions, physiological conformation and hormone receptors all indicate towards a cell type that is very active in regulating its surroundings.

Figure 1.2: Osteocytes in the lacunar-canalicular system. This is a confocal photomicrograph taken at 63x of basic fuchsin stained mouse cortical bone.

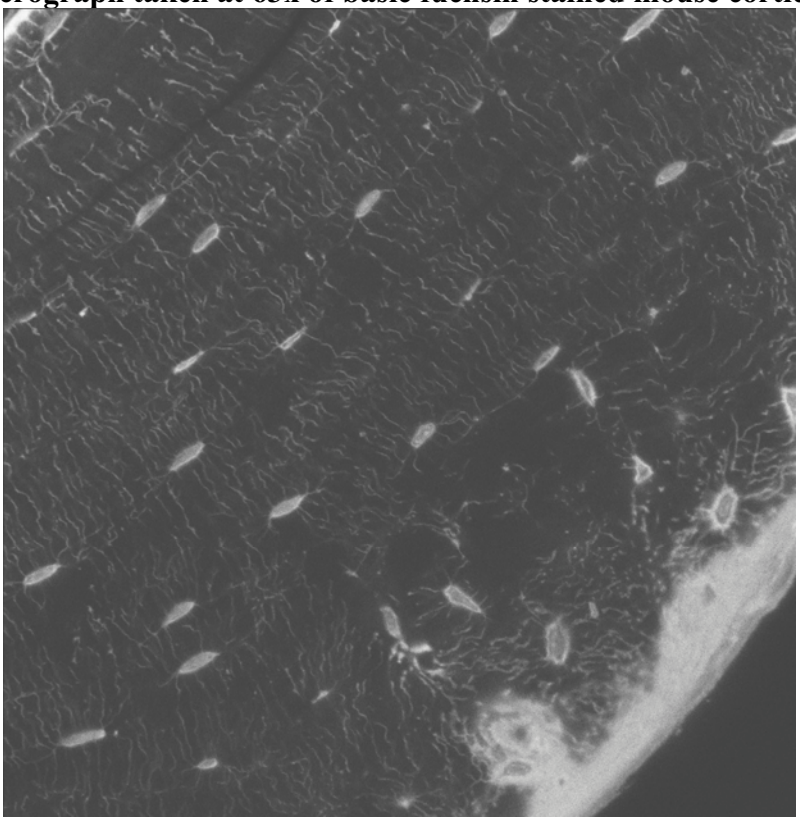

WHAT IS BONE REMODELING?

Bone is an extremely complex tissue system, being composed of multiple cellular elements, bone marrow components, and an elaborate extracellular matrix. The skeleton serves two major functions. It serves as a reservoir for minerals and as a structural framework to support muscles and vital organs [88]. Once growth and modeling of the skeleton are completed, bones continually alter their internal structure by a process called remodeling. It is important to note that modeling of bone happens primarily in children during growth where formation and resorption are independent and not linked processes [71]. Remodeling is different in the fact that it is a coupled process between formation

and resorption which occurs throughout adult life. The remodeling process consists of a coordinated effort by several bone cell types that make up the quantal unit called Basic Multicellular Unit (BMU) [61]. This process is initiated by bone resorption from the osteoclasts. Osteoclasts, the cells capable of resorbing bone, are multinucleated giant cells formed from hematopoietic precursors of the monocyte. They attach to the bone surface, sealing a resorbing compartment that they acidify by secreting H+ ions, which dissolves the bone mineral and exposes the organic matrix. Bone resorption is followed by bone formation of the osteoblasts; both processes are largely under control of the osteocyte. The osteocytes, as previously described above, are a terminally differentiated osteoblast that as become entombed within the bone matrix during bone formation. These cells maintain the surrounding matrix components and are the go-between for cellular communication of mechanical loads to the osteoblast and osteoclasts [73].

There are many factors that initiate bone remodeling, such as mechanics (removal of microdamage) and hormones (estrogen withdrawal). Mechanical usage has been widely studied and was first proposed by Frost's Mechanostat Theory, which correlated the biological mechanisms that fit skeletal mass and architecture to the needs of normal physical activities [54; 72]. Endocrinology influences such as circulating hormones exert control over bone remodeling, and crucial regulation is provided by many cytokines and growth factors that are the products of bone cells and the immune system's response to the hormones [15; 56]. Attempts have been made to explain the increased resorption and loss of bone with loss of estrogen, such as increased production of cytokines (IL-6, IL-1, TNF-α, RANKL), with the common mechanism being a deficiency in the coupling process [31; 55; 77]. Regardless of stimulus, the coupling of bone formation with

resorption following ovariectomy causes bone remodeling to be increased so that more of the bone surface is occupied by BMUs undergoing resorption and formation. Within each BMU, however, the amount of bone resorbed exceeds the amount of bone formed and therefore there is a net bone loss.

Bone remodeling is a necessary process in the body for mineral regulation, mechanical adaptation to a loading environment in order to reduce fracture (first described by Wolff) and to repair damage accumulated in the tissue [13; 54]. It is not energetically advantageous to make bone tissue randomly if only a certain site needs repair. Activation of this process is the phase that is least understood. The activation phase of remodeling involves an activating stimulus in which there is recruitment of osteoclast precursors, and migration to the specified site to initiate removal. An understanding of the local control of the remodeling activation would provide opportunities for therapeutic interventions regarding bone remodeling.

TARGETED VS NON-TARGETED REMODELING

Parfitt (1994) argued that bone remodeling could be either a 'stochastic' or 'targeted' process [94]. Targeted remodeling occurs when a microscopic region of bone is focally damaged or has otherwise outlived its functional lifespan. This region would be resorbed and replaced by a bone multicellular unit (BMU) that is "targeted" towards that region. Targeted remodeling to repair microdamage in bone was originally proposed by Frost (1960), and confirmed subsequently in numerous experimental studies where damage is created by fatigue loading in animal models [14; 34; 49]. In these studies, the increase in new remodeling response occurs subsequent to the generation of

microdamage, thereby supporting a direct relationship between the initiation of microdamage and local activation of repair. Further, these studies point to osteocyte injury around bone microdamage as the "target" focus for osteoclastic resorption. Bentolila et al found intracortical resorption surfaces occurring in regions of atypical osteocyte morphology following fatigue loading [6]. Verborgt et al previously demonstrated that osteocytes undergo apoptosis in bone areas immediately surrounding bone microdamage, and this apoptosis precedes and then co-localizes precisely with the location subsequent to bone resorption [126; 127]. Using a rat ulnar loading model, they defined a spatial association between microcracks, osteocyte apoptosis and new remodeling sites. Recent apoptosis inhibition studies by Cardoso et al demonstrated that osteocyte apoptosis plays a direct and controlling role in the activation and targeting of a microdamage remodeling response [*Figure 1.3*] [18].

Figure 1.3: The concept of targeted remodeling: removal and replacement of regions of bone that have outlived their mechanical or biological usefulness. Specifically, this schematic illustrates regions of interstitial bone that contain microdamage. Osteoclastic resorption colocalizes with these regions indicating that these regions of microdamage were "targeted" for removal. *Picture courtesy of Brad Herman.*

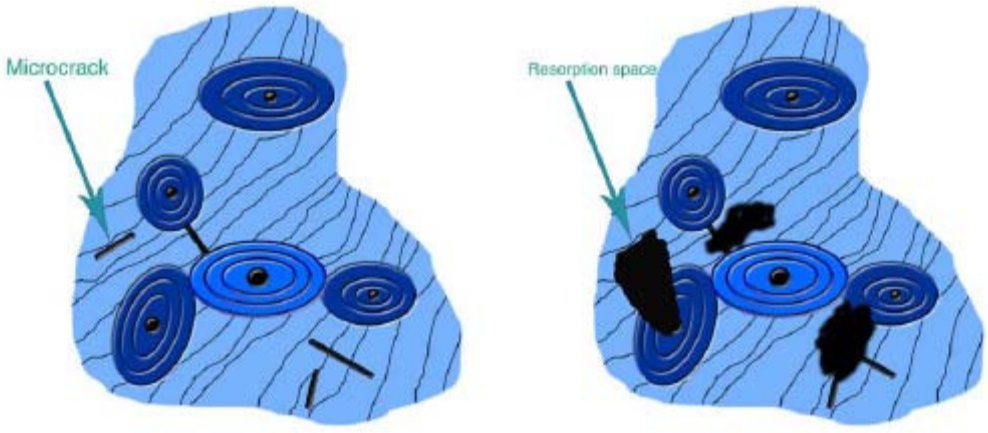

In contrast to targeted remodeling, Parfitt (1996) posited that stochastic remodeling occurs without any identifiable tissue focus or target for resorption of the tissue, as demonstrated in the generalized resorption increases seen after estrogen loss, glucocorticoid treatment and disuse [1; 40; 95; 123]. Treatments such as bisphosphonates that reduce bone turnover activity reduce the amount of stochastic and targeted remodeling by suppressing new remodeling areas and terminating osteoclast activity [35; 74; 98]. Deficiency of circulating hormones such as estrogen has largely been thought of as an inducer of stochastic remodeling because it is a global stimulus (or more properly considered a lack of stimulus). As this dissertation will demonstrate, attenuation of osteocyte apoptosis via estrogen withdrawal causes bone resorption that is targeted toward removal of dying osteocytes, and therefore has much more in common with targeted remodeling processes.

ESTROGEN'S ESSENTIAL ROLE IN THE BODY

Estrogens are a group of steroid compounds, named for their significance in the estrous cycle, and play an important role in growth, differentiation and function of many target tissues, including the female gonads, heart, and bone [78]. Estrogen is the common name for the female sex steroid composed of estrone (E1), estradiol (E2), and estriol (E3). Estrogen is synthesized from its precursor cholesterol and produced primarily by developing follicles in the ovaries, the corpus luteum, and the placenta [19]. Estrogen is important also in males, where it is produced by aromatization of testosterone in several tissues. Follicle-stimulating hormone (FSH) and Lutenizing Hormone (LH) stimulate the

production of estrogen in the ovaries for the regulation of different organ systems in the body, including the musculoskeletal and cardiovascular systems, as well as the brain.

To produce its action, estrogen can activate protein-kinase cascades using several different mechanisms [*Figure 1.4*]. The classical signaling pathway requires estrogen to bind to estrogen receptors (ER) located on the nuclear envelope. Most tissues other than bone exert their estrogen effects via this pathway [78; 138]. The activated estrogen-ER complex then binds directly to the estrogen-response elements (ERE) in the target gene promoters. Another mechanism for activation is called the ERE-independent genomic pathway, where nuclear estrogen-ER complexes are tied through protein-protein interactions to a transcription factor directly. The estrogen activates protein kinases via extranuclear function of the ER. Inhibition of apoptosis by estrogen requires nuclear accumulation of these protein kinases, with subsequent downstream transcription factors [97]. Previous studies implicate that sex steroids affect bone through non-genomic pathways [57; 117; 135]. They demonstrated that *in vitro* sex steroid-mediated anti-apoptotic effects on osteoblasts were mediated by non-genomic, sex non-specific activation of sex steroid receptors. Treatment of OVX animals with a estrogen-like compound (called estren) increased bone mass without affecting reproductive organs. Therefore, they suggested that estren is a mechanism-specific compound that reproduces only non-genomic signaling of estrogen [59].

Figure 1.4: Schematic Illustration of estrogen receptor (ER) signaling mechanisms. (1) Classical ER signaling pathway. Nuclear E2-ERs bind directly to the estrogen-response elements (ERE) in target gene promoters. (2 and 3) ERE-independent genomic actions. Nuclear E2-ER complexes are tied through protein-protein interactions to a transcription factor that contacts the target gene promoter. (4) Non-classical ER signaling pathways. Activation of protein-kinase cascades and non-genomic effects by ligand activated ERs and non-steroid receptors [7].

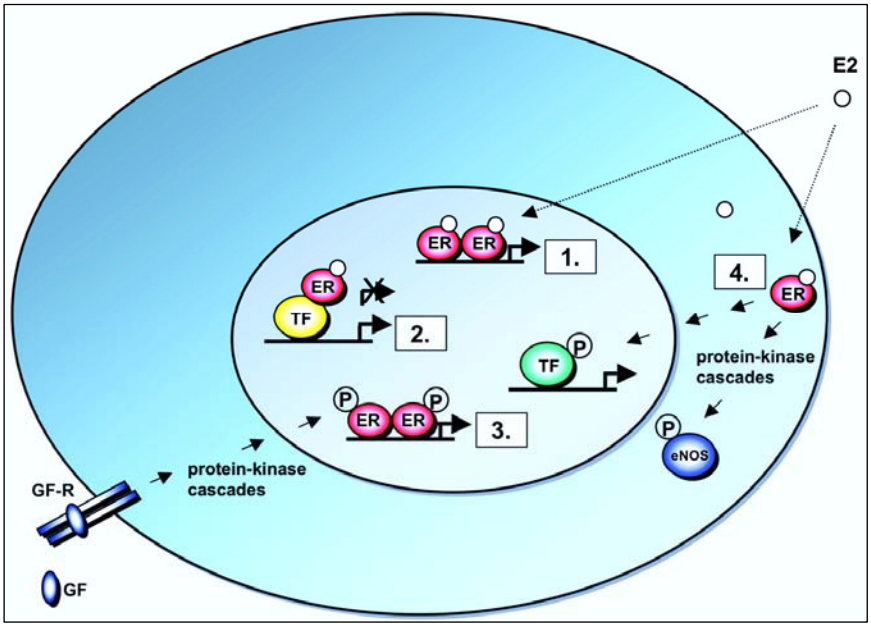

Estrogen studies investigating the role of estrogen as a potential athero-protective agent have shown it to inhibit both atherogenesis via regulation of endothelial FasL expression [2; 19]. Fas ligand (FasL) expression by the vascular endothelium inhibits the migration of inflammatory cells into the vessel wall, a crucial event for the development of atherosclerosis. Estrogen is a viability factor for many cell types and removal of this hormone has been shown to cause cell death in many tissue systems [23; 107; 116]. Ovariectomy studies examining endothelial, nerve and brain cell apoptosis levels have all shown increased apoptosis when the protective effects of estrogen are removed. Other studies have examined estrogen as a viability factor for cellular protection in the brain and heart in conjunction with IGF-1, and showed estrogen as an essential regulator of

neural and endothelial function [37; 83; 108]. Estrogen has also been implicated in maintaining nerve profile density in bone. Experiments done with ovariectomized animals observed substantial loss in innervation, indicating a functional link between bone loss after estrogen depletion and the nervous system [4]. The effects of estrogen have major implications on the immune system as well, with mediation by downregulating inflammatory immune responses and increasing antibody production [19; 121].

ESTROGEN AND BONE

The influence of estrogen on the remodeling skeleton is distinct in its ability to maintain an equilibrium set point for calcium levels in body fluids and strain levels (modulates the sensitivity and responsiveness of the mechanosensory control system) [92]. They are the major sex steroid affecting the growth, remodeling, and homeostasis of the skeleton [63]. For instance, during growth the epiphyseal closure at puberty in both sexes is dependent on estrogen. Estrogen protects the skeleton by suppressing rates of turnover and maintaining a focal balance between formation and resorption. This is maintained by increasing the lifespan of osteoblasts and embedded osteocytes, with minimal formation of osteoclasts. Loss of estrogen causes an imbalance in this regulation and therefore causes increased osteoblastogenesis and osteoclastogenesis independently, with mediation by osteocytes.

Osteoporosis initiated by estrogen removal is a model commonly used to simulate menopausal bone loss in animals [58; 75; 8991; 123; 124]. Estrogen deficiency is experimentally induced by ovariectomy (OVX), either surgically through the removal of

the ovaries, or chemically via estrogen receptor blockers [124]. OVX animal models have been used to isolate the effects of cytokines and receptors on estrogen deficient bone loss [87; 121]. For the studies presented in this dissertation, 17-week old female mice were used because skeletal growth is at a minimum [*Figure 1.5*], and combined with ovariectomy (OVX), it provides a model that allows us to study bone resorption.

Figure 1.5: Variation in femoral total area (Tt.Ar) and marrow area (Ma.Ar) among female mouse strains. Top: Changes in total area across development. Bottom: Changes in marrow area across development [100].

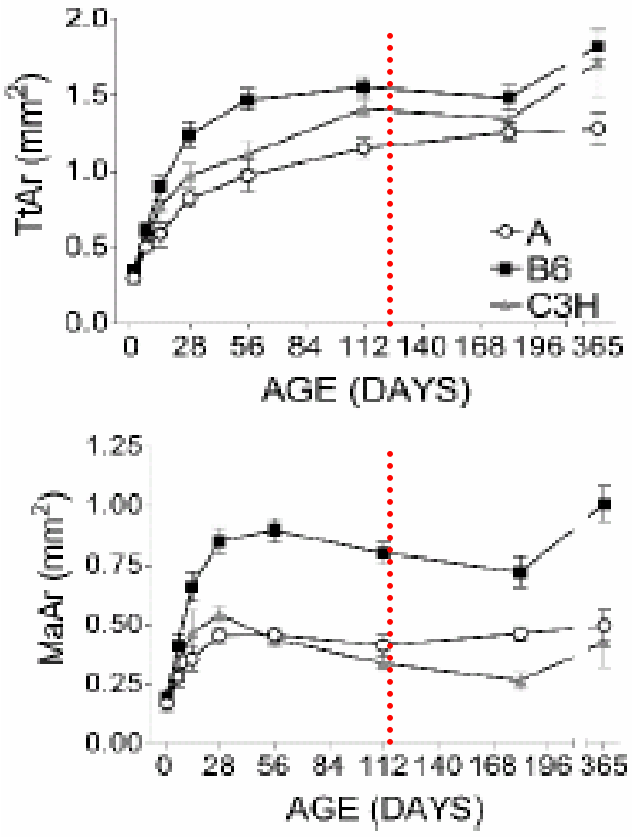

There are several mechanisms for estrogen-mediated effects on bone loss. It is a reasonable assumption that there is a combination of molecular actions of this hormone working together both directly on cells (as described above) and indirectly via other systems in the body. The main effect of OVX on bone cells is enhanced stimulation of resorption from increased osteoclastic bone resorption and osteocytes apoptosis [58; 68; 69]. This happens because the lack of estrogen elicits an increased circulation of pro-inflammatory cytokines (IL-1, IL-6, TNF-α, M-CSF). This inflammation enhances osteoclast formation and activates mature osteoclasts, thereby resulting in increased bone resorption. Pacifici et al have established an immuno-deficient model for cellular and molecular mechanisms responsible for OVX-induced bone loss in mice [91]. They showed that OVX mice with T-cell deficiency failed to lose bone, stimulate bone resorption, or increased M-CSF signaling, while OVX increased TNF-producing T-cells in bone marrow. Furthermore, after restoring $TNF^{+/+}$ T-cells, bone loss was induced; thus demonstrating a link between the immune system and bone physiology. Despite estrogens effects on bone marrow macrophages (T-cells), there are other regulatory systems that estrogen acts through in order to maintain bone turnover. Recent evidence points to the GH/IGF-1 axis could be involved. Recent work using liver IGF-1 deficient (LID) mice showed that the cortical response to ovariectomy-induced bone loss was altered in mice with low circulating IGF-1, with reduced resorption in LID mice [33].

There is also evidence that estrogen modulates the sensitivity of osteocytes to mechanical strain, free radical damage and glucocorticoid-induced apoptosis, which raises the question of estrogen's potential role as a protective agent and a potent antioxidant, not just a viability requirement [1; 3; 29]. Estrogen withdrawal studies show

decreased trabecular area, increased osteoclast number and an increase in serum calcium [71]. An ovariectomized rat trabecular longitudinal study using *in vivo* micro-CT observed changes in bone architecture over time, indicating that the bone remodeling process results in bone loss of certain trabeculae, thereby causing a realignment of bone and formation of new trabecular bone struts [72]. Studies such as these indicate that ovariectomy-induced bone loss should be appropriately described as a state of rapid bone metabolism in which remodeling is high and adaptation is accelerated, resulting in major changes over time. More recent studies utilizing an OVX rat model with left hindlimb suspension showed that sham-operated (E^+) bone of the suspended hindlimb maintained bone mass, but didn't aid in the geometry or strength of the bone, when compared to the contralateral limb that was loaded [92]. This study implicates that the actions of estrogen and loading are independent of one another.

POTENTIAL ROLE OF OSTEOCYTES IN BONE REMODELING

The lacunar-canalicular system (LCS) acts to connect all of the osteocytes within the bone to the cells of the bone surface. This system supports the idea that osteocytes are mechanoregulators and can sense load on the skeleton and translate those signals to formation or resorption [9; 10]. A newly published article by the Tatsumi group indicates that osteocyte-ablated mice exhibited fragile bone with intracortical porosity, microfractures, osteoblastic dysfunction, and trabecular bone loss [120]. Using a diphtheria toxin (DT) receptor only expressed in osteocytes, they injected DT for a 'loss-of function' study in grown mice, thereby not affecting the growth and developmental role of osteocytes. Their data shows that viable osteocytes are necessary to send

preventative signals against bone loss, and are also necessary for the bone to 'see' unloading. The findings that the loss of osteocytes results in not only reduced bone mass but compromised bone quality suggests that osteocyte deficiency may underlie bone fragility under various conditions, and that osteocytes therefore make an important target for the development of diagnostics and therapeutics for bone disease, as shown by osteoporosis. These data support previous theories that viable osteocytes prevent osteoclast activation, and that osteocytes surrounding damage illicit signals that direct osteoclast activity [123; 126]. There is a causal link between osteocyte apoptosis and initiation of remodeling; yet in all of the recently published data, a spatial and temporal relationship between osteocyte apoptosis and bone remodeling initiated by estrogen withdrawal has not been shown.

Since osteocytes are the predominant cell population in bone, constituting 90% of all bone cells, they are the most likely candidate source for osteoclasts recruitment signals, and aid in dictating the remodeling response. Osteocytes can indirectly influence bone remodeling by signaling to the bone-lining cells to produce RANKL or they can directly influence bone remodeling by producing RANKL and MCS-f, two known factors for osteoclastogenesis [73]. RANKL is essential for osteoclast differentiation via its receptor RANK located on the osteoclast membrane. Osteoprotegerin (OPG), a soluble decoy receptor, is produced by the osteoblast-lineage cell, binds to RANKL and prevents interaction with RANK on the osteoclast precursor. Since small amounts of MCSF are constitutively expressed in the bone microenvironment, it has been proposed that the relative expression of RANKL and OPG ultimately control osteoclastogenesis. Therefore, it is the ratio of RANKL to OPG that determines whether the bone-lining cell, the

osteoblast-lineage cell that is able to bind to the osteoclast precursor *in situ*, is able to stimulate osteoclastogenesis and ultimately, bone resorption [56]. Increased RANKL relative to OPG results in a pro-osteoclastogenic (ie, pro-resorptive) state. Conversely, increased OPG relative to RANKL results in an anti-osteoclastogenic (ie, anti-resorptive) state.

Osteocytes orchestrate the remodeling process via signaling to the other bone cell types. Osteocytes produce sclerostin, which regulates osteoblast activity by regulating RANKL expression in osteoblasts (osteoblast normally restrain their RANKL output) [99]. Recent data has given remarkable insight into the influence of osteocytes in bone remodeling. Ito et al used gene expression to show that allografts lacked RANKL, yet when it was added to the grafts, remodeling was comparable to control bone, clearly demonstrated the necessity for RANKL in bone remodeling [51]. In another study done by Gau et al, showed that osteocytes were negative regulators of osteoclastic activity directly [36]. Their work showed osteoclasts cultured on calvarial slices with living osteocytes inside failed to form their typical resorption signals, but when osteocyte apoptosis was induced strong osteoclastic resorption activity was observed. These allograft studies give insight into osteocytes as the primary cellular source of signals that initiate resorption.

OSTEOCYTE APOPTOSIS INITIATES REMODELING

There has been much work done in the field to try and elucidate the precise role of the osteocyte network in bone turnover signaling with many of these studies pointing towards osteocyte apoptosis. It has been reported that osteocyte density declines with age

and loss of estrogen accelerates the effects of aging via decreased defense against oxidative stress [1]. Osteocyte apoptosis has also been documented with estrogen deficiency, and glucocorticoid treatment [68; 81; 134]. Noble et al found a non-uniform distribution of apoptotic osteocytes among the femoral head, iliac crest, raising possibility of functional relationship between programmed osteocyte death and bone turnover [85]. Recent work done by Hedgecock et al demonstrated that regional variations in remodeling correlate with osteocyte apoptosis in rabit tibia mid-shafts [45]. Qiu et al reported that microdamage was found in cortical bone regions where osteocytes were dying, with increased empty lacunae [101]. Further, areas of less osteocytes were associated with increased microdamage and increased risk of fracture in femoral neck fracture cases [79]. Therefore, osteocyte apoptosis and its association of bone remodeling is becoming a common theme.

The phagocytic removal of apoptotic cells plays an important role in the body during development; tissue homeostasis and host defense [23]. The phagocytic removal of injured cells such as cells undergoing apoptosis can be considered largely beneficial for preservation of cellular homeostasis; therefore osteocyte apoptosis in the recruitment of osteoclastic macrophage cells in bone should illicit the same response.

There are two hypotheses by which death of osteocytes may lead to resorption. A dying osteocyte could decrease osteoclast inhibitory signals or activate osteoclasts to the scene. The first hypothesis, “loss of inhibition”, argues that osteocytes constitutively produce inhibitory signals which prevent recruitment of osteoclast precursors to the surface where bone is to be resorbed [72]. When osteocytes die, they no longer produce these inhibitory signals, thus creating a local environment that is attracts osteoclastic

activity. This theory does not hold up after previously discussing the allograft studies, due to the finding that *dead bone does not resorb*!

The second hypothesis is "cell mediated activation" of resorption wherein the osteocyte apoptosis itself is a pro-osteoclastogenic signal and/or the apoptosis upregulates pro-osteoclastogenic factor production in neighboring surviving osteocytes. Recent evidence shows that osteocyte apoptosis positively correlates to bone resorption by osteoclasts in growing bone, microdamage, and estrogen withdrawal [13]. Recent studies involving microdamage show that osteocytes adjacent to those undergoing apoptosis actively protect themselves against cell death by eliciting anti-apoptotic factors such as Bcl-2 [127]. Other studies examining the relationship of osteocyte apoptosis during bone formation concluded that osteocytes die and disperse nuclear fragments into the extracellular matrix, and that a majority of these osteocytes are phagocytosed by osteoclasts [12]. Although this early study did not provide direct evidence, it provides support for the idea that these neighboring cells could play an active role in signaling and/or targeting of osteoclastic bone resorption. More importantly, in the areas surrounding microdamage, the Verborgt study found that apoptosis preceded the activation of bone resorption, as will also be demonstrated in this proposal under Aim 1. More work done in our lab by Cardoso et al established a correlation between osteocyte apoptosis and osteoclast resorption, giving evidence that inhibiting fatigue-induced osteocyte apoptosis prevented activation of osteoclast resorption [17]. Therefore, osteocytes and the onset of apoptosis could prove a key relation to the signaling mechanisms that osteoclasts use to direct their resoptive response.

ANTIOXIDANTS AND BONE

Bone mineral density (BMD) measurements can not account for all the variation in bone strength. Measures of bone quality, architecture, and microdamage accumulation are now considered possible determinants of bone strength. Less well established is the impact of bone quality on impaired bone cellularity. Presence of viable and healthy osteocytes is essential to the bone's ability to remodel efficiently, to maintain mineralization and to repair accumulated microdamage. The number of viable osteocytes in the human femur, for example, decreases from 90% at ages 1-10 years, down to as low as 20% at age 90 [71]. Reasons for age-related loss of osteocytes are unclear, but apoptosis is thought to be caused by a penumbra of reasons such as estrogen loss and accumulated reactive oxygen species (ROS). ROS are generated from normal oxygen metabolism within the cell as well as produced exogenously in the body. They are also called oxygen free radicals, and include hydrogen peroxide, oxygen, and nitric oxide. Along these lines, a "Free Radical Theory of Aging" was first proposed by Harman (1956) that projected that aging is due to an accumulation of un-repaired damage from free radical attack on cells [44]. Aging causes a shift in the balance between pro-oxidative and antioxidative processes in the direction of oxidation [103; 125]. Therefore, aging results from an increase in oxidative damage to lipids, proteins, and DNA [43; 50; 125].

Oxidative stress is found to play a critical role in neurodegenerative diseases, such as Alzheimer's and Parkinson's disease, through degeneration of the neuron [23]. The brain is highly sensitive to oxidative stress due to high amounts of oxygen metabolism and low ROS defense system.It is thought that the effects of ROS on the brain and other

tissues are estrogen-receptor (ER) independent, and attributed to the antioxidant properties of estrogen [71]. Oxygen free radicals are also produced during ischemic injury and diabetes, and have been found to yield apoptosis in many different tissues such as lung, bone and heart [23; 24; 43; 50; 116]. Regardless of the cell type, the balance between ROS production and antioxidant defense determines the degree of oxidative stress and therefore the degree damage to the cells within the diseased tissue [32].

So where does estrogen fit in the picture? Many studies have shown that estrogen is an antioxidant that inactivates free radicals caused by metabolic waste, both directly and indirectly. Directly, prevention of oxidative stress-induced cell death has been found to be due to estrogen's conformation. There is a C3-OH moiety on the steroid A-ring of the molecule that mops up free radical damage within the cell [2; 71]. Studies investigating the possibility of estrogen as an antioxidant in osteocyte cell populations with H_2O_2 induced oxidative damage showed that with estrogen there was less apoptosis. Moreover, when ER-negative osteocytes were given estrogen and hydrogen peroxide, they yielded less apoptosis, thereby demonstrating an ER independent protection. Other studies in OVX-induced estrogen deficiency saw that there was increased accumulation of ROS in bone marrow, which led to increased TNF-α by activated T-cells [38]. Bone loss was prevented in OVX mice by either antioxidant administration.

Indirectly, estrogen is responsible for regulating the glutathione and thioredoxin pathways, which are the cells oxidative stress regulatory pathways. The cells defense mechanism against oxidative stress involves reduction of peroxides to harmless alcohols. Glutathione peroxidase oxidizes glutathione (GSH) to disulfide glutathione (GSSH), and glutathione reductase enzyme converts GSSH back to its reduced form GSH [*Figure 1.6*].

Estrogen is thought to maintain GSH within the cell by regulating reductase enzyme activity [63]. Reductase is found to decrease with aging, and therefore exaggerated with estrogen deficiency. It is important to note that aging overrides the acute effects of estrogen withdrawal, but loss of this valuable hormone greatly exaggerates the aging process.

Figure 1.6: The cellular glutathione pathway. Glutathione (GSH) mops up free radical damage and becomes inactive (GSSH). Reductase levels bring the glutathione back to an active state. Estrogen has been shown to regulate reductase levels.

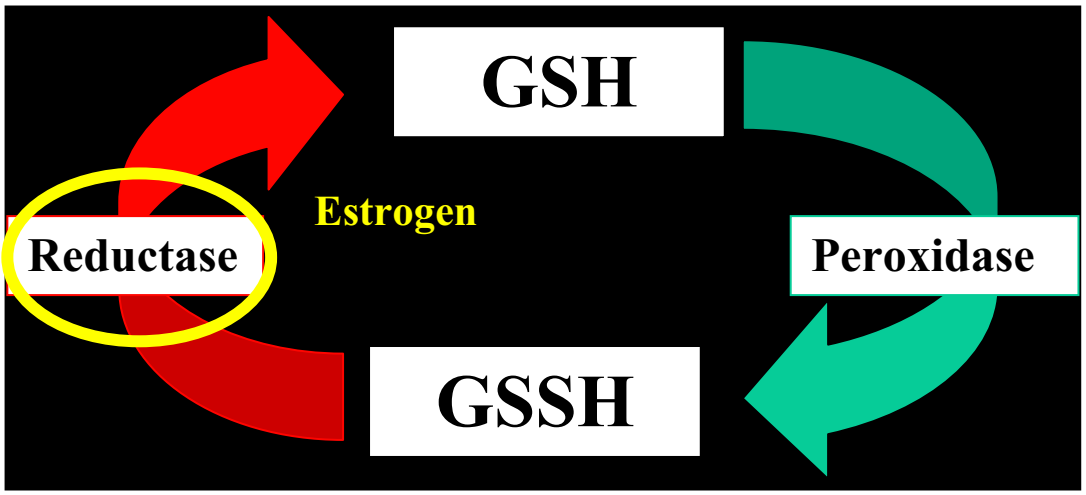

On a cellular level, oxidative stress leads to apoptosis that involves early phase cellular membrane phosphatidylserine (PS) exposure, and late phase degeneration of DNA [23; 43]. ROS can stimulate osteoclast formation and activity directly [38]. Studies using aged osteoblast cultures found that more RANKL is secreted with age, and OPG expression remained either unchanged or decreased, thereby altering the relationship between osteoblasts and osteoclasts [16]. This effect would be emphasized with estrogen

withdrawal because osteoclastogenesis would no longer be inhibited and osteoblasts would undergo apoptosis without estrogens protective effect. Ovariectomy induces a tissue-selective decrease in both ROS intracellular scavengers and inhibitors of ROS generation, which leads to local accumulation of ROS-induced protein damage. OVX also caused an increase in follicle-stimulating hormone, which is causative to a cytokine-driven increase in osteoclast formation. Another study examined the role of ROS accumulation and estrogens role in regulating the glutathione and thioredoxin pathways [63]. Their studies showed that reductase levels fell drastically post-OVX in marrow. Administration of the antioxidant NAC completely prevented bone loss, while BSO (L-buthione-(S, R)-sulphoximine) a specific inhibitor of glutathione synthesis, depleted glutathione and caused apoptosis in ovary-intact mice. Companion *in vitro* studies showed estrogen augmented osteoclastic expression of glutathione and thioredoxin reductases. The antioxidant NAC suppressed NF-κB activity and TNF-α expression in osteoclasts. Administration of BSO led non-OVX mice into a high turnover state, similar to estrogen withdrawal. These changes in histodynamics were identical to OVX-induced high turnover state where there is increased bone resorption that entrains an increased bone formation insufficient to replace bone lost. An important note to this study was that estrogen did not affect GSH, yet stimulated both glutathione and thioredoxin reductase levels. This was an important paper which demonstrated that antioxidant pathways are essential to osteocyte viability and that estrogen or other antioxidants (NAC) regulate these pathways via its maintenance of thioredoxin and glutathione reductase levels.

SUMMARY

Understanding the basic biological factors that contribute to bone loss after estrogen loss is fundamental to understanding bone health and disease. Evidence points to a role for osteocyte apoptosis in remodeling after estrogen withdrawal. Moreover, in other organ systems, apoptosis plays a pivotal role in governing normal turnover and response to injury. In other systems, turnover involves targeting of apoptotic cells and active signaling to the phagocytic cells to orchestrate the location of resorption. Although bone is regulated by estrogen, the mechanisms by which estrogen and its deficiency exert its directed effects on bone during remodeling remain unclear. Therefore, the overall goal of this dissertation is to better understand the role of osteocyte apoptosis in targeted bone remodeling after estrogen withdrawal. In Chapter 2, we characterize the spatial and temporal relationship between estrogen withdrawal, osteocyte apoptosis and bone resorption. In Chapter 3, we examine whether osteocyte apoptosis plays a comparable controlling role in the activation or targeting of osteoclastic resorption by inhibiting apoptosis. In Chapter 4, we examine the microenvironmental and biological differences that account for osteocyte apoptosis during estrogen withdrawal.

CHAPTER 2

SPATIAL AND TEMPORAL COUPLING OF OSTEOCYTE APOPTOSIS AND CONTROLLED BONE RESORPTION FOLLOWING ESTROGEN WITHDRAWAL IN MICE.

ABSTRACT

Introduction: Osteocyte apoptosis has been linked to bone resorption resulting from estrogen depletion and other resorptive stimuli; however, in those instances precise spatial and temporal relationships between the two events have not been clearly established. The purpose of this study was to characterize the patterns of osteocyte apoptosis in relation to bone resorption following ovariectomy in mice to test whether osteocyte apoptosis occurs preferentially in bone areas known to activate resorption in this model.

Materials and Methods: Adult female C57BL/6J mice (17 week old, n=5/group) underwent either bilateral ovariectomy (OVX) to activate bone resorption, or sham surgery (SHAM). Mice were euthanized on days 3, 7 and 14 days. Day 14 mice also received double calcein labels prior to sacrifice.

Diaphyseal 5μm cross-sections were stained by immunohistochemistry for activated caspase-3 as a marker of apoptosis. The percentages of Caspase-positive osteocytes (Casp+ Ot.) in eight tissue quadrants defined by the principal anatomical axes (anterior, posterior, medial, and lateral) were determined using an eyepiece grid reticule at 400X magnification.

Coronal 5 μm sections were cut from paraffin decalcified embedded distal femora to obtain metaphyseal trabecular bone sections. Immunohistochemical staining for cleaved caspase-3 was used to examine caspase-dependent apoptosis. Photomicrograph images were taken in 5 distinct metaphyseal regions, where percentages of Casp+ Ot. were determined using 400X magnification.

Results: OVX markedly increased osteocyte apoptosis in a non-uniform distribution throughout the femoral diaphyses. Increases in Casp+ osteocytes were located almost exclusively in the posterior diaphyseal cortex. In this region, the number of apoptotic osteocytes was nearly 800% higher than in sham controls ($p<0.005$). This increase in Casp+ osteocytes was seen by 3d post-OVX and persisted throughout the experiment ($p< 0.01$). Increases in resorption at 2 wks post-OVX also occurred along the posterior endocortical surface overlying the region of osteocyte apoptosis. The exacerbated osteocyte death preceded the increases in endocortical resorption ($p<0.005$).

Overall osteocyte apoptosis in trabecular metaphyseal trabecular bone of the distal femur was significantly elevated at 3 days post-OVX and remained elevated compared to the sham for the experimental period. Osteocyte apoptosis near resorption sites was dramatically elevated above that seen near quiescent surfaces.

Conclusions: The results of this study demonstrate that osteocyte apoptosis following estrogen loss occurs regionally, rather than uniformly throughout the cortex. Consistent with previous observations, we found that estrogen loss increased osteocyte apoptosis in both cortical and trabecular bone of the femur. However, we found that apoptotic osteocytes in cortical bone were overwhelmingly localized within the posterior cortical region, the area where subsequent endocortical resorption is known to occur after ovariectomy in B6 mice. In trabecular bone, we found the same relationship, with areas of apoptosis correlating to areas (within 20 μm) of resorption. That a similar spatial and temporal coupling between osteocyte apoptosis and bone resorption occurs in cancellous bone, after ovariectomy argues that osteocyte apoptosis may play a universal role in the local regulation of bone remodeling, in both cortical and cancellous bone compartments.

INTRODUCTION

Estrogen is the major sex steroid affecting the growth, remodeling, and homeostasis of the female skeleton [102]. Estrogen deficiency in postmenopausal women frequently leads to osteoporosis, a metabolic bone disease characterized by low bone mass and associated with increased risk of fracture, and is one of the most prevalent degenerative disease worldwide [55]. Similarly, ovariectomy clearly induces an osteoporotic bone phenotype in mice [81]. The main effect of OVX on bone is enhanced stimulation of resorption from increased osteoclastic bone resorption and osteocytes apoptosis [123; 124]. The coupling of bone formation with resorption after estrogen withdrawal following ovariectomy causes bone remodeling to be increased so that more of the bone surface is occupied by bone multi-cellular units (BMU) undergoing resorption and formation. Within each BMU, however, the amount of bone resorbed exceeds the amount of bone formed and therefore there is a net bone loss.

There has been much work done in the field to try and elucidate the precise role of the osteocyte network in bone turnover signaling. Osteocyte apoptosis plays an essential role in targeted bone remodeling induced by fatigue damage [126; 127]. Apoptosis occurs specifically in osteocytes near microdamage sites and precedes the onset of bone resorption; moreover, inhibition of apoptosis in vivo is sufficient to prevent osteoclastic resorption due to fatigue. Osteocyte apoptosis has also been linked to bone resorption resulting from estrogen depletion and other resorptive stimuli [1; 5; 56]. Noble et al found a non-uniform distribution of apoptotic osteocytes among the femoral head, iliac crest, raising possibility of functional relationship between programmed osteocyte death

and bone turnover [85]. Recent work done by Hedgecock et al demonstrated that regional variations in remodeling correlate with osteocyte apoptosis in rabit tibia mid-shafts [45]. Published studies from our lab have demonstrated that post-ovariectomy, there was an increased (+422%) posterior endocortical remodeling in the B6 mouse model at 4 weeks post-surgery in a specific region of bone [66].

The findings that the loss of osteocytes results in not only reduced bone mass but compromised bone quality suggests that osteocyte deficiency may underlie bone fragility under various conditions, and that osteocytes therefore make an important target for the development of diagnostics and therapeutics for bone disease, as shown by osteoporosis. A causal link between osteocyte apoptosis and initiation of remodeling has previously been demonstrated; however a spatial relationship between osteocyte apoptosis and bone remodeling initiated by estrogen withdrawal has not been shown. The purpose of this study is to characterize the patterns of osteocyte apoptosis in relation to bone resorption following ovariectomy in mice, and to test whether osteocyte apoptosis occurs preferentially in bone areas known to activate resorption in cortical and cancellous bone.

METHODS AND MATERIALS

Animal Model and Procedures

Fifty-five (17-week old) female, C57BL/6J mice were used in this study. Twenty-five animals underwent bilateral ovariectomy (OVX) using a dorsolateral approach under Avertin anesthesia. An additional 25 animals underwent sham surgery in which ovaries were exteriorized and replaced in the abdominal cavity, with all wounds suture closed. A group of 5 control mice (BASAL) was sacrificed at the beginning of the

study. All animals were weighed at surgery and at sacrifice. At 1,3,7,14, and 21 days following surgery, groups of OVX and SHAM animals (n=5 each) were anesthetized as above and blood samples were collected by retro-orbital bleeding, after which the animals were euthanized by cervical dislocation.

Tissue Collection and processing

At necropsy, uteri were harvested and weighed to confirm the effectiveness of ovariectomy. Femora were dissected, cleaned of soft tissue and fixed in 10% neutral buffered formalin for 48 hr at 4˚C. Right femora were decalcified in formic acid solution for 3 days with daily changes. Bones were then embedded in paraffin and mid-diaphyseal 5 micron cross-sections cut and adhered to charged slides.

The distal mid-shaft femur was then reoriented in paraffin, and 5 μm coronal sections were cut and stained for cleaved caspase-3 to indicate caspase-dependent apoptosis in metaphyseal and epiphyseal trabecular bone.

Left femora remained undecalcified for cortical bone histomorphometry following the methacrylate embedding using bulk staining procedures [62; 66]. Mid-diaphyseal cross sections were cut (150 micron thickness) using a Leica 1600 Sawing Microtome (Leica Instruments, Nussloch, Germany), polished to 30 micron thickness with silicon carbide grinding paper (Buehler, Lake Bluff, IL, USA), and cover-slipped with non-fluorescing mounting medium for bone histomorphometric analysis.

Immunohistochemistry

The spatial and temporal patterns of osteocyte apoptosis were assessed in the right mid-diaphyseal femoral cortex using immunohistochemistry for apoptotic markers at various time points (1d, 3d, 7d, 14d, 21d) post-ovariectomy. These time points were used to examine osteocytes before resorption activation (1d, 3d), at early osteoclastic phase (7d), and at peak resportion (14d, 21d) in this model [66]. To detect osteocyte apoptosis, sections were incubated with primary antibody to cleaved (activated) caspase-3, an effector caspase required for regulated cell death [114]. Sections were deparaffinized, rehydrated and then treated with 3% hydrogen peroxide to block endogenous peroxidase activity. Antigen retrieval was performed using a methanol-NaOH based solution for 30 minutes at room temperature (DeCal Retrieval Solution, Biogenex, San Ramon, CA). Before addition of primary antibodies, non-specific tissue binding was blocked by incubating tissue sections in 10 percent rabbit serum in PBS for 30 minutes at room temperature. Sections were incubated with rabbit anti-mouse cleaved caspase-3 primary antibody (#9661, Cell Signaling Technologies, Danvers MA) at 1:50 dilution in Antibody Diluent (DakoCytomation, Carpinteria, CA) to identify cells undergoing apoptosis. Sections were incubated in primary antibody overnight at 4˚C in a humidified chamber. Detection was performed using a goat anti-rabbit secondary antibody labeled with a Horseradish Peroxidase conjugate and developed with a DAB substrate chromogen system (DakoCytomation, Carpinteria, CA) ; fast-green was used as a counterstain. Optimal dilution for the primary antibody was determined using internal positive control tissues (growth plate) that were treated in identifcal fashion to experimental bone

samples. For negative staining controls, immunostaining was performed with normal sera instead of primary antibody.

Measurement of osteocyte apoptosis

Apoptotic (caspase-positive) and non-apoptotic (caspase-negative) osteocytes were counted under brightfield microscopy at 400X magnification using a 10mm x 10mm eyepiece grid reticule [*Figure 2.1*]. Caspase+ osteocytes were counted through the entire cortical width for each of eight sampling regions around the bone cross section. Each sampling region was further divided into 10 equal area sub-regions extending from the periosteal to the endosteal surface. Numbers of caspase-positive and negative osteocytes were determined, and osteocyte apoptosis was expressed both as a percentage of total cells in the regions of interest.

Figure 2.1: Data collection schematic for spatial distribution of osteocyte apoptosis around the femoral mid-shaft. A: anterior, P: posterior, L: lateral, M: medial. Four sampling axes were established. Two axes corresponded to the principal anatomic axes of the tissue (antero-posterior and medio-lateral) and the two axes were rotated by 45 degrees (AM, AL, etc). Grids (only the posterior segment is shown) were established parallel and perpendicular to the sampling axes, bordered by the endosteal and periosteal surfaces.

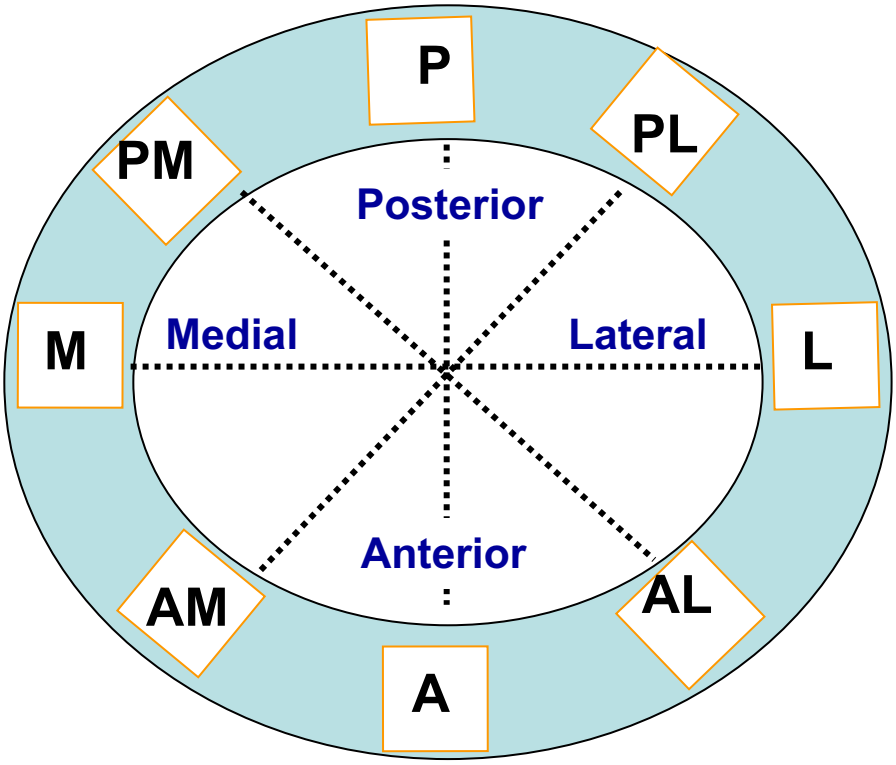

To quantify osteocyte apoptosis in trabecular bone of the distal femur, photomicrograph images were taken from 9 distinct regions of trabecular bone using bright field microscopy at 400X magnification. Images were then imported into Adobe Photoshop [Adobe Systems, San Jose, CA] where Casp+ and Casp- Ot. were identified, counted, and labeled [*Figure 2.2*]. Resorption surfaces were also identified and labeled. Subsequently, a grid of fixed area (80 μm x 80 μm total area with each box 10 μm x 10

μm) was overlaid onto the image in such a way that the x-axis was flush against the resorption surface. The grid allowed for the accurate measurement of both the x and y distance between Casp+ Ot and resorption surfaces, as well as length of resorption surface itself. Recorded osteocyte presence was within 20 μm of the resorption surface center in both the positive and negative x-direction, and less than or equal to 40 μm down from the surface in the y-direction. This area is consistent with the size of a typical bone remodeling unit (hemiosteon). Measurements taken included: Casp+ Ot. (%), Resorption surface length (μm), bone Volume Fraction (%), and spatial distribution mapping of Casp+ Ot.

Figure 2.2: Photomicrograph of data collection schematic for metaphyseal trabecular bone of murine distal right femur.

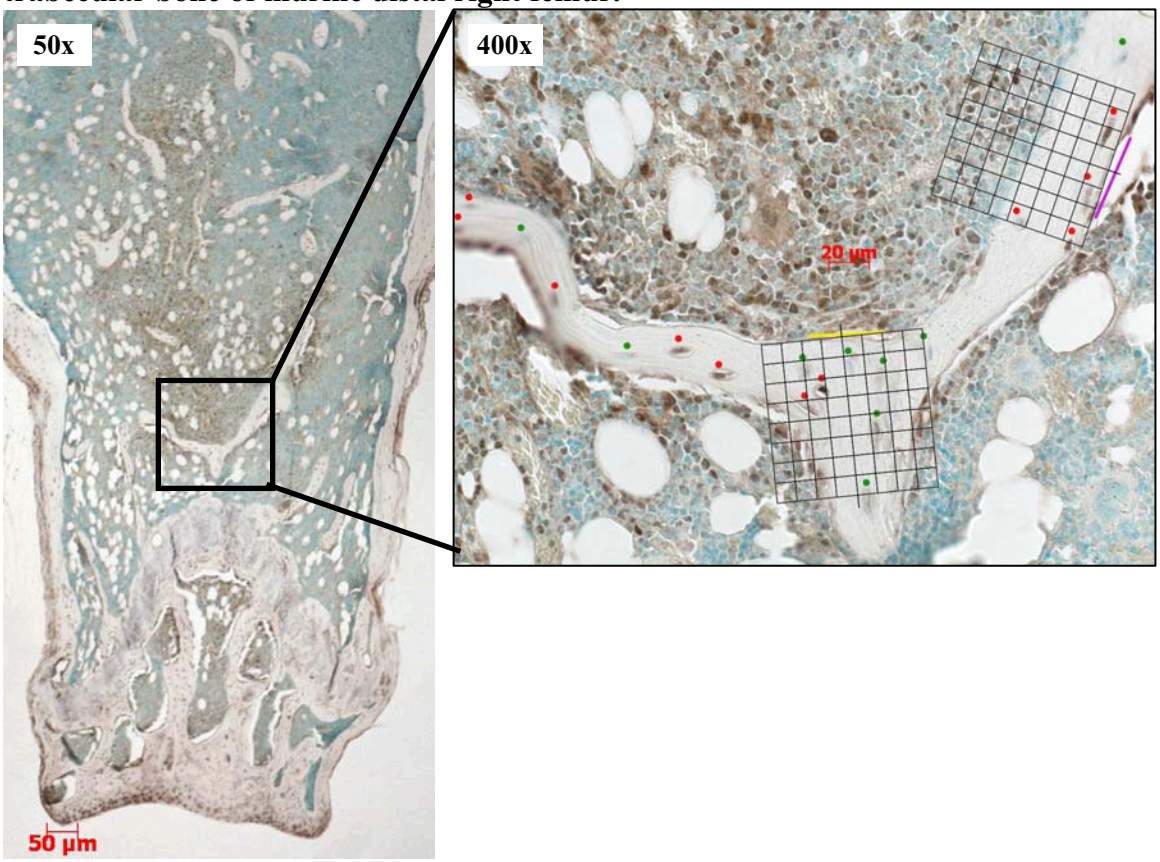

Bone Histomorphometry

Histomorphometry was performed using OsteoMeasure (Osteometrics, Atlanta, GA, USA) connected to a Zeiss Axioskop microscope. Static indices included total periosteal area (T.Ar; mm^2), marrow area (Ma.Ar; mm^2), cortical bone area (Ct.Ar = T.Ar – Ma.Ar; mm^2), and cortical width (Ct Wi; μm). Bone resorption was assessed by eroded surface (Er.Pm/B.Pm; %); bone formation indices were assessed by labeled surface (L.Pm/B.Pm; %), and bone formation rate (BFR/B.Pm; μm/day x 100) on both periosteal and endosteal surfaces using an OsteoMeasure system (Osteometrics, Atlanta, GA, USA) connected to a Zeiss Axioskop microscope.

Confocal Microscopy

Undecalcified sections were viewed using a confocal laser scanning microscope (TCS, Leica Microsystems, Wetzlar, Germany) to examine micro-architectural and morphological differences that were present between osteocytes in the regions of high and low apoptosis. A 63X magnification oil immersion objective lens with 514 nm wavelength excitation was used to view fluorescent Villanueva staining [6]. Each image used for measurement was formed by stacking 10 sequential images taken at 0.5 μm intervals in order to recreate a comparable thickness to histology slides. Images were collected for the posterior region (area of high apoptosis) and anterior medial region (area of low apoptosis), and imported into Adobe Photoshop where a calculated ROI was taken from each image to normalize the data collection area. All images were then imported into quantitative image software (IMAQ Vision Builder; National Instruments, Austin

TX) with optimized threshold settings and counted for number of lacunae and canaliculi, lacunae perimeter and area.

Statistical Analysis

Differences in the Caspase+ osteocyte numbers over time were tested using one-way ANOVA and repeated separately for each time point examined. Differences in osteocyte apoptosis between OVX and sham at each site were tested using the Mann-Whitney test. A regression ANOVA was used to assess the change in osteocyte apoptosis over time, starting after the spike seen post-OVX. Differences in apoptotic activity and bone resorption activity in trabecular bone were tested using Mann-Whitney Comparison Test. Results were expressed as mean ± SD for each group. Analyses for all statistical analyses and performed using the Graphpad Prism 3.0 software program [GraphPad Software, San Diego, CA].

RESULTS

General Changes after OVX

Ovariectomy resulted in an 85 percent decrease in uterine weight by 3 weeks ($p < 0.001$) confirming successful estrogen loss in all ovariectomized mice (data not shown). By 3 weeks post-OVX, there was a 23 percent increase in body weight and a 2-fold increase in gonadal fat relative to age-and weight-matched sham controls ($p < 0.005$).

Osteocyte apoptosis post-OVX

Ovariectomy caused an approximate 2-fold overall increase in osteocyte apoptosis within the femoral cortex (226.3% increase; $p < 0.01$). However, this increase in apoptosis was not uniformly distributed around the diaphyseal cortex. Rather, increases in Casp+ osteocytes were confined almost exclusively to the posterior regions of the diaphyseal cortex [*Figure 2.3*].

Figure 2.3: Image of (A) a Caspase-positive osteocytes and (B) a caspase-negative osteocytes within the endocortical region of the cortical mid-diaphysis of murine femur, 400X magnification.

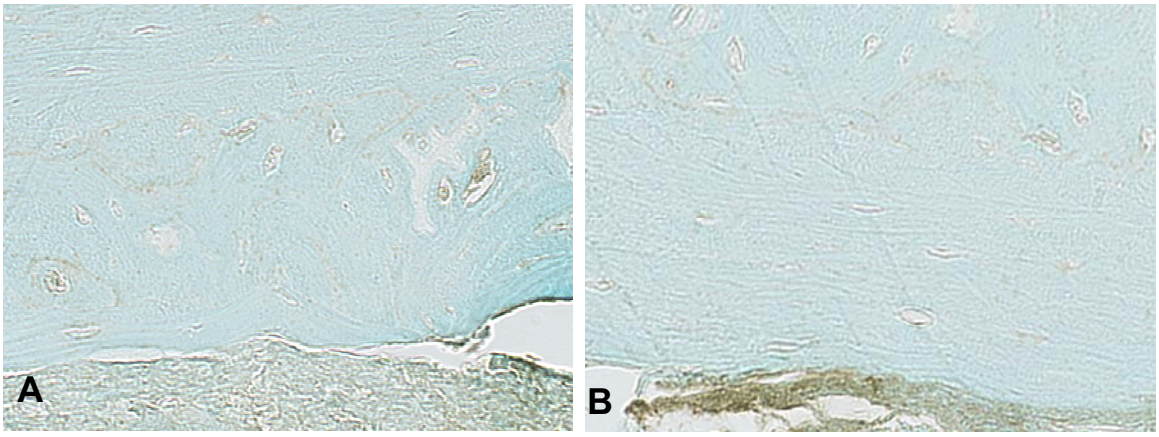

In these areas, apoptotic osteocyte numbers were 500-800 percent higher than in the comparable bone regions of sham controls [*Figure 2.4;* $p<0.005$]. A thin region (within ~50 μm of the periosteal surface) containing apoptotic osteocytes was observed in the immediate periosteal sub-region of the anterior lateral (AL) cortex, but this did not significantly alter the mean for the AL sampling region ($p > 0.20$). Within the posterior cortical regions osteocyte apoptosis was concentrated in the inner one-third to one-half of the cortex.

Figure 2.4: Distribution of apoptotic osteocytes around the femoral mid-shaft 7 days post-ovariectomy (#p<0.02; *p<0.01). There was a significantly elevated amount of apoptotic osteocytes in the posterior regions of the femoral cortex (PM, P, PL).

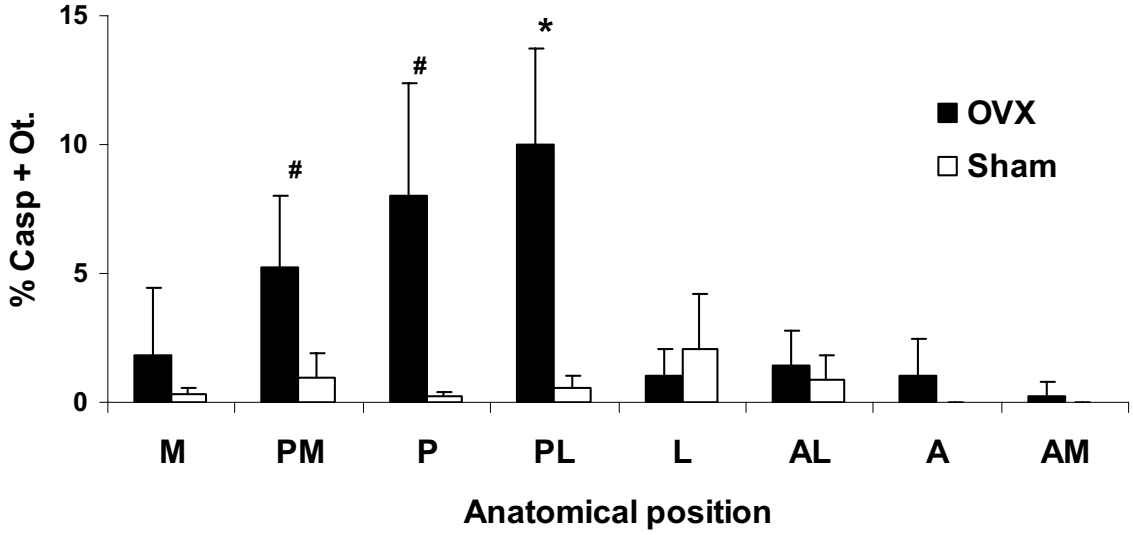

The distribution of osteocyte apoptosis around the femoral cortex was similar at all experimental time points (data not shown). Osteocyte apoptosis post-OVX in the posterior femoral cortex was dramatically increased after day 1, and decreased slowly thereafter (linear regression analysis between days 1 and 21; $p < 0.16$). However, even at 21 days post-OVX, osteocyte apoptosis had not returned to control levels [*Figure 2.5;* $p < 0.01$].

Figure 2.5: Osteocyte apoptosis over time for posterior region. Osteocyte apoptosis was significantly increased (*p < 0.005; ** p <0.01) when compared to the sham after the first day post-ovariectomy and remained elevated over the experimental time periods (linear regression analysis between days 1 and 21 OVX slope = -0.2 ± 0.1, p < 0.16).

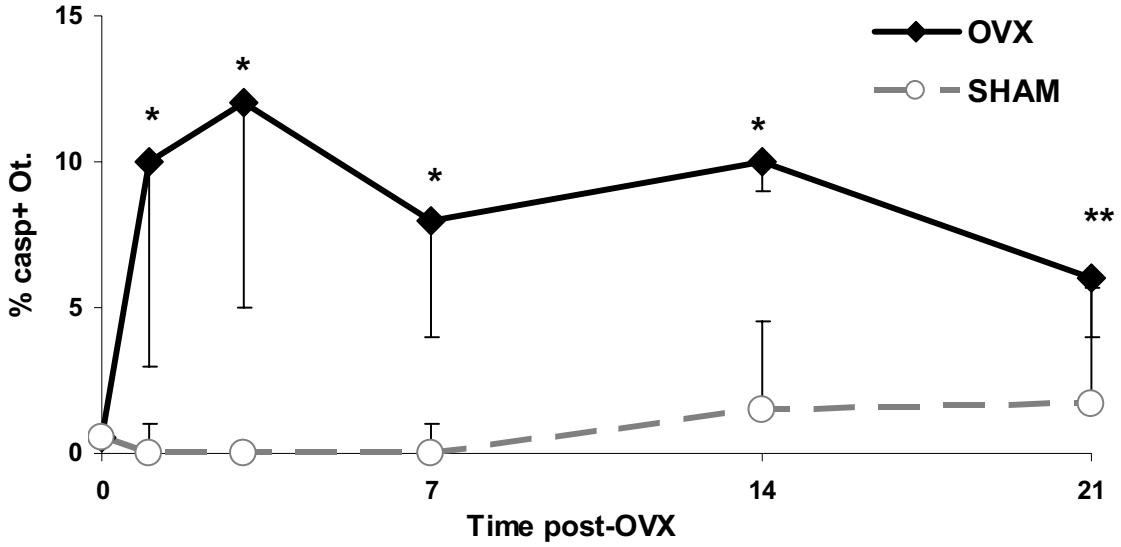

Overall osteocyte apoptosis in metaphyseal trabecular bone of the distal femur was significantly elevated at 3 days post-OVX and remained elevated compared to the sham for the experimental period [*Figure 2.6*].

Figure 2.6: Ostocyte apoptosis in metaphyseal trabecular bone over time (* p <0.01). Ostoecyte apoptosis was significantly elevated at 3 days post-OVX and remained elevated compared to sham.

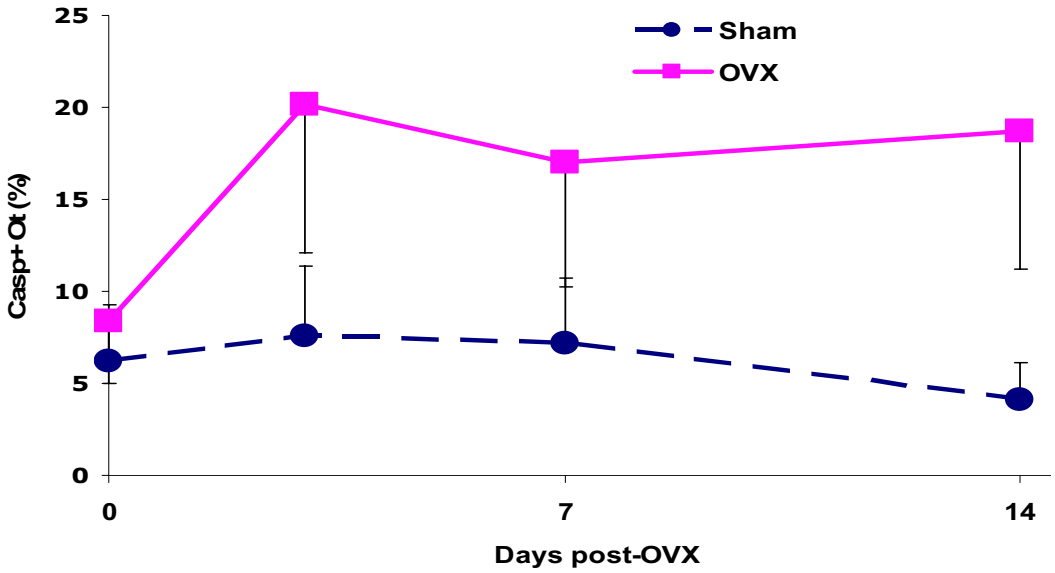

Endocortical resorption post-OVX

Increases in endocortical resorption over baseline were not seen until 7 days post-OVX and were not elevated significantly until 14 days after OVX ($p < 0.004$). Both of these time points were well after the post-OVX induced increases in osteocyte apoptosis [*Figure 2.7*]. All endocortical resorption post-OVX occurred solely at surfaces adjacent to the regions of osteocyte apoptosis.

Figure 2.7: Endocortical resorption after ovariectomy (*p < 0.004). A resorption differential when compared to the sham was first exhibited after 14 days post-ovariectomy.

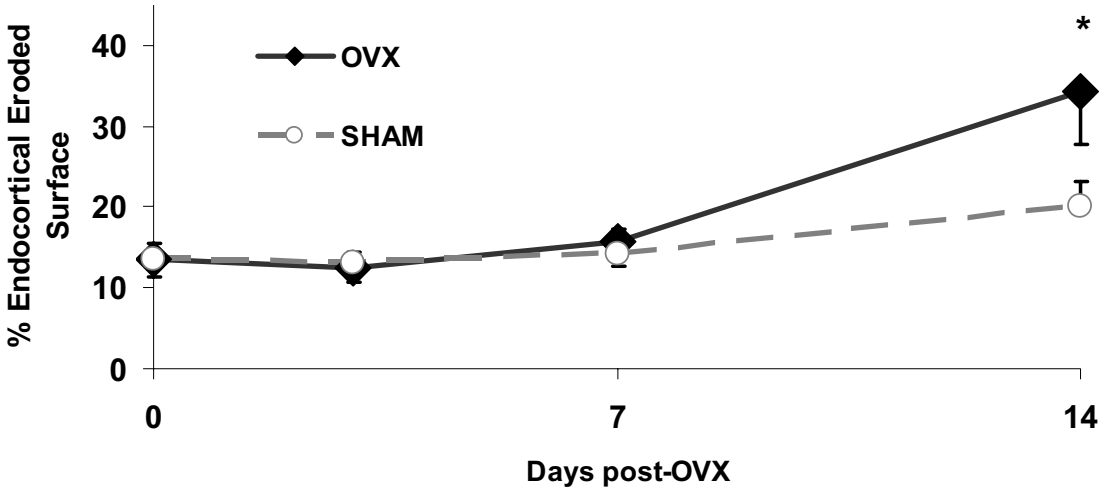

Resorption surface lengths in trabecular metaphyseal bone were identical to control at 3 days and were significantly elevated at 7 and 14 days post-OVX [*Figure 2.8*]. This indicates that elevated apoptosis seen by 3d post-OVX [*Figure 2.6*] preceded onset of resorption in trabecular bone. Osteocyte apoptosis was dramatically elevated above that seen near quiescent sites, regardless of hormonal status [*Table 2.1*]. The early time point indicates that there was no difference between OVX and SHAM, but shows that areas of resorption, regardless of stimulus, have elevated apoptosis.

Figure 2.8: Trabecular bone resorption surface length over time. Resorption surface lengths were identical to control at 3 days, and then significantly elevated at 7 and 14 days (*p < 0.005).

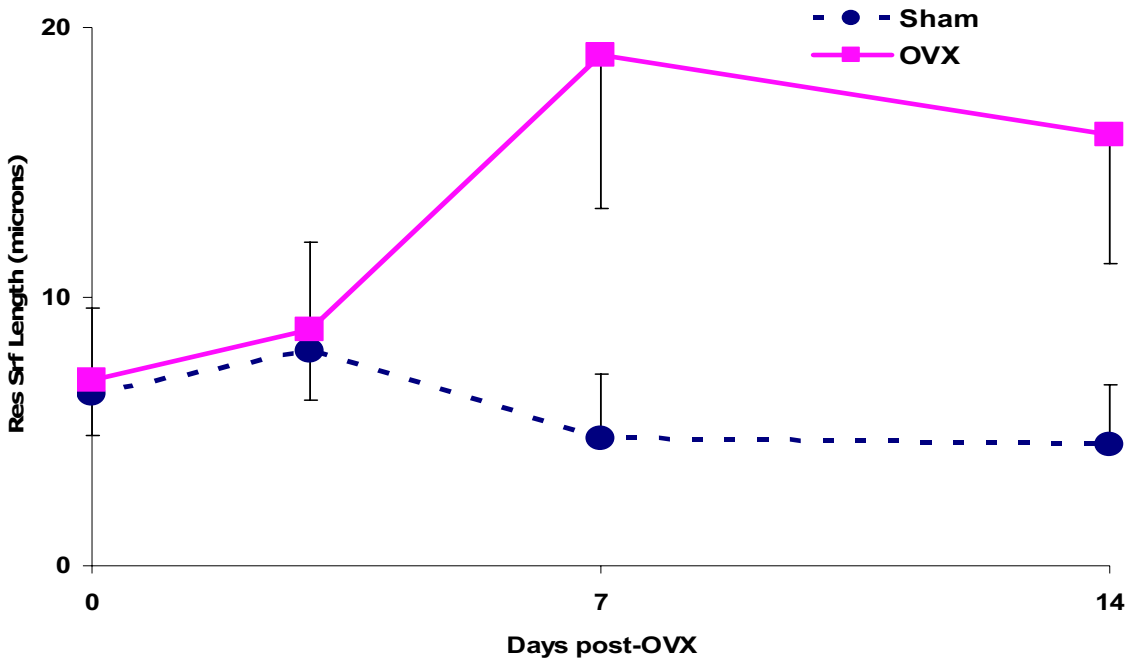

Table 2.1: Apoptotic Ot (%) at bone surrounding Resorption and Quiescent Sites 3 days post-surgery (*p< 0.002 R vs Q).

Site	OVX	SHAM
Resorption	42.60*	44.00*
Quiescent	8.87	7.83

Confocal Microscopy

Confocal microscopy images revealed morphological and micro-environmental differences between areas of high and low apoptosis. The posterior regions that have increased apoptosis are structurally distinct, comprised largely of compacted cancellous

bone, whereas the anterior regions of the transverse cortical sections that exhibit low amounts of apoptosis are comprised of lamellar bone tissue [*Figure 2.9*]. Measurements of morphological features within the different regions of cortical bone indicate a significant difference in canalicular density between compacted cancellous and lamellar bone tissue, with compacted cancellous bone having slightly more osteocytes and significantly less canaliculi ($p<0.0005$) than the lamellar bone regions [*Table 2.2*].

Figure 2.9: Photomicrographs of Compacted Cancellous (CC) and Lamellar (L) bone regions within the mid-diaphyseal femoral cortex.

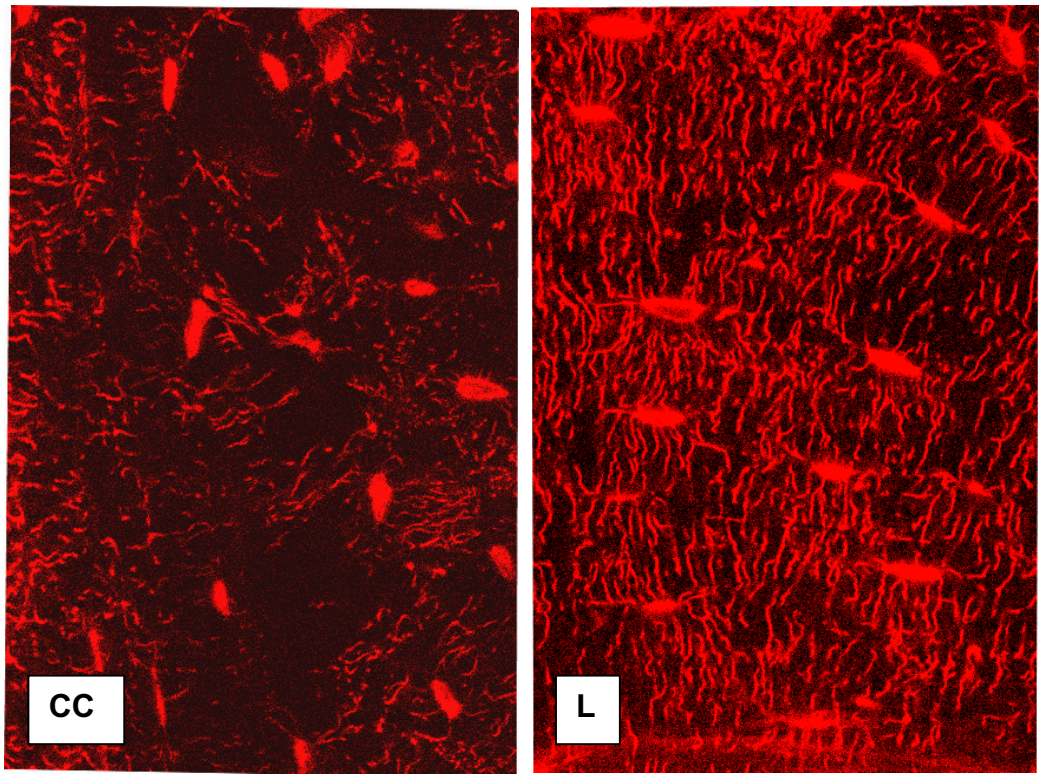

Table 2.2: Measurements (±SD) of morphological features of lacunar-canalicular system within regions of cortical bone indicate a significant difference in canalicular density between CC and L .p < 0.0005 for t-test canalicular density. Parameters are as follows: Oc. Den = osteocyte density (ROI), Can. Den = # canaliculi/um2 (ROI), d = canalicular length (1/sqrt Oc Den).**

Tissue Type	Oc. Den	Can. Den**	d
	#/mm2	#/um2	um
Compacted Cancellous (CC)	652 *(170)*	0.183 *(0.03)*	39.17 *(76)*
Lamellar (L)	593 *(102)*	0.216 *(0.04)*	41.08 *(98)*

DISCUSSION

The current study demonstrates that following estrogen loss, osteocyte apoptosis in cortical bone occurs at specific regions, rather than uniformly throughout the cortex. Moreover, these areas of increased apoptosis occur within cortical regions that subsequently will be resorbed after OVX [66]. Increased osteocyte apoptosis in these areas was evident within days after estrogen loss, while increases in resorption were evident only 1-2 weeks after estrogen withdrawal. Thus, the results demonstrate that osteocyte apoptosis after estrogen withdrawal precedes resorption.

The current studies reveal that osteocyte apoptosis in response to estrogen depletion occurs in discrete regions of the bone, and these regions are the ones that undergo resorption after OVX in mouse femoral diaphyses. This spatial and temporal relationship between osteocyte apoptosis and resorption after estrogen loss correspond exactly to the spatial and temporal coupling of microdamage to osteocyte apoptosis and resorption. Previous studies have shown apoptosis after estrogen withdrawal but did not

examine the microstructural location of this cell death or its relationship to the subsequent activation of bone resorption [123; 124]. Their findings demonstrated that estrogen deficiency leads to a higher prevalence of apoptotic osteocytes, and clarified the role of estrogen in the maintenance of osteocyte viability, yet lacked a direct correlation between osteocyte apoptosis and onset of bone resorption.

Parfitt (1994) argued that bone remodeling could be either a 'stochastic' or 'targeted' process [94]. Targeted remodeling occurs when a microscopic region of bone is focally damaged or has otherwise outlived its functional lifespan. This region would be resorbed and replaced by a bone multicellular unit (BMU) that is "targeted" towards that region. Targeted remodeling to repair microdamage in bone was originally proposed by Frost (1960), and confirmed subsequently in numerous experimental studies where damage is created by fatigue loading in animal models [14; 34; 49]. In these studies, the increase in new remodeling response occurs subsequent to the generation of microdamage, thereby supporting a direct relationship between the initiation of microdamage and local activation of repair. Further, these studies point to osteocyte injury around bone microdamage as the "target" focus for osteoclastic resorption. Bentolila et al found intracortical resorption surfaces occurring in regions of atypical osteocyte morphology following fatigue loading [6]. Verborgt et al previously demonstrated that osteocytes undergo apoptosis in bone areas immediately surrounding bone microdamage, and this apoptosis precedes and then co-localizes precisely with the location subsequent to bone resorption [126; 127]. Using a rat ulnar loading model, they defined a spatial association between microcracks, osteocyte apoptosis, and new remodeling sites. Recent apoptosis inhibition studies by Cardoso et al demonstrated that

osteocyte apoptosis plays a direct and controlling role in the activation and targeting of a microdamage remodeling response [17; 18]].

In contrast to targeted remodeling, stochastic remodeling occurs without any identifiable tissue focus or target for resorption of the tissue, as demonstrated in the generalized resorption increases seen after estrogen loss, glucocorticoid treatment and disuse [1; 41; 75; 76]. However, our current studies in cortical bone reveal that osteocyte apoptosis after estrogen loss occurs in a preferential (non-random) manner. Moreover, this activation is highly consistent in its distribution and co-localizes with areas that will undergo resorption, thus demonstrating that there is a temporal and spatial coupling between osteocyte apoptosis and bone resorption after estrogen loss which resembles that seen in targeted repair of bone microdamage. Although largely considered to be stochastic response, these data show that osteocyte apoptosis after estrogen deficiency is orchestrating a targeted remodeling process.

The current studies were first performed in murine femoral cortical bone, where the straightforward tubular diaphyses present several distinct advantages in testing the relationship between osteocyte apoptosis and the bone remodeling response. The femoral cortex location gives a discrete and highly consistent anatomical location to study the spatial distribution of apoptosis. Although estrogen deficient bone loss has largely been characterized in trabecular bone, our cortical based model first utilized the same biology and surface-dependent phenomenon previously shown in cancellous bone [35; 77; 93; 110; 128]. Given that we established the relationship using a cortical bone model, our next studies examined whether these same spatial couplings exist in cancellous bone as well. The results of the trabecular bone study showed the exact relationship: estrogen

loss leads to an increase in the osteocyte apoptosis in cancellous bone. Moreover, this increase in osteocyte apoptosis precedes the increase in bone resorption caused by estrogen loss. Finally, this increase in osteocyte apoptosis following estrogen loss occurs focally, rather than uniformly throughout the cancellous bone, with apoptosis concentrated ultimately at resorption sites. This similar spatial and temporal coupling between osteocyte apoptosis and bone resorption in cancellous bone post-OVX argues that osteocyte apoptosis is a universal role in the local regulation of bone remodeling, regardless of bone tissue types.

Confocal images taken in the regions of bone expressing increased apoptosis led us to the discovery that these cells are residing in bone that is structurally distinct; it is comprised largely of compacted cancellous bone rather than the lamellar bone [*Figure 2.9*]. It remains obscure why osteocytes in this region of the bone are preferentially affected by estrogen withdrawal. Temporal growth and development images of calcein-labeled (labels mineralization front) transverse mid-diaphyseal mouse femurs reveal that the posterior region, where osteocyte apoptosis concentrates after OVX, is the oldest tissue and thus the oldest osteocytes of the mouse femoral cortex [100]. Since the regions of increased apoptosis correspond to the oldest areas of the femoral cortex, it seems reasonable to speculate that the older osteocytes also have more cumulative stress (oxidative, DNA damage, etc), and are therefore more at risk when the protective effect of estrogen is removed. Estrogen is well established as an antioxidant with its regulation of glutathione and thioredoxin pathways [71]. Loss of estrogen has been shown to accelerate the effects of aging on bone by decreasing defense against reactive oxygen species (ROS) with its reduced ability to regulate the cells' antioxidant defense. The

osteocytes in oldest tissue appear to be inherently more primed for apoptosis because of their age, therefore removal of estrogen leads to the removal of the protective effect against oxidative damage [2; 63]. Previous studies done in our lab demonstrated that solute transport is also reduced with age via impaired lacunar properties (density, surface area, volume) [139]. These age- and microenviroment-related differences could influence the way osteocytes within certain regions of bone respond differently to estrogen deprivation, and will be discussed extensively in Chapter 4 of this dissertation.

The issue of how osteocyte signaling directs osteoclast resorption is unclear. It is much more evident is that once osteoclasts which are one of the professional phagocytic cell lineage (macrophages), encounter apoptotic debris, they likely participate in the removal process. In other cell types which undergo apoptosis, molecular signals are generated in order to identify them as targets for phagocytic elimination by neighboring cells [42; 107; 116]. In bone, osteoclast recruitment from the neighboring bone marrow and the onset of resorption may depend on signals from apoptotic osteocytes as well as signals produced by surviving osteocytes near sites of apoptosis. Because of the mid-cortex apoptotic pattern in our model, and the manner of endocortical surface remodeling, it is possible that there is an intervening zone of viable osteocytes that receive apoptotic diffusing signals and relay those to the bone lining cells and/or osteoclasts. The directed response may either be from the dying cells directly, or paracrine signaling of the osteocytes to their neighboring cells that initiates the osteoclast attraction. Other investigators have argued that the loss of osteocytes has lead to loss of inhibition activity, suggesting an alternative relationship that might explain the targeting of osteoclasts to the areas of resorption [11; 120]. More recently, apoptosis was confirmed to be a necessary

and controlling step in the initiation of bone resorption, giving evidence that inhibiting fatigue-induced osteocyte apoptosis with a pan-caspase inhibitor prevented activation of osteoclast resorption [17; 18]. Therefore, osteocytes and the onset of apoptosis are proving to be a key relation to the signaling mechanisms that osteoclasts use to direct their resorptive response to site-specific areas of bone for removal.

In summary, we have demonstrated that estrogen withdrawal by ovariectomy promotes osteocyte apoptosis in cortical bone immediately post-OVX and remains elevated over time. The elevated apoptosis was increased in regions that will undergo resorption, and precedes the increase in resorption. Moreover, this temporal and spatial coupling between osteocyte apoptosis and bone resorption after estrogen loss strongly resembles that seen in targeted repair of bone microdamage, and is a consistent relationship in both cortical and cancellous bone. This apoptosis is found in a non-uniform distribution that is anatomically consistent throughout the femoral mid-diaphyseal cortex, as well as within 20 μm of resorption sites in trabecular bone. Our results indicate that not all osteocytes within cortical and cancellous bone are at equal risk for apoptosis after estrogen loss. The regions of elevated apoptosis are found almost solely within compacted cancellous bone or the oldest type of bone tissue in cortical bone. The data suggest that dying osteocytes, irrespective of the cause in cortical or cancellous bone, become targets for osteoclast recruitment and resorption. Thus, osteocyte apoptosis may represent a common pathway for activating and targeting bone resorption in response to diverse stimuli.

ACKNOWLEDGEMENTS

This work was supported by grants AR41210 from NIAMS. We thank Damien Laudier for assistance with specimen preparation, and Dr. Shoshanna Yakar and Dr. Brad Herman for their helpful discussions. Thanks to Bin Hu, M.D. and Adrian Woo, who were my initial mouse ovariectomy team, and were a tremendous help in facilitating 50 successful surgeries. Also, special thanks to Joe Pinero and Alex Sinofsky who did the data collection for the trabecular bone and cortical bone histomorphometry, respectively. They were a constant source of help and comic relief for the three months that I worked with them.

CHAPTER 3

INHIBITION OF OSTEOCYTE APOPTOSIS PREVENTS ACTIVATION OF BONE REMODELING IN CORTICAL BONE AFTER ESTROGEN WITHDRAWAL.

ABSTRACT

Introduction: Osteocyte apoptosis is spatially and temporally linked to estrogen-deficiency induced endocortical remodeling, but mechanistic relationships among these events have not been established. Here we report that osteocyte apoptosis is necessary to initiate endocortical remodeling in response to estrogen withdrawal.

Materials and Methods: Adult female C57BL/6J mice (17 weeks old) underwent either bilateral ovariectomy (OVX) to activate bone resorption, or sham surgery (SHAM). To test whether osteocyte apoptosis plays a regulatory role in the initiation of bone resorption after estrogen loss, one group of OVX mice received the pan-caspase inhibitor, QVD-OPh (MP Biomedicals, Livermore, CA, 20mg/kg/day) to inhibit osteocyte apoptosis (OVX+QVD). Remaining experimental groups received either QVD or DMSO Vehicle as follows: SHAM+QVD, SHAM+Veh, OVX+Veh. Mice were euthanized at 14 days.

Diaphyseal 5μm cross-sections were stained by immunohistochemistry for activated caspase-3 and γH_2AX, markers of caspase-dependent and –independent apoptosis respectively. The percentages of Caspase-positive osteocytes (Casp+ Ot.) in eight tissue quadrants defined by the principal anatomical axes (anterior, posterior, medial, and lateral) were determined using an eyepiece grid reticule at 400X magnification.

Coronal 5 μm sections were cut from paraffin decalcified embeddeddistal femora to obtain metaphyseal trabecular bone sections. Immunohistochemical staining for cleaved caspase-3 was used to examine caspase-dependent apoptosis.

Photomicrograph images were taken in 5 distinct metaphyseal regions, where percentages of Casp+ Ot. were determined using 400X magnification .

Results: Following ovariectomy, apoptosis was increased dramatically (OVX+Veh) by more than 3-fold over control and SHAM levels. Treatment with QVD in OVX animals suppressed this osteocyte apoptosis, with levels in QVD-treated samples equivalent to baseline. Osteoclastic resorption increased only in OVX+Veh animals. QVD treatment completely prevented this OVX-induced increase in osteoclastic activity.

Following OVX, apoptosis in metaphyseal trabecular bone was increased dramatically (OVX+Veh) by more than 2-fold over control and SHAM levels. Treatment with QVD in OVX-animals suppressed this osteocyte apoptosis in trabecular bone as well, with levels in QVD-treated samples equivalent to baseline.

Conclusions: Osteocyte apoptosis is necessary to activate endocortical remodeling, as well as increased cancellous bone resorption, following ovariectomy-induced estrogen withdrawal. Early apoptotic events following estrogen deficiency may largely determine the subsequent course of bone remodeling in both cortical and cancellous bone.

INTRODUCTION

Apoptosis is an active process of programmed cell death that is important during development and in disease [112]. In bone, turnover of cells and matrix occurs during a process called remodeling wherein osteoclastic resorption removes and osteoblastic infilling replaces microscopic regions of bone that have outlived their functional life span [14; 94]. Perhaps the best-characterized example of a region of bone reaching the end of its life occurs after fatigue-induced microdamage. This remodeling of bone occurs in a

non-stochastic and lesion specific manner that has been termed ‘targeted remodeling’ by Parfitt and others [34; 49; 94]. Verborgt and coworkers demonstrated that osteocytes undergo apoptosis in bone areas immediately surrounding bone microdamage, and this apoptosis precedes and then co-localizes precisely with the location subsequent to bone resorption [126; 127]. This correlation between osteocyte apoptosis and targeted remodeling was further demonstrated by Emerton et al who demonstrated that apoptosis via immunohistochemical staining of activated caspase-3 orchestrates the remodeling process after estrogen withdrawal in a spatially and temporally specific manner [30]. This tight spatial and temporal coupling of osteocyte apoptosis to bone microdamage, estrogen withdrawal and directed bone remodeling has led to the hypothesis that osteocyte apoptosis is a key controlling step in the activation and/or targeting of osteoclastic resorption in response. In the current studies we tested this hypothesis in an in vivo ovariectomy model. We employed a broad-spectrum caspase inhibitor to determine if modulation of osteocyte apoptosis in vivo would alter the onset of endocortical bone remodeling in the mid-diaphyseal cortical bone model previously used.

Apoptosis is characterized by a series of distinctive morphological and biochemical changes (DNA laddering, formation of vesicles etc), with mediation by cysteine proteases (caspases) that uniquely cleave substrates specifically. Caspases are synthesized in their inactive form in the cytosol as either dimeric or monomeric [28]. They must undergo proteolysis after the aspartic acid is cleaved to be in its active form for initiation of pathway cascade [80]. The apoptosis process utilizes 3 main pathways; caspase 3/9, caspase 12 (not human), and caspase 8/10 pathways. The former two pathways are activated when cytochrome C is released from the mitochondria into the

cytosol and causes caspase activation. The caspase 8/10 pathway is activated by ligand binding to the death receptors of the TNF-α family. Caspases can be divided into 2 groups based on their functional roles; upstream (caspase 2, 8, 9, 10) are responsible for initiation of caspase activation cascades. Downstream or effector caspases (caspase 3, 6, 7) are responsible for the actual demolition of the cell.

Apoptosis inhibitors work by blocking activation of proteases (such as caspases) into their active form, or by binding to the already active protease. Studies done to compare several inhibitors using actinomyocin D as an apoptosis inducing agent found that an inhibitor called Q-VD-OPh (quinolyl-valyl-O-methylaspartyl-[-2, 6-difluorophenoxy]-methyl ketone) was significantly more effective in preventing apoptosis than others for all three caspase pathways [20]. The reagent is stable in solution, irreversibly binds at the active cysteine site of the caspase and is non-toxic at high doses, even though it was found to be effective at 1/10 lower doses than other inhibitors [20; 96]. The ability to use such low doses eliminates problems associated with vehicle concentrations or non-specificity typically associated with other inhibitors, and also has increased cost effectiveness. Recent apoptosis inhibition studies by Cardoso et al demonstrated that osteocyte apoptosis plays a direct and controlling role in the activation and targeting of a microdamage remodeling response [18]. These inhibitors provide the opportunity to pharmacologically modulate osteocyte apoptosis *in vivo*. In the current studies, we used this *in vivo* inhibitor approach to test whether osteocyte apoptosis plays a controlling role in the activation and targeting of osteoclastic resorption in both cortical and trabecular bone after estrogen withdrawal.

METHODS AND MATERIALS

Animal Model and Procedures

Under IACUC-approval, twenty-four adult female C57BL/6J mice (17 week old, Jackson Laboratory, Bar Harbor, ME) underwent either bilateral surgical ovariectomy (OVX) using a dorsolateral approach under 5% Avertin anesthesia (30 uL/g BW) or sham surgery (SHAM) in which ovaries were exteriorized and replaced in the abdominal cavity. Following surgery, all animals received subcutaneous injections of Buprenex, (0.1 uL/g BW) for analgesia. All animals were weighed at surgery and at sacrifice. In addition, all animals received calcein (10 mg/kg) labels at 4 and 10 days prior to sacrifice in order to assess bone formation sites. Mid-diaphysis femur tissue sections were examined at baseline (0 days) and 14 days after ovariectomy to examine responses of apoptotic osteocytes and their neighboring cells.

In vivo apoptosis inhibition

Apoptosis inhibitors of the caspases have been successfully used in animal models that attenuate cell death and minimize tissue damage following ischemic injury to brain, gut and heart [52; 67; 96; 137]. These inhibitors provide a unique opportunity to pharmacologically modulate osteocyte apoptosis *in vivo*. The apoptosis inbitor chosen for this study was a pan-caspase inhibitor Q-VD-OPh (quinolyl-valyl-O-methylaspartyl-[-2, 6-difluorophenoxy]-methyl ketone; MP Biomedicals, Livermore, CA) and was administered via intraperitoneal injection (IP) twice daily for 2 days prior to surgery in order to acclimatize the animals to the inhibitor. Post-surgery, animals were treated twice daily, 12h apart, for 14d to test whether continuous suppression of osteocyte apoptosis

would alter the activation of endocortical bone resorption in the mid-diaphysis of the femur. Dosages of 20 mg/kg/day of QVD (diluted in DMSO) were administered. Dosing frequency was determined by previous studies to test osteocyte apoptosis suppression after inducing fatigue-loading microdamage [17]. Treatments continued until sacrifice.

To test whether osteocyte apoptosis plays a regulatory role in the initiation of bone resorption after estrogen loss, one group of OVX mice (n=6) received the pan-caspase inhibitor, QVD-OPh to inhibit osteocyte apoptosis (OVX+QVD). Previous studies showed this dosing regimen prevented fatigue-induced osteocyte apoptosis, while other studies had established that pan-caspase inhibitors have no direct effect on osteoclast recruitment or differentiation [17]. Remaining experimental groups (n=6 mice/group) received either QVD or DMSO Vehicle as follows: SHAM+QVD, SHAM+Veh, OVX+Veh. Mice were euthanized 14 days post-OVX to sample the peak resorption period in this model [66].

Tissue Collection and processing

Uteri were harvested and weighed to confirm the effectiveness of ovariectomy. Femora were dissected, cleaned of soft tissue and fixed in 10% neutral buffered formalin for 48 hr at 4˚C. Right femora were decalcified in formic acid solution for 3 days with daily changes [62]. When decalcification was completed, samples were processed and embedded in paraffin. Left femora were processed undecalcified for cortical bone histomorphometry. Bones were cut transversely using a low-speed diamond saw, and both segments bulk-stained with Villanueva. Ground mid-diaphyseal sections (60 μm) were used for histomorphometric analysis.

The distal mid-shaft femur was then reoriented in paraffin, and 5 μm coronal sections were cut and stained for cleaved caspase-3 to indicate caspase-dependent apoptosis in metaphyseal and epiphyseal trabecular bone.

Mid-diaphyseal segments of the contra-lateral femurs were bulk stained in Villanueva stain and then embedded in poly-methyl methacrylate with 15% dibutyl phthalate (Fisher Scientific) as previously described [62; 65]. Cross-sections of mid-diaphyseal segments were cut at 150 micron thickness using a Leica 1600 Sawing Microtome (Leica Instruments, Nussloch, Germany), polished to 30 micron thickness with silicon carbide grinding paper (Buehler, Lake Bluff, IL, USA) and cover-slipped with non-fluorescing mounting medium for standard bone histomorphometric analysis.

Measurement of osteocyte apoptosis

The spatial patterns of osteocyte apoptosis were assessed in mid-diaphyseal femoral cortex by immunohistochemistry for apoptotic factors at 14d post-ovariectomy. This time point was used to sample osteocytes at peak resportion [66]. Mid-diaphyseal cross-sections and distal femur coronal section of the paraffin embedded diaphysis were cut at 5-micron thickness and adhered to positively-charged slides. Sections were deparaffinized, rehydrated and then treated with 3% hydrogen peroxide to block endogenous peroxidase activity. Sections were then pretreated for antigen retrieval for 30 minutes at room temperature with a methanol-NaOH based solution (DeCal Retrieval Solution, Biogenex, San Ramon, CA). Before addition of primary antibodies, non-specific tissue binding was blocked by incubating the tissue sections in 10% titred rabbit serum in PBS for 30 minutes at room temperature. Sections were incubated in primary

antibody overnight at 4°C in a humidified chamber. Cleaved (activated) caspase-3 (#9661, Cell Signaling Technologies, Danvers MA) at dilutions of 1: 50 were used as the marker for osteocyte apoptosis which has been previously demonstrated to occur in response to ovariectomy and fatigue-induced matrix damage [30; 126]. Adjacent sections were also stained with rabbit anti-mouse γH2AX antibody (AB3369, Chemicon, Temecula, CA) at dilutions of 1: 300 to test for caspase-independent apoptotic pathway activation [105]. HRP-labeled polymer (DakoCytomation, Gllostrup, Denmark) was used for secondary detection; toludine blue was used as a counterstain. Optimal dilutions for the primary antibody were determined using internal positive control tissues (growth plate). For negative staining controls, immunostaining was performed with normal sera instead of primary antibody.

Apoptosis Quantification

To quantify osteocyte apoptosis, cells were counted using bright field microscopy at 400X magnification using a 10mm x 10mm eyepiece grid reticule. Previously, we reported that osteocyte apoptosis in mouse cortical bone after OVX is almost exclusively confined to the posterior cortex [30]. Thus, in the current study we observed changes in osteocyte apoptosis within this same posterior region. The selection for sampling regions is based on previous studies that demonstrated increased osteocyte apoptosis in non-lamellar bone tissue found within the posterior axis of transcortical sections, when compared with lamellar bone tissue of the anterior axis. Caspase+ osteocytes were counted through the entire cortical width for each of eight sampling regions around the bone cross section [*Figure 2.2 of Chapter 2*]. Each sampling axis grid was further divided

into 10 equal area sub-regions extending from the periosteal to the endosteal surface. The number of caspase-positive and negative osteocytes, as well as empty osteocyte lacunae per mm^2 of bone was determined and the frequency of osteocyte apoptosis (Casp+ Ot, and γH_2AX+ Ot) was expressed as a percentage of total cells in the region of interest.

To quantify osteocyte apoptosis in trabecular bone of the distal femur, photomicrograph images were taken from 5 distinct regions of metaphyseal trabecular bone using bright field microscopy at 400X magnification. Images were then imported into Photoshop where Casp+ and Casp- Ot. were identified, counted, and labeled [*Figure 3.1*]. Resorption surfaces were also identified and labeled. Subsequently, a grid of fixed area (80 μm x 80 μm total area with each box 10 μm x 10 μm) was overlaid onto the image in such a way that the x-axis was flush against the resorption surface. The grid allowed for the accurate measurement of both the x and y distance between Casp+ Ot and resorption surfaces, as well as length of resorption surface itself. Recorded osteocyte presence was within 20 μm of the resorption surface center in both the positive and negative x-direction, and less than or equal to 40 μm down from the surface in the y-direction. This area is consistent with the size of a typical bone remodeling unit (hemiosteon). Measurements taken included: Casp+ Ot. (%), Resorption surface length (μm), bone Volume Fraction (%), and spatial distribution mapping of Casp+ Ot.

Figure 3.1: Photomicrograph of data collection schematic for metaphyseal trabecular bone of murine distal right femur.

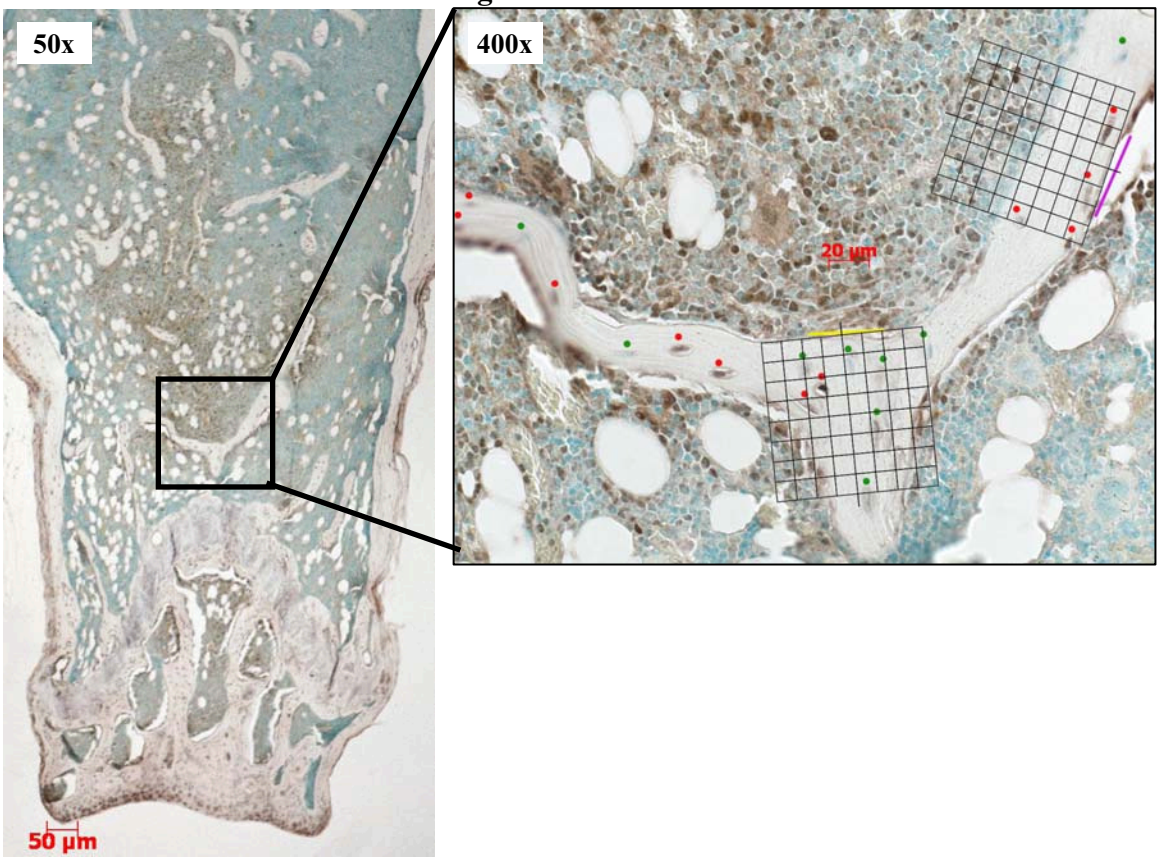

Bone Histomorphometry

Histomorphometry was performed using OsteoMeasure (Osteometrics, Atlanta, GA, USA) connected to a Zeiss Axioskop microscope. Static indices included total periosteal area (T.Ar; mm^2), marrow area (Ma.Ar; mm^2), cortical bone area (Ct.Ar = T.Ar – Ma.Ar; mm^2), and cortical width (Ct Wi; µm). Bone resorption was assessed by eroded surface (Er.Pm/B.Pm; %); bone formation indices were assessed by labeled surface (L.Pm/B.Pm; %), and bone formation rate (BFR/B.Pm; µm/day x 100) on both periosteal and endosteal surfaces.

Statistical Analysis

Differences in the Casp+ Ot, or γH2AX+ Ot among groups were tested using one-way ANOVA with Tukey's Multiple Comparison Test for posthoc testing using the Graphpad Prism 3.0 software program [Graphpad Software, San Diego, CA]. Differences in apoptotic activity and bone resorption activity in trabecular bone were tested using Mann-Whitney Comparison Test. Results were expressed as mean ± SD for each group. Significance was reported at a minimum $p < 0.05$ for all statistical analyses performed.

RESULTS

General Changes after OVX

Ovariectomy resulted in an approximately 80 percent decrease in uterine weight by 14 days ($p< 0.002$) in both OVX+Veh and OVX+QVD groups, confirming successful estrogen loss in all ovariectomized mice and demonstrated that the apoptosis inhibitor did not alter systemic response to estrogen loss (data not shown). By 14 days post-OVX, there was a 4 percent increase in body weight relative to age-and weight-matched sham controls ($p < 0.005$).

Apoptosis Inhibition

Following ovariectomy, osteocyte apoptosis was dramatically increased (OVX+Veh) by more than 3-fold over control and SHAM levels [*Figure 3.2a and Figure 3.2b*]. Treatment with QVD-OPh for 14 days after ovariectomy effectively suppressed osteocyte apoptosis to control levels, with levels in QVD-treated samples equivalent to Control group.

Figure 3.2a: Image of caspase stained osteocytes within the posterior endocortical region of the mid-diaphysis of murine femur, 400X magnification. Scale Bar = 50 microns.

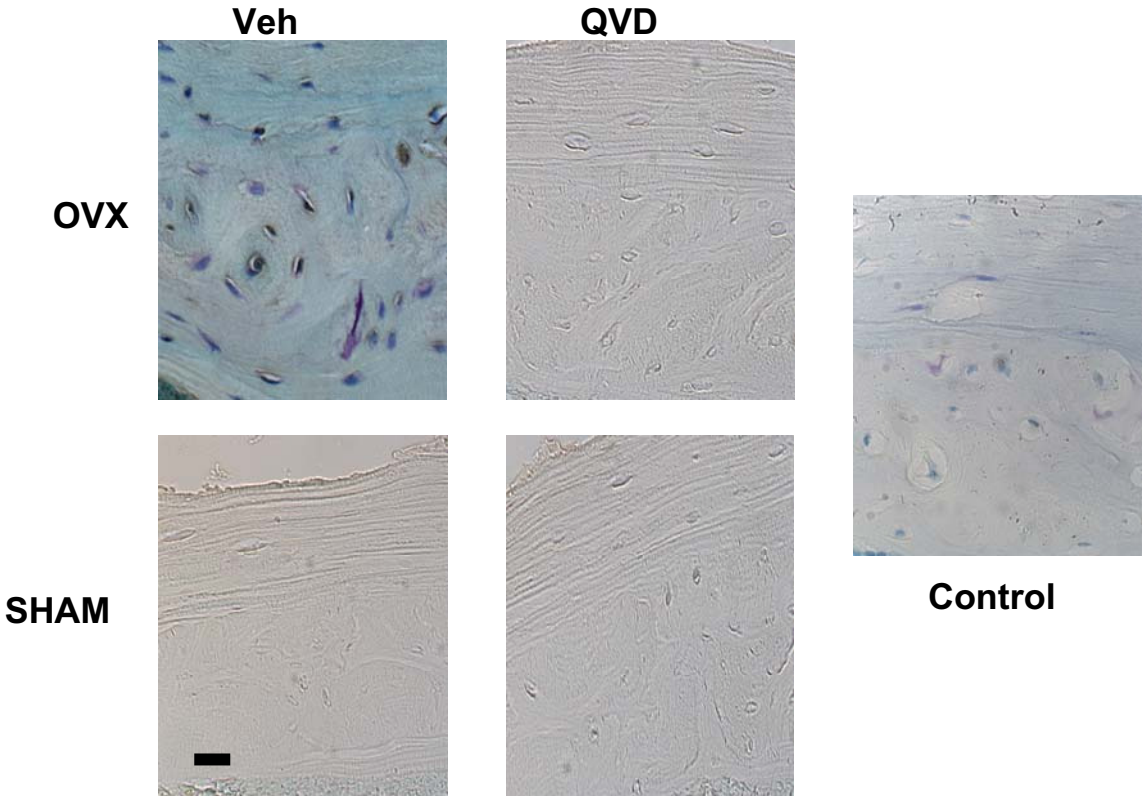

Figure 3.2b: Activated caspase-3 osteocyte apoptosis at 14 days post-OVX with and without apoptosis inhibitor treatment in the posterior (P) region (*p < 0.005). Elevated apoptosis shown in OVX+Veh only.

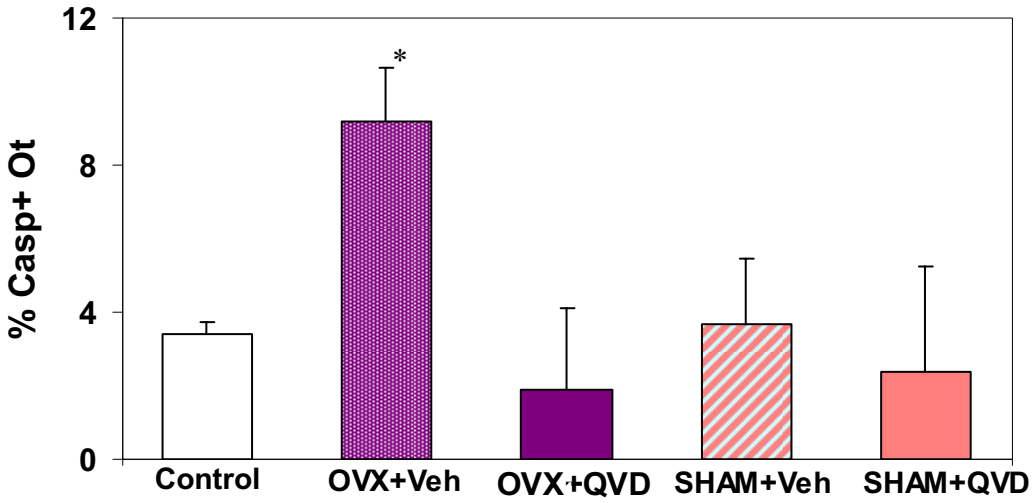

Staining for γH_2AX showed similar results with increases in staining in osteocytes post-OVX, and suppression of this cell death marker in the QVD treated OVX group [*Figure 3.3a and Figure 3.3b*].

Figure 3.3a: Image of γH_2AX stained osteocyte within the posterior endocortical region of the mid-diaphysis of murine femur, 400X magnification. Scale Bar = 50 microns.

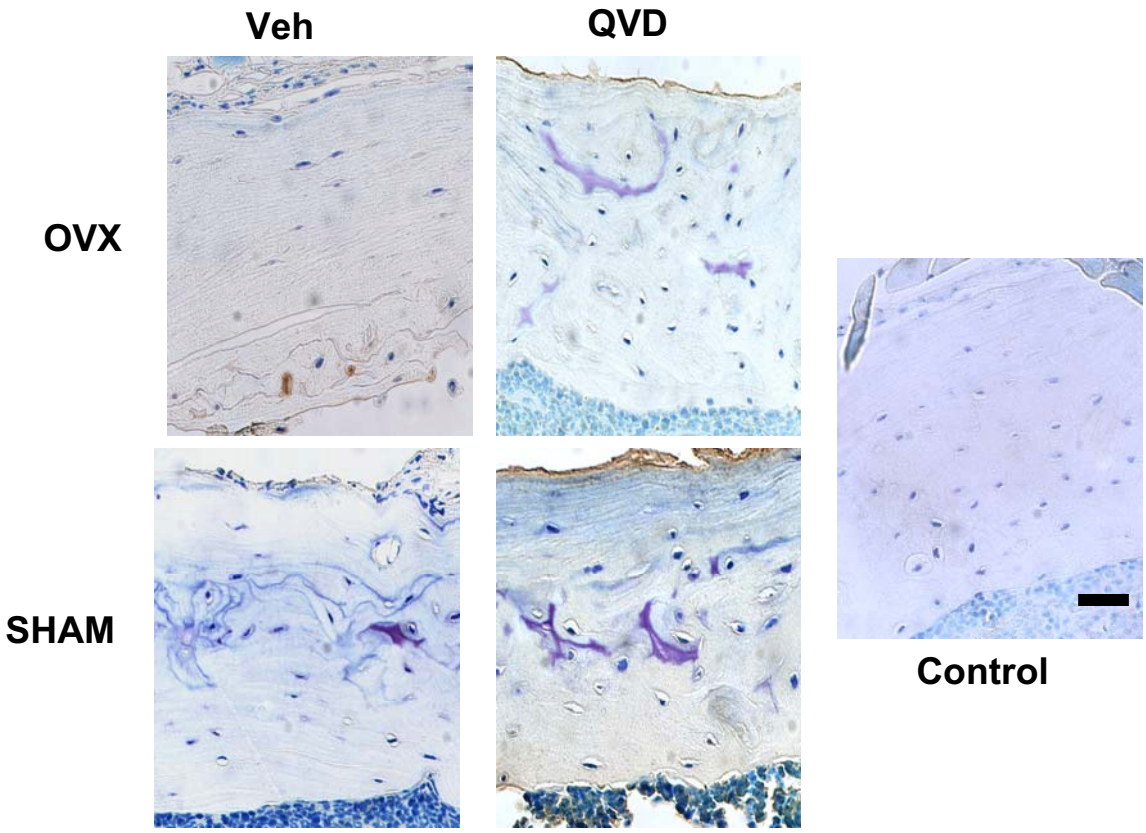

Figure 3.3b: Phosphorylated H_2AX osteocyte apoptosis at 14 days post-OVX with and without apoptosis inhibitor treatment in the posterior (P) region (*p < 0.005). Elevated apoptosis shown in OVX+Veh only.

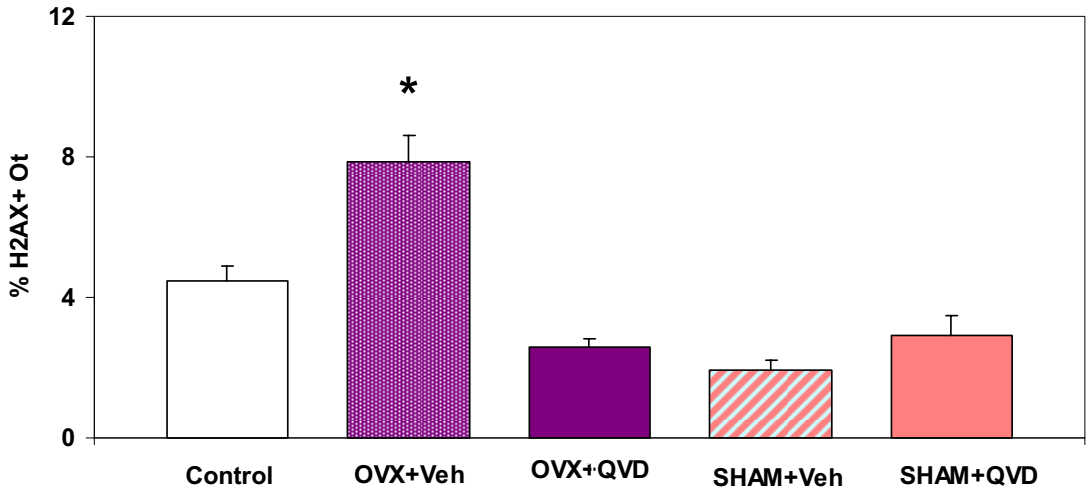

Following ovariectomy, apoptosis was increased dramatically (OVX+Veh) in metaphyseal trabecular bone by more than 2-fold over control and SHAM levels [*Figure 3.4; $p < 0.036$*]. Treatment with QVD in OVX animals suppressed this osteocyte apoptosis, with levels in QVD-treated samples equivalent to baseline.

Figure 3.4: Activated caspase-3 osteocyte apoptosis at 14 days post-OVX with and without apoptosis inhibitor treatment in the metaphyseal trabecular region of distal femur (*p < 0.036). Elevated apoptosis shown in OVX+Veh only.

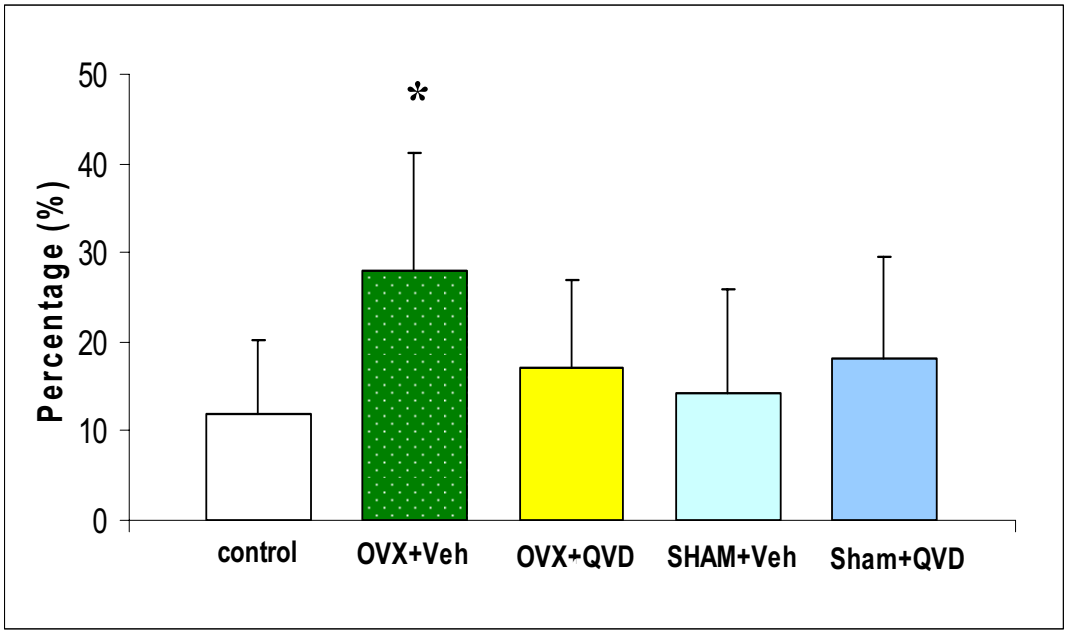

Endocortical resorption post-OVX

Endocortical resorption was activated by estrogen withdrawal, with osteoclastic remodeling increased only in the OVX+Veh animals [*Figure 3.5*]. This endocortical resorption occurred solely at surfaces adjacent to the regions of osteocyte apoptosis. Treatment with QVD completely prevented this OVX-induced increase in osteoclastic activity, with erosion levels consistent with control groups.

Figure 3.5: Endocortical resorption at 14 days post-OVX with and without apoptosis inhibitor treatment in the posterior (P) region (*p < 0.01). Data shows significantly elevated erosion rates in the OVX+Veh only.

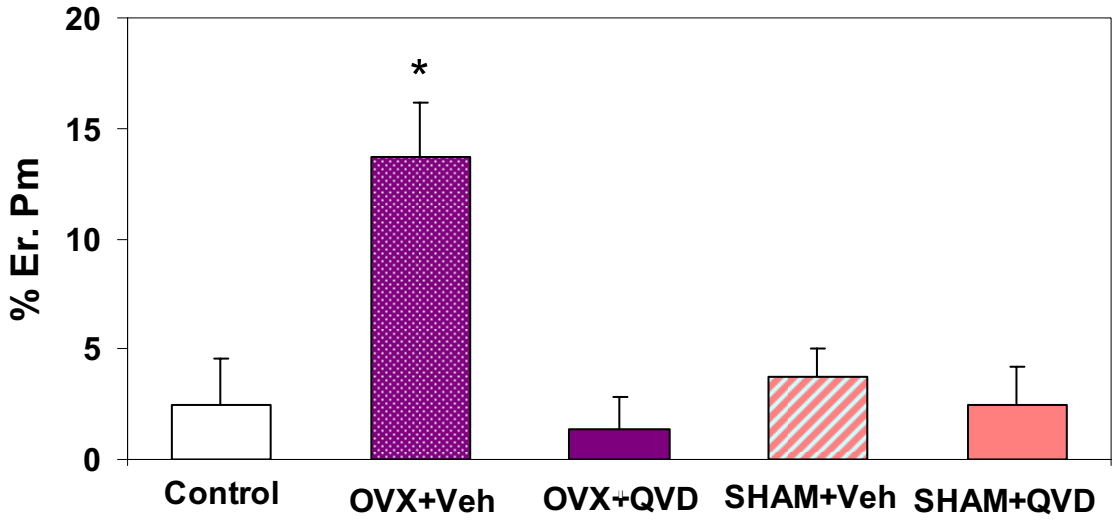

Trabecular resorption post-OVX

Osteoclastic resorption surface was increased in OVX+Veh animals [*Figure 3.6; p <0.012*]. QVD treatment completely prevented OVX-induced increases in osteoclastic activity for metaphyseal trabecular bone.

Figure 3.6: Resorption surface length in microns at 14 days post-OVX with and without apoptosis inhibitor treatment in the metaphyseal trabecular region of distal femur (*p < 0.012). Data shows significantly elevated erosion rates in the OVX+Veh only.

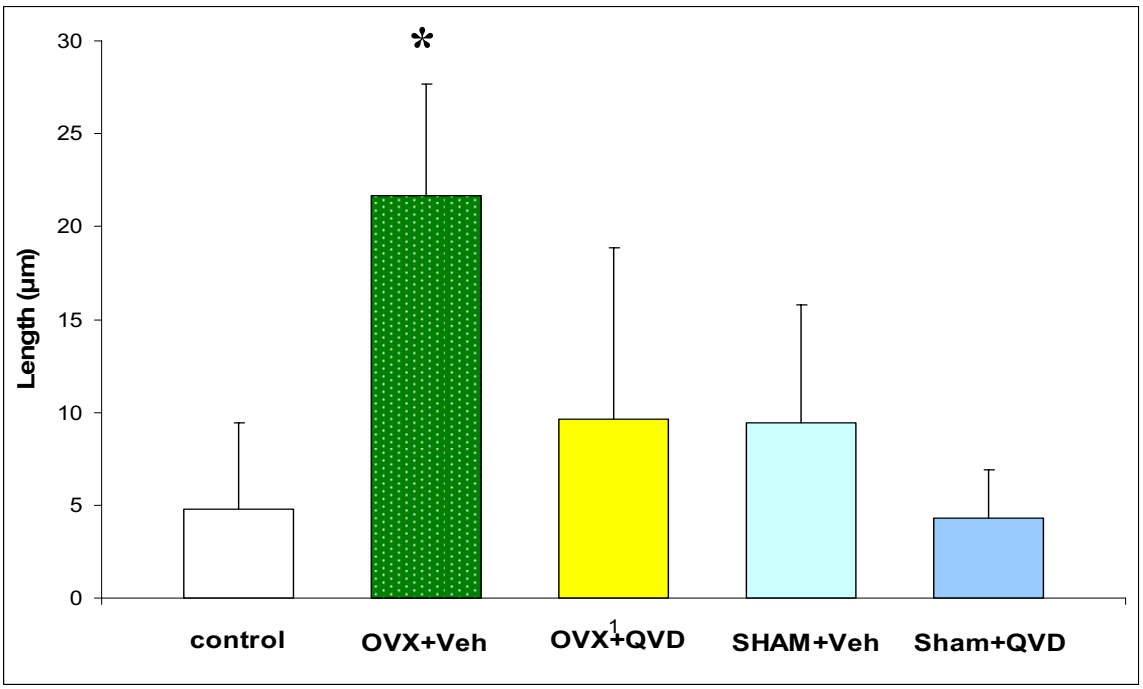

DISCUSSION

In the current studies, we utilized a novel systemically active caspase inhibitor, QVD, against apoptosis induced by ovariectomy. We examined the effects of QVD specifically because it is a new generation broad-spectrum caspase inhibitor that offers improvements in stability and toxicity over other benchmarked caspase inhibitors [20; 137]. It is much more potent than previously used inhibitors, and blocks apoptosis mediated by the three major apoptotic pathways: caspase-9/2, caspase-8/10, and caspase-12.

In the present studies, prevention of osteocyte apoptosis by a pan-caspase inhibitor completely blocked the activation of bone resorption in response to OVX-induced estrogen withdrawal in both cortical bone and cancellous bone. There is previous evidence for apoptotic death as well as activation of caspase-3, the effecter caspase involved in all three caspase pathways, after ovariectomy [30]. Caspases have been used in many studies as an endpoint for apoptotic cell death, therefore presenting a target for pharmacological modulation of apoptosis in our study [67; 112]. Despite the success in minimizing tissue damage, the use of apoptosis inhibitors that lack cell type specificity raises the question of its ability to inhibit resorption directly via osteocyte signaling, or indirectly inhibiting resorption via actions on the differentiation or activity of osteoclasts. Previous *in vitro* experiments in our lab found that formation of TRAP+ multinucleated cells isolated from rat marrow were unaffected by QVD at high concentrations [17]. Since pan-caspase inhibitors do not directly affect osteoclast differentiation or function, the results indicate that osteocyte apoptosis is required to activate osteoclastic resorption subsequent to estrogen loss.

Bone resorption after estrogen loss has been widely considered a stochastic remodeling process since it lacks a defined targeting focus, as previously demonstrated with microdamage. In microdamage, however, the targeting focus for resorption is not the damage itself but rather signals emanating from apoptotic cells and their surviving neighbors near damage sites. Spatial and temporal correlations between bone microdamage, estrogen withdrawal in cortical and cancellous bone, osteocyte apoptosis and bone remodeling led us previously to hypothesize that osteocyte apoptosis is a key controlling factor in the activation and targeting of osteoclastic resorption following

estrogen deficiency. The current studies demonstrate that continuous pharmacological suppression of osteocyte apoptosis using a pan-caspase inhibitor prevented increased cell death and activation of osteoclastic resorption in both cancellous and cortical bone, thereby arguing strongly that osteocyte apoptosis is indeed required to activate bone resorption after estrogen loss regardless of bone tissue type. Since blocking osteocyte apoptosis prevented OVX-induced bone resorption as it previously did for microdamage remodeling, it suggests that both processes are targeted, and that osteocyte apoptosis may initiate a common pathway for activating and targeting resorption in response to diverse stimuli.

Apoptosis plays an important role both in human embryonic development and in adult tissue homeostasis. Apoptosis is the most common mechanism by which the body eliminates damaged or unneeded cells without local inflammation from leakage of cell contents. Apoptosis is activated through two different pathways; extrinsic and intrinsic. The intrinsic pathway is triggered from within the cell by developmental cues or severe cell stress, such as DNA damage. The extrinsic pathway is activated when a pro-apoptotic ligand, such as endogenous Fas ligand or APO_2 ligand/tumor necrosis factor (TNF)-related apoptosis-inducing ligand (APO_2L/TRAIL), binds to pro-apoptotic receptors [Figure 3.7]. The extrinsic and intrinsic pathways converge via activation of intracellular enzymes called 'caspases', which are intracellular protease enzymes that break down the cell. This is important to our study, because regardless if estrogen withdrawal elicits apoptosis via intrinsic or extrinsic pathways, it is inhibited during the universal caspase activation. The caspase cascade ultimately triggers cell death through the destruction of cellular proteins, which are important for cell viability. The caspase

cascade plays a vital role in the induction, transduction, amplification and execution of apoptotic signals within the cell. The caspases are a group of intracellular cysteine enzymes that upon activation through the intrinsic and/or extrinsic pathways destroy essential cellular proteins, leading to controlled cell death. There are two tiers of caspase activation during apoptosis. Initiator caspases are activated through the apoptosis-signaling pathways and activate the effector caspases which, in an expanding cascade, carry out apoptosis. Caspase cascades are initiated through an assembly of many protein complexes that trigger activation of the initiator caspases (2, 8, 9, 10) which are then released and able to activate the downstream effector caspases such as caspase 3, 6 and 7.

Figure 3.7: Apoptosis pathway signaling for apoptosis (Source: *http://www.researchapoptosis.com*).

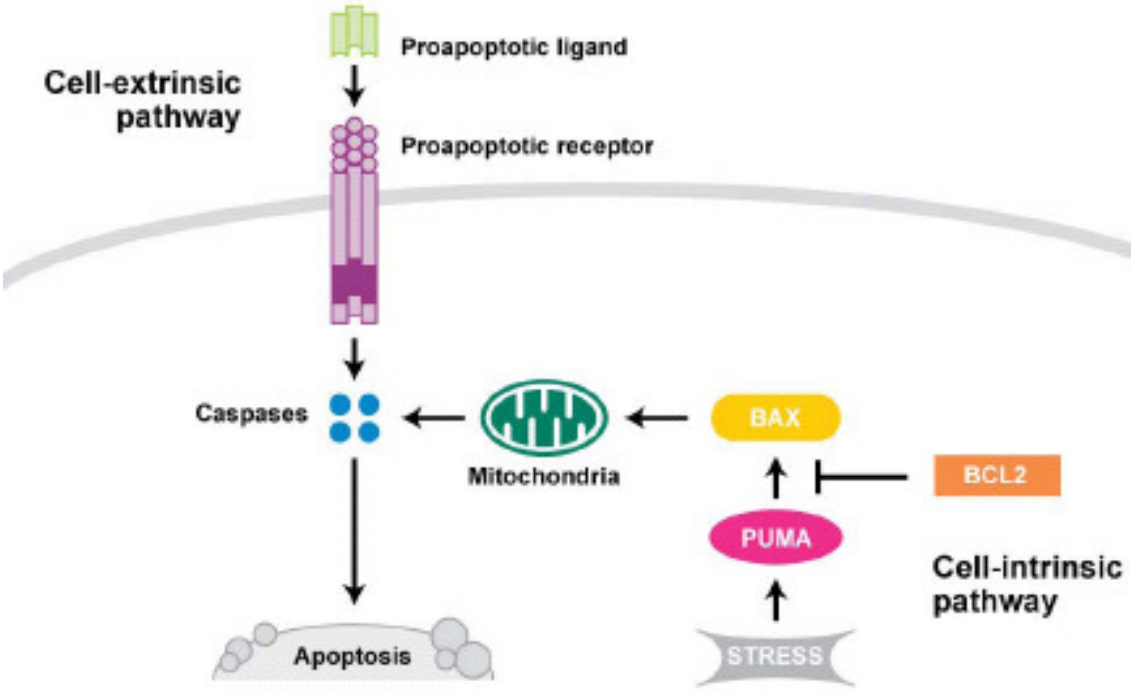

Whether surviving osteocytes are the cells that produce the signals to attract osteoclast progenitors are still unclear; moreover, the molecular mechanisms linking osteocyte death to osteoclast recruitment have yet to be established. There are many different theories that involve osteocytes and the pro-resorptive signaling they are associated with. The first, 'loss of inhibition theory', says when osteocytes die, they no longer produce these inhibitory signals, thus creating a local environment that is attracts osteoclastic activity. This theory does not hold up since previous studies examining resorption on living and non-living allografts only showed osteoclastic lesions on living allografts, thereby showing that dead bone does not resorb [111]. The second theory, 'cell mediated activation' in which dying osteocytes and neighboring osteocytes produce osteoclastogenic signals that direct the response [22; 46; 60; 72]. Recent evidence shows that osteocyte apoptosis positively correlates to bone resorption by osteoclasts in growing bone, microdamage, and estrogen withdrawal [35]. Recent studies involving microdamage show that osteocytes adjacent to those undergoing apoptosis actively protect themselves against cell death by eliciting anti-apoptotic factors such as Bcl-2 [127]. This provides support for the idea that these neighboring cells could play an active role in signaling and/or targeting of osteoclastic bone resorption. More work done in our lab by Cardoso et al established a correlation between osteocyte apoptosis and osteoclast resorption, giving evidence that inhibiting fatigue-induced osteocyte apoptosis prevented activation of osteoclast resorption [16]. Therefore, osteocytes and the onset of apoptosis could prove a key relation to the signaling mechanisms that osteoclasts use to direct their resorptive response.

Phosphorylated H_2AX, is associated with a caspase-independent apoptotic pathway after DNA damage (unraveling of the histone proteins) when phosphorylated [16; 105]. The histone H_2AX has a motif unique to it that becomes rapidly phosphorylated (γH_2AX) in cells and animals when the DNA double-strand breaks are exposed during apoptosis. When phosphorylated, γH_2AX appears in apoptosis because of endonuclease activity in caspase- independent activation. During apoptosis, a cell is rendered incapable of proliferation or reversal of the apoptosis once this histone is phosphorylated. We wanted to utilize this marker to check for caspase-independent initiated apoptosis to verify that the apoptotic response that was driving the remodeling response in our system was caspase-dependent, and also to accommodate for other apoptotic pathways. Our results showed increases in γH_2AX+ osteocytes post-OVX in cortical bone (staining was not done in cancellous bone), and suppression of this cell death marker in QVD-treated OVX group. This indicates that both markers are following the same trend and that there is some non-caspase mediated apoptosis, but in smaller amounts, thereby showing caspase-dominant mediation.

In summary, we have demonstrated that osteocyte apoptosis plays a fundamental role in the initiation of bone remodeling in response to ovariectomy, regardless of bone tissue type. Prevention of osteocyte apoptosis completely blocked the activation of trabecular and cortical bone resorption in response to ovariectomy-induced estrogen withdrawal. Since QVD does not directly affect osteoclastic differentiation or function, our results indicate that osteocyte apoptosis is required to activate osteoclastic resorption. Since blocking osteocyte apoptosis prevented OVX-induced bone resorption as it previously did for microdamage remodeling, it suggests that both processes are targeted,

and that osteocyte apoptosis may initiate a common pathway for activating and targeting resorption in response to diverse stimuli.

ACKNOWLEDGEMENTS

This work was supported by NIH grant AR 41210. We thank Bin Hu for his assistance in the ovariectomy surgeries, Damien Laudier for assistance with specimen preparation, and Marissa Steinberg who did the data collection for the trabecular bone and was a constant source of help and comic relief for the short three months I was honored to work with her.

CHAPTER 4

RELATIONSHIP OF BONE TISSUE AGE, MICROSTRUCTURE AND OXIDATIVE STRESS ACCUMULATION TO OSTEOCYTE APOPTOSIS REGIONS.

ABSTRACT

Introduction: Our previous studies reveal that the osteocyte apoptosis regions correspond to the oldest areas of mouse femoral cortex, and also suggest reduced lacunar-canalicular connectivity of osteocytes in regions prone to apoptosis after estrogen loss. These observations leads us to hypothesize that 1) diminished transport to osteocytes in these regions and 2) the older osteocytes have accumulated more oxidative damage and are therefore more at risk when the recently demonstrated protective effect of estrogen against oxidative stress/damage are removed after estrogen withdrawal. This study examines extrinsic and/or intrinsic differences that lead to the non-stochastic pattern of osteocyte apoptosis seen in mouse cortical and cancellous bone tissues after estrogen loss, as previously described in Chapter 2 and 3 of this dissertation. The purpose of this study was to begin to understand the mechanisms behind why osteocytes in specific regions of the bone undergo apoptosis with estrogen withdrawal, while those in other regions do not.

Materials and Methods: Our experimental design to observe mechanistic differences of osteocytes in regions of high and low apoptosis consists of two parts: First, an *in vivo* tracer study was used to examine transport in areas of high and low apoptosis, combined with a mathematical model utilizing modified Fick's Law. Normalized region of interest (ROI) input values from mid-diaphyseal femur of the sacrificed animals were then compared with our mathematical model to give a functional measurement of transport within these regions. Second, we examined molecular biology differences of osteocytes via immunohistochemical staining for cumulative stress damage from the mid-diaphyseal regions of high and low apoptosis.

Results: The *in vivo* tracer model reveals that regions of high apoptosis (posterior region) have fewer canalicular connections than the lamellar bone of the anterior region, and thereby reduced transport efficiency. Areas of high apoptosis also yield elevated staining for oxidative stress marker 8-OhdG.

Conclusions: Estrogen withdrawal promotes osteocyte apoptosis in consistent regions that subsequently undergo resorption, with increased apoptosis in the posterior region of cortical bone. Microarchitectural differences between the areas of high and low apoptosis (the regions of lamellar vs. non-lamellar bone) reveal that the osteocytes in this region are less connected to their neighboring osteocytes with significantly fewer canalicular connections. The reduced connections therefore imply that the osteocyte population of the posterior region is subject to less efficient transport of signaling molecules that travel via bone fluid flow through the LCS. Estrogen loss attenuates this response with its antioxidant capabilities to reduce the amount of free radicals, as well as its ability to regulate the glutathione and thioredoxin pathways. These age- and microanatomical-related differences make osteocytes more sensitive to a system perturbation, thereby influencing the way osteocytes within certain regions of bone respond differently to estrogen deprivation.

INTRODUCTION

It has been previously established that estrogen deficiency promotes osteocyte apoptosis in murine cortical bone in a non-random anatomical distribution [30]. The regions demonstrating increased apoptosis are structurally distinct, comprised largely of

less well organized compact bone (non-lamellar) rather than lamellar bone. The visible differences in microarchitecture suggest different lacunar-canalicular connectivity for osteocytes within these structurally unique regions. Bone's lacunar-canalicular porosity is believed to be a continuous interstitial fluid pathway through which osteocytes obtain nutrients and dispose of wastes. Transport of intercellular signaling molecules through the lacunar-canalicular system (LCS) is also an important means of communication among osteocytes. The kinetics of *in vivo* fluid flow through bone greatly depends upon the permeability characteristics and the degree of connectivity within the LCS [119; 130; 131]. Therefore, differences between tissue types (newer lamellar vs. older non-lamellar bone) in morphology and microstructure of the LCS could account for a reduced diffusive propagation of essential signaling molecules needed for osteocyte viability. A previous study done with different sized tracers injected into the LCS indicated that molecules (<6nm) readily passed from bone capillaries to osteocyte lacunae in rat long bone [130].

It remains obscure why osteocytes in this region of the bone are preferentially affected by estrogen withdrawal. Temporal growth and development images of calcein-labeled (labels mineralization front) transverse mid-diaphyseal mouse femurs reveal that the posterior control region, where osteocyte apoptosis concentrates after OVX, is the oldest tissue and thus contains the oldest osteocytes of the mouse femoral cortex [100]. Previous studies have also demonstrated that solute transport is reduced with age via impaired lacunar properties (density, surface area, volume) [139]. As the regions of increased apoptosis correspond to the oldest areas of the femoral cortex, it seems reasonable to speculate that the older osteocytes, which are less interconnected than those

in lamellar bone, also have more cumulative stress (oxidative, DNA damage, etc) and are therefore more at risk when the protective effect of estrogen is removed.

Numerous studies have shown that estrogen is an antioxidant that inactivates free radicals caused by metabolic waste, both directly and indirectly. Directly, prevention of oxidative stress-induced cell death has been linked to estrogen's conformation. There is an -OH moiety on the C3 position of the steroid A-ring of the estrogen molecule that mops up free radical damage within the cell [71]. Estrogen is also well established as an antioxidant indirectly with its regulation of glutathione and thioredoxin pathways [63; 71]. Loss of estrogen has been shown to accelerate the effects of aging on bone by decreasing defense against reactive oxygen species (ROS) with its reduced ability to regulate the cells' antioxidant defense, yet these studies did not localize the older cells or its relationship to aging induced remodeling [2; 129]. Thus, we posit that osteocytes within the posterior region of cortical bone have accumulated greater damage either due to age or transport differentials. We also hypothesize that older cells that accumulate this damage are inherently more primed for apoptosis, and the first to die when estrogen is withdrawn.

This study examines the extrinsic and/or intrinsic differences that lead to the non-random pattern of osteocyte apoptosis seen in our previous studies. Our goals were two-fold: First, we experimentally tested transport differences among regions of high and low apoptosis by utilizing an *in vivo* tracer study. This allowed us to quantify and compare morphology differences seen in LCS microanatomy among tissue types to estimate transport efficiency. Secondly, we examined metabolic stress state differences in regional

osteocytes that account for the spatial distribution of osteocyte apoptosis after estrogen withdrawal.

METHODS AND MATERIALS

Our experimental design to examine mechanistic differences of osteocytes in regions of high and low apoptosis consisted of two parts. An *in vivo* tracer dye study was performed to study osteocyte microanatomy differences in regions of high and low apoptosis after estrogen loss. A mathematical model for solute transport efficiency, previously developed in our lab, was used to compare transport efficiency between these two compartments [131; 133]. Lastly, we tested for differences in osteocyte cumulative stress damage by *in situ* immunohistochemical staining in the mid-diaphyseal regions of high and low apoptosis.

In Vivo Tracer Experimental Model

Animal Preparation: Skeletally mature C57BL/6J mice (n=6, 17 weeks old; Jackson Laboratory, Bar Harbor, ME) were injected with a tracer solution composed of 0.8% Reactive Red (MW: 1470, Sigma-Aldrich) and 0.2 mg/g BW 488-Alexa Fluor labeled Albumin (# A13100, MW: 66,000, Invitrogen) in PBS in order to examine diffusive transport of different size molecules within the LCS of high and low apoptosis regions. Mice were anaesthetized via intraperitoneal injection of Avertin (1mL/100g BW), and an injection of freshly made tracer solution (0.2 mL per animal) was slowly infused into the tail vein and allowed to circulate for 5 minutes post-injection. Animals were sacrificed via cervical dislocation without recovery from anesthesia. Femurs and

tibias from both hind limbs were harvested by dissection, with care taken to keep the periosteum intact.

Tissue Collection and Processing: Whole bones were placed in 90% alcohol for 24 hours at 4˚C and then 100% alcohol for 24 hours (changed 3 times) using a modified dehydration process [39]. Bones were cleared in methylsalicylate for 24 hours (2 changes) and then embedded in PMMA. Femoral mid-diaphysis were cut in cross-section using a diamond blade saw and then polished to a final thickness of 70 μm. Sections were mounted on glass slides and cover-slipped with Eukitts mounting medium for confocal microscope.

Confocal Microscopy: Undecalcified sections were viewed using a confocal laser scanning microscope (TCS, Leica Microsystems, Wetzlar, Germany) to examine micro-architectural and morphological differences that were present between osteocytes in the regions of high and low apoptosis. The optimal detection of fluorescent labeling of reactive red used a 543-nm argon laser excitation, while Alexa-Fluor 488 utilized a 488-nm excitation. All images were obtained using a 63X oil immersion objective. Z-stacks of ~50um depth were collected for each ROI within the posterior and anterior medial quadrants of the mid-diaphyseal femoral cortex, which corresponds to the same regions where Emerton et al showed high and low osteocyte apoptosis after estrogen loss [30]. The calibrated 6” x 9” ROI was taken from each image to normalize the data collection area [*Figure 2.9; Chapter 2 of this dissertation*]. There were 5 consecutive images taken of every region per animal (n=6), giving a total of 30 images per region. All images were then imported into ImageBuilder software with optimized threshold settings and counted

for number of lacunae and canaliculi, lacunae perimeter and area that was labeled with Reactive Red (1nm) and AlexaFluor 488 labeled albumin (6nm).

The mid-diaphysis of a femur from a baseline animal (not injected with tracer) was stained with Toluidine Blue (Aldrich Co, Milwaukee, WI) and used as negative controls to count osteocyte lacunae and blood vessels for the tracer-injected animals (data not shown). Consecutive sections were unstained and imaged via confocal microscopy in order to make sure there was no auto-luminescence from the PBS or bone tissue that would yield a staining artifact.

Transport Mathematical Model: Image measurements from IMAQ Vision Builder software were imported into a two-compartment model that was modified by Wang et al to examine radial spreading of a representative signaling molecule, PGE_2, from one osteocyte lacuna to its neighbor [131] [*Figure 4.1a,b*]. The model describes the diffusion of the molecules through connecting canaliculi into the lacunae of adjacent cells with a zero initial concentration. Diffusion between adjacent osteocyte layers is one-dimensional in the radial direction (which account for ~80% of total canaliculi emanating from a lacunae) [132]. Mathematically, the model reduces to two well-mixed pools connected by a linear channel [*Figure 4.1c*]. Concentrations in the canaliculi C(x,t) and within the sink lacunae $C_s(t)$ are governed by Fick's second and first law, respectively, where D is the diffusion coefficient of the molecules; x is the distance from the source reservoir; V_s is the sink volume; N is the number of connecting canaliculi; and A_{fc} is the cross-sectional area for the fluid annulus in one canaliculus. The equations were solved and an approximate solution was obtained [$\boldsymbol{Cs(t)/C0 = 1-exp(-t/\tau)}$]. This equation was used to solve for the solute concentration, where τ is the time constant required for C_s to

reach 63% of the initial concentration [$\tau=d_2/(V_rD)$]. *Vr* is the ratio of fluid volume between canaliculi and the sink lacuna [$V_r=(NA_{fc}d)/V_s$].

Figure 4.1: Two-compartment model. (A) Confocal image of two neighboring osteocytes [courtesy of Wang et al 2006]. (B) Mathematical model of solute transport from source to sink. (C) Fick's second and first law of diffusion, respectively.

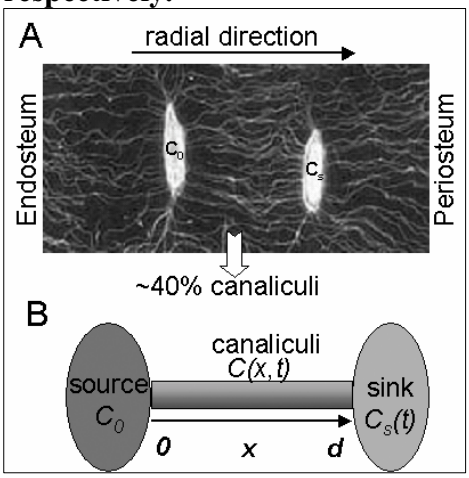

$$D\frac{\partial^2 C}{\partial x^2}=\frac{\partial C}{\partial t}$$

$$V_s\frac{dC_s(t)}{dt}=-(NA_{fc})D\frac{\partial C(d,t)}{\partial x}$$

Model Parameters: D is set at 3.3 x 10^{-6} cm^2/sec, as measured for fluorescein in previous LCS tracer studies using B6 mice [131]. Canalicular length was obtained from osteocyte number density [*d=1/sqrt(Oc.Den)*]. Lacunar volume (V_s) and surface area (*S*) were calculated from the radii of the three principal axes [132]. Number of connecting canaliculi was half of the canaliculi emanating radially from the cell (~40% of total canaliculi of one lacuna), which was calculated from the surface area and canalicular number density (*N=40%*S*Can.Den*). The relative volume ratio V_r was calculated for each region, and parameters were input [*Table 4.1*].

Statistical Analysis: Differences in osteocyte density and canalicular density between posterior and anterior regions were tested using Students T-test for the

computational model and tracer study measurements. Results were expressed as mean ± SD for each group. Analyses for all statistical analyses and performed using the Graphpad Prism 3.0 software program [GraphPad Software, San Diego, CA].

Osteocyte Cumulative Stress

Choice of candidate molecules. Evidence suggests that cells increase apoptosis as they age, and estrogen attenuates this response via accumulation of free radical and metabolic damage [2; 69; 76; 93; 128]. **HIF-1α** (Hypoxia Inducible Factor-1α) is produced in response to hypoxic stress [113; 115]. Immunostaining for this gave us an indication if the cells within the posterior and anterior regions of mid-diaphyseal cross-sections were intrinsically more stressed, or primed for apoptosis when estrogen is removed.

Nucleic acids can be oxidized by ROS, with 20 oxidative –specific lesions discovered in DNA and RNA [103]. One of these lesions exposed is 8-hydroxyguanine (8-OhdG), which is highly measurable and known specifically for its mutagenic effect. Therefore, we stained for **8-OhdG**, a marker specific to oxidative stress accumulation that has been previously demonstrated to be elevated in diabetic bone [43; 50]. Liver tissue from a diabetic mouse was used as additional positive staining control for the antibody.

Animal Preparation: Sham-operated cortical femur transverse sections from the right femora of 17-week old female C57BL/6J mice from the previous study in Chapter 2 of this dissertation (estrogen loss and osteocyte death) were used to examine cellular

stress levels between regions of high and low apoptosis (posterior and anterior regions). Sections from sham animals at 1 and 3 days following surgery were used for immunohistochemistry staining of DNA oxidative damage and metabolic stress markers.

Tissue Collection and Processing: Femora were dissected, cleaned of soft tissue and fixed in 10% neutral buffered formalin for 48 hr at 4˚C. Right femora were decalcified in formic acid solution for 3 days with daily changes. Bones were then embedded in paraffin and mid-diaphyseal 5-micron cross-sections cut and adhered to charged slides.

Data collection: Osteocytes were counted under brightfield microscopy at 400X magnification using a 10mm x 10mm eyepiece grid reticule. Positively stained osteocytes were counted through the entire cortical width for the posterior (P) and anterior (A) sampling regions around the bone cross section. Each sampling region was further divided into 10 equal rows extending from the periosteal to the endosteal surface. Numbers of stained osteocytes were determined, and expressed as a percentage of total cells in the regions of interest.

Statistical Analysis: Differences in osteocyte staining for HIF-1α or 8-OhdG between OVX and sham at each time point were tested using the Mann-Whitney test. Results were expressed as mean ± SD for each group. Analyses for all statistical analyses and performed using the Graphpad Prism 3.0 software program [GraphPad Software, San Diego, CA].

RESULTS

In Vivo Tracer Experimental Model

Five minutes post-injection, both tracers showed identical labeling patterns despite their difference in size (Reactive Red and labeled-Albumin at 1 and 6 nm, respectively). The labeling of Reactive Red and labeled-Albumin was extensive, with the dye found in most blood vessels, osteocyte lacunae and canalicular channels [*Figure 4.2*]. The labeling for both tracers was found to be identical and extensive despite the 5-nm difference in tracer diameter, indicating accurate transport regardless of size. Control sections of bone showed no staining, confirming that the staining in the injected sections was not an artifact.

Figure 4.2: Confocal images of posterior (P) and anterior (A) transverse cortical sections injected with labeled albumin and calcein. Red box indicates normalized ROI that was imported into IMAQ Vision Builder to quantitate lacunar and canalicular density.

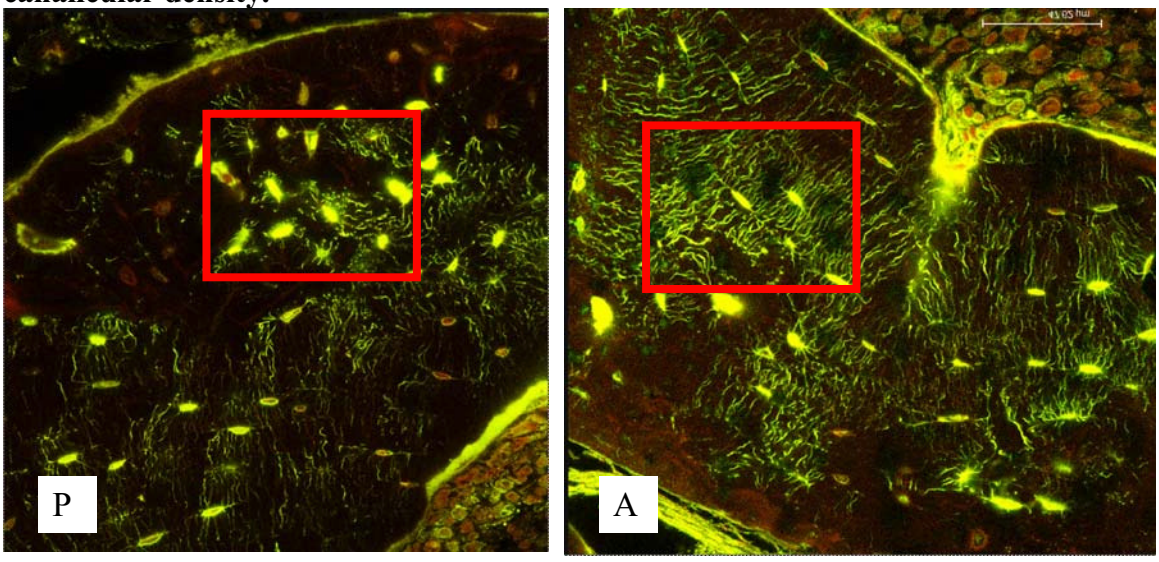

The mathematical model to estimate transport efficiency predicts that the diffusion through the LCS results in exponential concentration increases of small

signaling molecules in lacunae adjacent to the source, until a plateau is reached. However, based on differences in lacunar size, and canalicular density the spreading should occur most rapidly in lamellar bone as opposed to non-lamellar bone where osteocyte apoptosis is concentrated. Our results show estimated time constants of 55 and 70 seconds for anterior and posterior bone tissue, respectively [*Table 4.1*]. There was significantly less canalicular connections in the posterior region, where osteocyte apoptosis is elevated, thereby accounting for the main difference in the time constants between tissue regions.

Time constants (τ) for the two regions (tracer study) were input into the previously described equation, and solved for solute concentrations within the lacunae. Similar curves are seen for the two different regions of bone calculated, with all curves approaching the same plateau [*Figure 4.3*].

Table 4.1: Morphological features of LCS within regions of cortical bone. **p < 0.0003 for experimental tracer dye measurements using Students T-test for canalicular density (P vs A).

Tissue Region	Oc. Den	Can. Den	d	τ
	#/mm^2	#/um^2	µm	sec
Posterior (tracer)	539	0.095**	43.06	70.10
Anterior (tracer)	622	0.123	40.09	55.80

Parameters are as follows; Oc. Den = osteocyte density (ROI); Can. Den = # canaliculi/um^2 (ROI); d = canalicular length (1/sqrt Oc Den); τ = calculated time constant (seconds).

The Mann-Whitney analyses showed no significant difference in osteocyte density between the lamellar and non-lamellar regions of bone. However, there was a significant difference in canalicular density ($p < 0.005$). The density of osteocytes

labeled with Reactive Red was similar to Toluidine-labeled controls (data not shown). No pairwise differences were found to be significant ($p < 0.05$) among the examined group means for lacunae area or perimeter.

Figure 4.3: Transport efficiency (solute concentration within lacunae) for different regions after 5 minute circulation of tracers. Time constants were 55 seconds for the anterior region (low apoptosis), and 70 seconds for the posterior region (high apoptosis). Graph shows that the model accurate estimates how the system behaves.

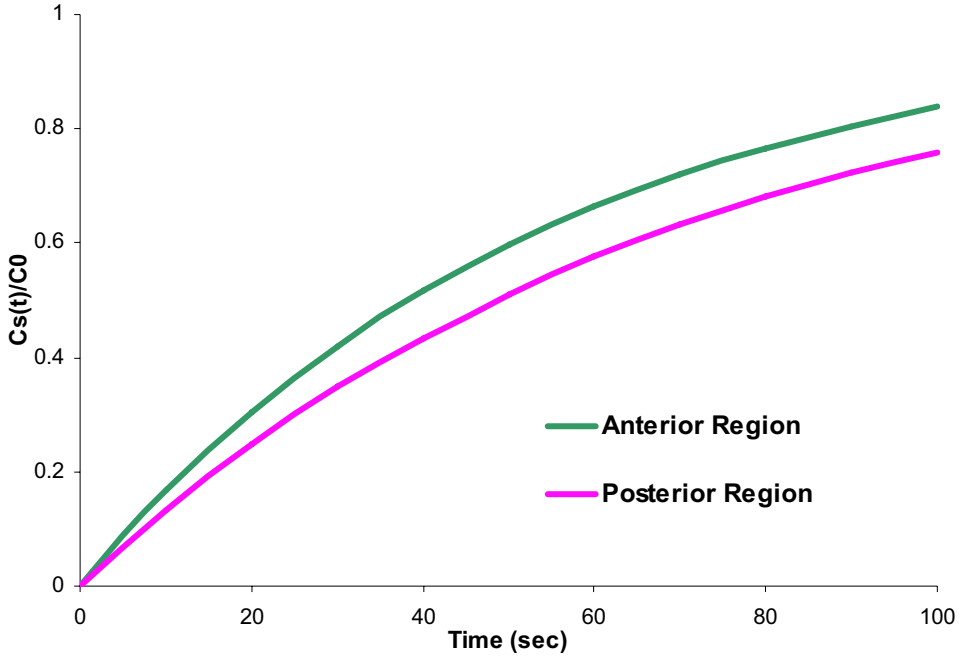

Osteocyte Cumulative Stress

There was minimal staining of HIF-1alpha in control bone regions of the transverse sections (<1%). There was no significant difference in osteocyte apoptosis for either posterior or anterior regions of the bone ($p < 0.45$) [*Figure 4.4*].

Figure 4.4: HIF-1α + osteocytes within regions of transverse murine cortical bone of the femur.

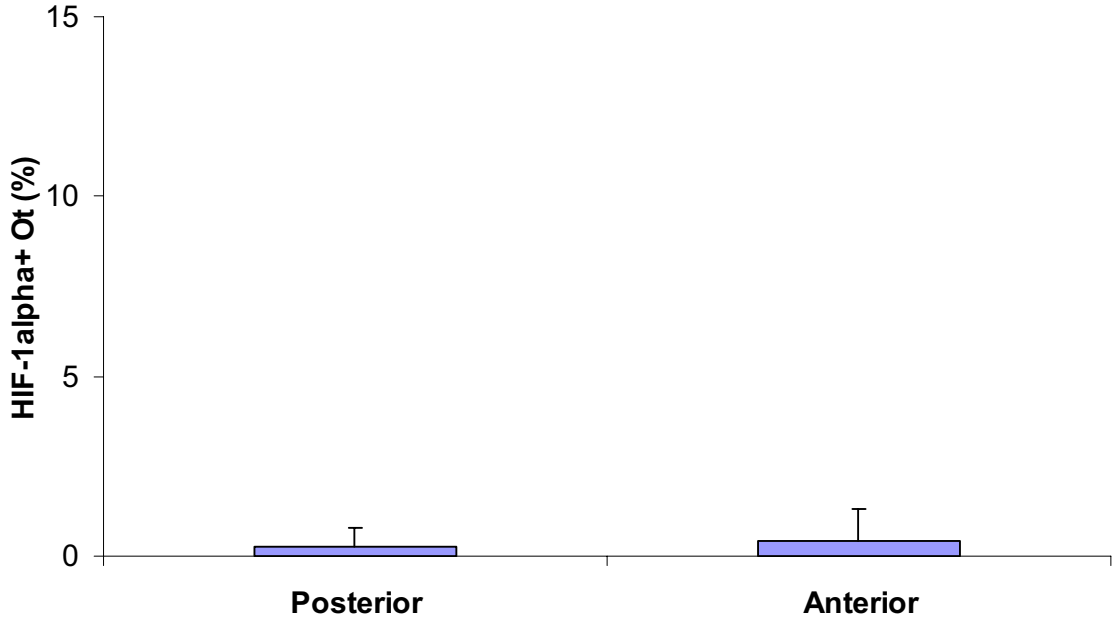

Immunohistochemical staining for oxidative stress marker 8-OhdG was elevated in the exact location where osteocyte apoptosis is elevated, the posterior region, by more than 7-fold when compared to the anterior region [***Figure 4.5***].

Figure 4.5: 8-OhdG + Ot, an oxidative stress marker for DNA/RNA damage, within posterior and anterior regions of transverse murine cortical CONTROL bone of the femur.

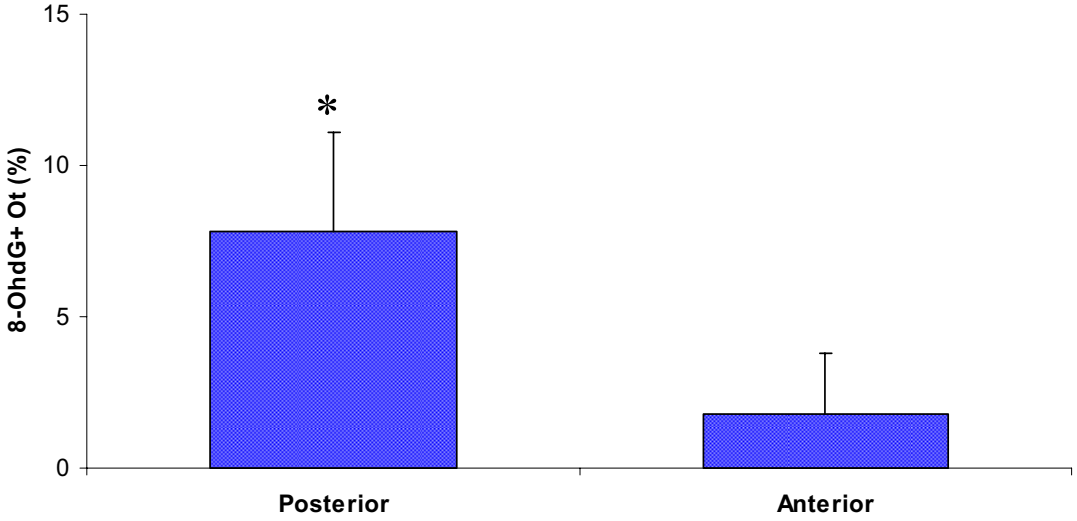

DISCUSSION

The current study examined the extrinsic and/or intrinsic differences that account for the non-random pattern of apoptosis demonstrated in previous chapters of this dissertation. Our current studies show that the osteocytes most susceptible in our system contain high levels of pre-existing DNA oxidative damage, with dramatically elevated levels of impairment exactly within the same area (posterior region) of high apoptosis. Thus, its reasonable to posit that osteocytes within the posterior region of cortical bone have accumulated greater damage and that these cells are' living closer to the edge'; i.e., more sensitive to apoptosis during a system perturbation such as estrogen withdrawal.

Staining for DNA oxidative stress marker 8-OhdG revealed significant staining within the exact areas that contain increased apoptosis, the posterior region that is largely composed of compacted cancellous bone. Our 8-OhdG staining for control bone caused a

7-fold increase in oxidative damage in the same regions known to undergo apoptosis. This early upregulation in oxidative stress damage activity could be the driving factors for the elevated levels of apoptosis seen after loss of estrogen's protective effect. Positive-staining osteocytes for this marker yielded higher amounts (8% ± 4% in control posterior) than osteocyte apoptosis via caspase-3 staining (2% ± 3% in control posterior; see *Figure 2.4* of Chapter 2 of this dissertation). These results point towards the fact that these cells are inherently more primed for damage, and are more easily damaged when estrogen's antioxidant protection is removed. We believe that estrogen loss exacerbates the apoptosis already seen in these regions.

Estrogen is well established as an antioxidant with its regulation of glutathione and thioredoxin pathways [71]. Loss of estrogen has been shown to accelerate the effects of aging on bone by decreasing defense against reactive oxygen species (ROS) with its reduced ability to regulate the cells' antioxidant defense. The osteocytes in oldest tissue appear to be inherently more primed for apoptosis because of their age, therefore it seems a reasonable speculation that removal of estrogen leads to the removal of the protective effect against oxidative damage. Recent studies have shown that the balance between ROS production and antioxidant defense determines the degree of oxidative stress [32; 38; 63; 71]. Aging cells accumulate more oxidant-damaged nuclear and mitochondrial DNA, as well as RNA. These studies infer that older cells are intrinsically more damaged. When an environmental factor is introduced, such as estrogen withdrawal, an increase in ROS would perturb the normal reduction-oxidation balance, and cause previously damage-accumulated cells to shift into a state of oxidative stress. When this stress is severe, the survival of the cell is dependent upon its ability to adapt or to resist

stress and repair the damage. With osteocytes in the posterior region situated in a less-optimal microenvironment, it is possible that these osteocytes respond to insult by undergoing apoptosis, whereas osteocytes in the anterior region would maintain viability.

Our previous study examined the micro-environmental differences within the regions where there were high levels of apoptosis. Confocal images taken in the regions of bone expressing increased apoptosis (posterior region of mid-diaphyseal cortical bone) led us to the discovery that these cells are residing in bone that is structurally distinct; it is comprised largely of compacted cancellous bone whereas anterior regions (mounts of apoptosis) are comprised of lamellar bone tissue. Areas of high apoptosis exhibit a 'woven-like' bone that is less organized and has a visual difference in structure. Temporal growth and development images of calcein-labeled (labels mineralization front) transverse mid-diaphyseal mouse femurs reveal that the posterior region, where osteocyte apoptosis concentrates after OVX, is the oldest tissue and thus the oldest osteocytes of the mouse femoral cortex [100]. However, the age differential between the cells in the lamellar and non-lamellar bone is around the order of 4-6 weeks, so we are not sure if this age difference is a valid factor.

We undertook an experimental dye tracer transport study to examine compartmental differences in transport between areas of high and low apoptosis (posterior and anterior) using different sized tracers. Bone LCS porosity is a continuous interstitial fluid pathway that is vital to osteocytes for nutrient and waste disposal [119]. Previous tracer studies showed that less than 6 nm pass readily from bone capillaries to lacuna, therefore transport differences modeled in the first portion of our study could be examined real time in order to elucidate whether there was indeed impaired transport in

high apoptosis regions [25; 130]. The gathered images indicated that there were identical and extensive labeling patterns despite tracer size differences and both tracer dyes were accurately reaching all bone tissue areas. The *in vivo* tracer dye patterns from the mid-diaphyseal femurs also reveaedl that there was a significantly reduced canalicular density in regions of high apoptosis. When these image measurements were imported into diffusion equations and solved for solute concentration there was decreased transport efficiency found in the posterior regions that are largely composed of compacted cancellous bone. The osteocytes in these regions show markedly slower transport due to fewer connections. Time constant differences between the anterior (τ = 55 sec) and posterior region (τ = 70 sec) show that the reduced canalicular connections impair transport to osteocytes in the posterior region [*Figure 4.3*]. Previous studies have shown that transport of intracellular signaling molecules through the LCS is an important means of cellular communication, as well as essential for nutrient delivery and removal [AJP 2008]. These regional differences in microanatomy could affect propagation patterns and timing of key signaling molecules, therefore yielding a greater baseline 'stress' for cells in this region with reduced ability to receive nutrients and remove wastes due to less efficient transport. Because of this reduced cell connectivity, it seems reasonable to speculate that the posterior region would be more dramatically affected by any sort of changes (i.e. estrogen withdrawal).

Previous studies have implicated that a disruption in transport produces hypoxic stress, and up-regulation of HIF-1α in surrounding microdamage [48; 118; 119]. Our immunostaining for this marker showed minimal to no staining in either posterior or anterior regions of the control bone, with positive-staining cells percentages slightly less

than previously shown apoptosis percentages for control bone in these regions. Since HIF-1α is an acute response protein, if these cells are in a hypoxic environment then they must be adapted to it, and the estrogen does not play a substantial role in the mechanism behind the elevated apoptosis in these regions. Previous work has found acutely elevated HIF-1α expression 1-hour post ischemia reperfusion in liver cells, and 6-hrs in hypoxic chondrocytes [26; 84]. In both of these cases, however, the hypoxic event was an immediate and isolated event, not a gradual adjustment to its microenvironment, as would be the case for the osteocytes situated in the areas of high apoptosis. Early work examining protein synthesis patterns were examined in rat brain after ischemia, and analyzed at different blood flow reductions [53]. Even small reductions in blood flow caused reduced amounts of protein synthesis, showing that cells are affected by small variations, and therefore are a more 'sluggish' cell that has reduced ability to clean up metabolic wastes. More recent studies have confirmed that reduced transport due to ischemia cause increased ROS in brain and nerve cells with reduced GSH levels found as soon as 30 minutes after ischemia, and is maintained over long term hypoperfusion [27; 104]. These lines of evidence indicate that it is possible that the reduced transport and increased oxidative damage could be linked factors attributing to the high apoptosis regions that we are seeing in our study. Therefore it is important to note that a functional study using the tracers at immediate time points such as 30 seconds and 1 minute is needed to truly 'tease out' the effects of non-saturated transport. We need to go to a more physiological level to do a functional confirmation of the model, not just the 5 minute saturated time point that gave us more of an 'architecture' result.

Estrogen studies investigating the role of estrogen as a potential athero-protective agent have shown it to inhibit both atherogenesis via regulation of endothelial FasL expression [2; 19]. Fas ligand (FasL) expression by the vascular endothelium inhibits the migration of inflammatory cells into the vessel wall, a crucial event for the development of atherosclerosis. Other studies have examined estrogen as a viability factor for cellular protection in the brain and heart in conjunction with IGF-1, and showed estrogen as an essential regulator of neural and endothelial function [37; 83; 108]. Further, other studies have shown protective effects of estrogen on apoptosis of other cell systems, such as nerve viability and umbilical endothelial cells during ischemia [21; 106]. These studies and others [64] demonstrate the significance of estrogen as a protectant against hypoxia-induced injury and provide the groundwork for future studies to examine differences between areas of known high apoptosis and low apoptosis after estrogen is withdrawn.

In summary, estrogen withdrawal promotes osteocyte apoptosis in consistent regions that subsequently undergo resorption, with increased apoptosis in regions of compacted cancellous bone tissue. Whether the osteocyte apoptosis is a result DNA oxidative damage, or age and reduced transport efficiency, or a combination of both that puts them at risk is unknown. We previously hypothesized that the osteocytes that are older and less connected to their neighboring osteocytes are at higher risk for oxidative stress and/or lower levels of anti-apoptotic protection. These older cells are contained within a matrix that closely resembles woven bone, or tissue that was quickly constructed as the animal was rapidly growing. Microanatomy differences between the areas of high

and low apoptosis (the regions of lamellar vs. non-lamellar bone) reveal that the osteocytes in this region are less connected to their neighboring osteocytes with significantly fewer canalicular connections. The reduced connections therefore imply that the osteocyte population of the posterior region is subject to less efficient transport of signaling molecules that travel via bone fluid flow through the LCS. The microanatomy and age of these osteocytes indicate that cells in this region of high apoptosis have accumulated more damage, and are therefore living 'closer to the edge'. Estrogen loss attenuates this response with its antioxidant capabilities to reduce the amount of free radicals, as well as its ability to regulate the glutathione and thioredoxin pathways. In conclusion, these age- and microenviroment-related differences make osteocytes more sensitive to a system perturbation, thereby influencing the way osteocytes within certain regions of bone respond differently to estrogen deprivation.

ACKNOWLEDGMENTS

The authors would like to thank Cesare Ciani, PhD and Susannah Fritton, PhD for their thought-provoking discussions and help in the experimental design of the tracer study, as well as for the gift of the Reactive Red powder. We would also like to thank Marvin Lin and John Salig for their expertise and aid in performing the tail vein injections.

CHAPTER 5

GENERAL CONCLUSIONS AND FUTURE DIRECTIONS.

GENERAL CONCLUSIONS

The goal of this dissertation was to better understand the role of osteocyte apoptosis in targeted bone remodeling after estrogen withdrawal, which is fundamental to understanding bone health and disease. In other organ systems, apoptosis plays a pivotal role in governing normal turnover and response to injury. In other systems, turnover involves targeting of apoptotic cells and active signaling to the phagocytic cells to orchestrate the location of resorption. Although bone is regulated by estrogen, the mechanisms by which estrogen and its deficiency exert its directed effects on bone during remodeling remain unclear. Previous studies have alluded to a role for osteocyte apoptosis in remodeling after estrogen withdrawal, but specific localizations of this response to bone remodeling have never been examined.

Our first objective was to characterize the spatial and temporal relationship between estrogen withdrawal, osteocyte apoptosis and bone resorption. It was previously demonstrated that estrogen withdrawal induces regionally consistent bone loss [66]. We used the same well-characterized murine system because it demonstrated highly consistent patterns of cortical bone resorption after estrogen withdrawal, and induced estrogen deficiency by surgical ovariectomy. Osteocyte apoptosis was then sampled at early time points post-ovariectomy in mid-shaft femoral cortex in order to sample both pre-osteoclast and active resorptive time points. Sampling of osteocytes apoptosis along the major anatomical axes was assessed using immunohistochemistry combined with histomorphometry for resorptive surface measurements of the mid-diaphyseal femur sections. We later incorporated trabecular bone from the distal metaphyseal femur from the same animals to examine whether the same relationship existed in trabecular bone.

The results of this study demonstrate that osteocyte apoptosis following estrogen loss occur regionally, rather than uniformly throughout the cortex. Consistent with previous observations, we found that estrogen loss increased osteocyte apoptosis in both cortical and trabecular bone of the femur. However, we found that apoptotic osteocytes in cortical bone were overwhelmingly localized within the posterior cortical region, the area where subsequent endocortical resorption is known to occur after ovariectomy in B6 mice. In trabecular bone, we found the same relationship, with areas of apoptosis correlating to areas (within 20 μm) of resorption. There was increased osteocyte apoptosis as early as 1 day after the initial stimulus of estrogen deprivation, and this apoptosis remained elevated over time. Endocortical resorption was greatly enhanced after ovariectomy, and the exacerbated osteocyte death preceded the increases in endocortical resorption. That a similar spatial and temporal coupling between osteocyte apoptosis and bone resorption occurs in cancellous bone, after ovariectomy argues that osteocyte apoptosis may play a universal role in the local regulation of universal bone remodeling, in both cortical and cancellous bone compartments.

Our results indicate that not all osteocytes within cortical and cancellous bone are at equal risk for apoptosis after estrogen loss. Confocal images taken in the regions of bone expressing increased apoptosis led us to the discovery that these cells are residing in bone that is structurally distinct; it is comprised largely of compacted cancellous bone rather than the lamellar bone. The regions of elevated apoptosis are found almost solely within compacted cancellous bone or the oldest type of bone tissue in cortical bone. Temporal growth and development images of calcein-labeled (labels mineralization front) transverse mid-diaphyseal mouse femurs reveal that the posterior region, where

osteocyte apoptosis concentrates after OVX, is the oldest tissue and thus the oldest osteocytes of the mouse femoral cortex [100]. The data suggest that dying osteocytes, irrespective of the cause in cortical or cancellous bone, become targets for osteoclast recruitment and resorption. These results have important clinical implications since resorption-modifying treatments administered to post-menopausal patients are often initiated after bone remodeling has already begun.

In Chapter 3, we examined whether osteocyte apoptosis is required to initiate bone resorption after estrogen withdrawal. Previous work in our lab demonstrated that inhibiting osteocytes apoptosis after fatigue-induced microdamage prevented activation of osteoclastic resorption, and showed that osteocytes apoptosis is a required step for activation of bone resorption [17]. This observation raised the fundamental question of whether osteocyte is necessary to initiate remodeling in diverse stimuli such as estrogen withdrawal. In order to determine if apoptosis is a controlling and necessary step after estrogen deficiency, we administered pharmacological inhibition (pan-caspase inhibitor) to the same murine model in order to modulate osteocytes apoptosis and compare the amount of bone remodeling exhibited. Osteocyte apoptosis was then sampled at 14 days post-ovariectomy in mid-shaft femoral because our earlier study demonstrated visible onset of resorption by this time point. Sampling of osteocytes apoptosis along the major anatomical axes was assessed in the same manner as our first study, using immunohistochemistry combined with histomorphometry for resorptive surface measurements of the mid-diaphyseal femur sections. We again later incorporated trabecular bone from the distal metaphyseal femur from the same animals to examine whether the same relationship existed in trabecular bone.

Our results showed osteocyte apoptosis plays a comparable controlling role in the activation or targeting of osteoclastic resorption by inhibiting apoptosis. This was demonstrated by suppression of osteocyte apoptosis using a pan-caspase inhibitor to prevent increased cell death, which completely blocked the activation of bone resorption in response to OVX-induced estrogen withdrawal in both cortical bone and cancellous bone, thereby arguing strongly that osteocyte apoptosis is indeed required to activate bone resorption after estrogen loss regardless of bone tissue type. Since blocking osteocyte apoptosis prevented OVX-induced bone resorption as it previously did for microdamage remodeling, it suggests that both processes are targeted, and that osteocyte apoptosis may initiate a common pathway for activating and targeting resorption in response to diverse stimuli.

Our final objective was to examine the microenvironmental and biological differences that account for osteocyte apoptosis during estrogen withdrawal. This study was important to understand why osteocytes in specific regions of the bone undergo apoptosis with estrogen withdrawal, while those in other regions do not. Our previous studies already revealed that the osteocyte apoptosis regions correspond to the oldest areas of mouse femoral cortex, and also suggest different lacunar-canicular connectivity for osteocytes in these regions. These observations leads us to hypothesize that 1) diminished transport to osteocytes in these regions and 2) the older osteocytes have accumulated more oxidative damage and are therefore more at risk when the recently demonstrated protective effect of estrogen against oxidative stress/damage are removed after estrogen withdrawal. Our experimental design to examine mechanistic differences of osteocytes in regions of high and low apoptosis consisted of: 1) an *in vivo* tracer dye

study to study osteocyte microanatomy differences in regions of high and low apoptosis after estrogen loss. A mathematical model for solute transport efficiency, previously developed in our lab, was then used to compare transport efficiency between these two compartments [132]. 2) We tested for differences in osteocyte cumulative stress damage by *in situ* immunohistochemical staining in the mid-diaphyseal regions of high and low apoptosis.

The data showed that the osteocytes most susceptible in our system contain high levels of pre-existing DNA oxidative damage, with dramatically elevated levels of impairment exactly within the same area (posterior region) of high apoptosis. Staining for DNA oxidative stress marker 8-OhdG revealed significant staining within the exact areas that contain increased apoptosis, the posterior region that is largely composed of compacted cancellous bone. We previously hypothesized that the osteocytes that are older and less connected to their neighboring osteocytes are at higher risk for oxidative stress and/or lower levels of anti-apoptotic protection. These older cells are contained within a matrix that closely resembles woven bone, or tissue that was quickly constructed as the animal was rapidly growing. Microanatomy differences between the areas of high and low apoptosis (the regions of lamellar vs. non-lamellar bone) reveal that the osteocytes in this region are less connected to their neighboring osteocytes with significantly fewer canalicular connections. The reduced connections therefore imply that the osteocyte population of the posterior region is subject to less efficient transport of signaling molecules that travel via bone fluid flow through the LCS. The microanatomy and age of these osteocytes indicate that cells in this region of high apoptosis have accumulated more damage, and are therefore living ‘closer to the edge’. Estrogen loss

attenuates this response with its antioxidant capabilities to reduce the amount of free radicals, as well as its ability to regulate the glutathione and thioredoxin pathways. Whether the osteocyte apoptosis is a result DNA oxidative damage, or age and reduced transport efficiency, or a combination of both that puts them at risk is unknown. In conclusion, these age- and microenviroment-related differences make osteocytes more sensitive to a system perturbation, thereby influencing the way osteocytes within certain regions of bone respond differently to estrogen deprivation. A better understanding of the algorithm of mechanisms behind the demonstrated osteocyte apoptosis after estrogen withdrawal is needed.

Together, the results of this dissertation have great clinical significance because they provide increased comprehension of factors that initiate remodeling, which is fundamental towards improving resorption-modifying treatments currently administered to osteoporosis patients. This work furthers the understanding of the factors that activate targeted remodeling, which are essential to understand bone health and disease. Moreover, the mouse models used in these studies were a remarkable resource for understanding the link between bone cell health and initiation of remodeling after hormonal deprivation. By understanding the relationship between osteocyte apoptosis and metabolic bone remodeling, our knowledge of bone health can be improved.

FUTURE DIRECTIONS

The relationship between osteocyte apoptosis and bone remodeling after estrogen withdrawal were observed in adult female cortical and cancellous bone. It was then confirmed that osteocyte apoptosis plays a controlling and necessary for activation of bone remodeling by using a pan-caspase inhibitor administered systemically. These compounds are non-specific, in that they suppress any cell type utilizing caspase activation to induce apoptosis. That being said, other cell types, such as bone lining cells, and their role in directed osteoclast resorption were not studied. Although the study was important to show the role of osteocyte apoptosis during a time of minimal growth (minimal osteoclast and osteoblast activity), the clinical use of these apoptosis-inhibiting agents is not practical. Currently, the only other agents with demonstrated anti-apoptotic effects and bone selectivity are bisphosphonates [97; 98]. Therefore, an osteocyte-specific apoptosis inhibitor would allow conditional osteocyte-specific modulation of cell death.

Previously, we established that blocking osteocyte apoptosis prevents initiation of resorption. However, another fundamental question is whether osteocyte apoptosis acts to initiate remodeling, or if ongoing osteocyte apoptosis is required for the resorption process once started? Our results from Chapter 2 [Figure 2.5] show that osteocyte apoptosis is elevated as early as 1 day after estrogen withdrawal, and that this apoptosis remained elevated over the 3-week time study. This question has particular clinical significance with resorption-modifying treatments being initiated after increased remodeling has begun.

Future studies could use pharmacological apoptosis inhibitors to modulate osteocyte apoptosis at selected times during the temporally well-defined sequence post-ovariectomy, in order to tease out the effects of osteocyte apoptosis on initiation versus sustainability phases of the resorption response. Our previous study examined the time points to sample osteocytes before resorption activation (1d, 3d), at early osteoclastic phase (7d), and at peak resorption (14d, 21d). Incorporation of apoptosis inhibition would be administered at certain time intervals post-OVX to intervene in the bone resorption process.

Our previous findings (Chapter 2) that estrogen withdrawal induces immediate osteocyte apoptosis in the inner 1/3 of the cortex, with less than 10% of the cells becoming apoptotic. This begs the question of the role of viable osteocytes to the directed response of osteoclasts. Osteocyte up-regulation of osteoclast recruitment and differentiation factors, as well as anti-apoptotic signaling in surrounding cells have been found in regions of bone known to undergo remodeling in response to fatigue [48; 127].

Understanding the role that non-apoptotic osteocytes play towards is an important aspect to the targeted remodeling story. Future studies would be needed to determine if osteocytes, both viable and apoptotic, in areas known to remodel increase their expression of pro-osteoclastogenic signals. This would allow us to directly assess the spatial and temporal patterns of pro-osteoclastic signals (RANKL, OPG and Bcl-2) involved in the osteoclast recruitment and differentiation pathway for our previously studied bone region after estrogen deprivation. Signaling factors would be examined by immunohistochemistry with spatial and temporal distribution measured by histomorphometry.

Our third study examined the mechanisms that account for regions of high apoptosis. We started this pilot study using only control cortical bone in order to try and elucidate what makes regions of high apoptosis intrinsically/extrinsically more primed for apoptosis after a stimulus such as estrogen withdrawal. These studies should be opened up to include trabecular bone, in order to elucidate if the same mechanisms initiating apoptosis in cortical bone is the driving factor in trabecular bone as well. Also, these same regions should be examined for differences that OVX make.

Also, more work needs to be done to further examine the tissue 'age' question that older cells have accumulated more ROS. The cells residing in the older tissue (the posterior non-lamellar bone that accounts for high regions of apoptosis) are only an estimated 4-6 weeks old. Does this age differential matter? A future study is needed to test this question by immunostaining for oxidative stress levels in bone of the same age, but different tissue type (lamellar bone).

This dissertation (Chapter 4) demonstrated that cells residing in the tissue of the posterior region containing non-lamellar bone have fewer canalicular connections, higher amounts of oxidative damage and levels of apoptosis. In order to more closely examine the relationship between oxidative stress accumulation and cell connectivity, a future experiment would incorporate a quantitative analysis of connectivity amongst individual damaged cells. This would include double staining with a histological dye and also staining for oxidative damage. Then, the number of canalicular processes for individual cells expressing positive staining for damage would be compared with the amount of canalicular connections for un-damaged osteocytes.

The results of this dissertation have emphasized the import role of osteocytes, the predominant cell type in bone, in orchestrating the remodeling process after estrogen loss. This work furthers the understanding of the factors that activate targeted remodeling, which are essential to understand bone health and disease. Moreover, the mouse models used in these studies were a remarkable resource for understanding the link between bone cell health and initiation of remodeling after hormonal deprivation. Further work with apoptosis inhibitors and modified improved (osteocyte-specific) compounds can be used to map to further tease out the role of osteocytes in bone resorption directly. In addition, since 10% of cells are undergoing apoptosis, the role of the remaining 90% viable cells in dictating the osteoclasts to targeted areas needs to be teased out using an immunohistochemical and histomorphometry approach. Through these future experiments we hope to advance our understanding of osteocytes role in metabolic bone remodeling, and to promote the development of diagnosis, prevention, and treatment methodologies aimed at controlling post-menopausal osteoporosis.

REFERENCES

1) Aguirre, J. I., L. I. Plotkin, et al. (2006). "Osteocyte apoptosis is induced by weightlessness in mice and precedes osteoclast recruitment and bone loss." J Bone Miner Res **21**(4): 605-15.

2) Almeida, M., L. Han, et al. (2007). "Skeletal involution by age-associated oxidative stress and its acceleration by loss of sex steroids." J Biol Chem **282**(37): 27285-97.

3) Amant, C., P. Holm, et al. (2001). "Estrogen receptor-mediated, nitric oxide-dependent modulation of the immunologic barrier function of the endothelium: regulation of fas ligand expression by estradiol." Circulation **104**(21): 2576-81.

4) Bakker, A. D., J. Klein-Nulend, et al. (2005). "Additive effects of estrogen and mechanical stress on nitric oxide and prostaglandin E2 production by bone cells from osteoporotic donors." Osteoporos Int **16**(8): 983-9.

5) Bellido, T. (2006). "Downregulation of SOST/sclerostin by PTH: a novel mechanism of hormonal control of bone formation mediated by osteocytes." J Musculoskelet Neuronal Interact **6**(4): 358-9.

6) Bentolila, V., T. Boyce, et al. (1998). "Intracortical remodeling in adult rat long bones after fatigue loading." Bone **23**: 275-81.

7) Bjornstrom, L. and M. Sjoberg (2005). "Mechanisms of estrogen receptor signaling: convergence of genomic and nongenomic actions on target genes." Mol Endocrinol **19**(4): 833-42.

8) Bonewald, L. F. (2004). "Osteocyte biology: its implications for osteoporosis." J Musculoskelet Neuronal Interact **4**(1): 101-4.

9) Bonewald, L. F. (2007). "Osteocyte messages from a bony tomb." Cell Metab **5**(6): 410-1.

10) Bonewald, L. F. (2007). "Osteocytes as dynamic multifunctional cells." Ann N Y Acad Sci **1116**: 281-90.

11) Bonewald, L. F. and M. L. Johnson (2008). "Osteocytes, mechanosensing and Wnt signaling." Bone **42**(4): 606-15.

12) Bronckers, A. L., W. Goei, et al. (1996). "DNA fragmentation during bone formation in neonatal rodents assessed by transferase-mediated end labeling." J Bone Miner Res **11**(9): 1281-91.

13) Burr, D. B. (2002). "Targeted and nontargeted remodeling." Bone **30**(1): 2-4.

14) Burr, D. B., M. R. Forwood, et al. (1997). "Bone microdamage and skeletal fragility in osteoporotic and stress fractures." Journal Bone Mineral Research **12**: 6-15.

15) Burt-Pichat, B., M. H. Lafage-Proust, et al. (2005). "Dramatic decrease of innervation density in bone after ovariectomy." Endocrinology **146**(1): 503-10.

16) Cao, J. J., T. J. Wronski, et al. (2005). "Aging increases stromal/osteoblastic cell-induced osteoclastogenesis and alters the osteoclast precursor pool in the mouse." J Bone Miner Res **20**(9): 1659-68.

17) Cardoso, L., B. Herman, et al. (2008). "Osteocyte apoptosis controls activation of intracortical remodeling in response to fatigue." Journal Bone Mineral Research **manuscript in revision for publication**.

18) Cardoso, L., D. Laudier, et al. (2005). Inhibition of osteocyte apoptosis prevents activation of bone remodeling after fatigue in vivo. 52nd Annual Meeting of the Orthopaedic Research Society.

19) Carlsten, H. (2005). "Immune responses and bone loss: the estrogen connection." Immunol Rev **208**: 194-206.

20) Caserta, T. M., A. N. Smith, et al. (2003). "Q-VD-OPh, a broad spectrum caspase inhibitor with potent antiapoptotic properties." Apoptosis **8**(4): 345-52.

21) Chen, G. D., S. Z. Wu, et al. (2008). "[Protective effects of estrogen on mitochondria in human umbilical vascular endothelial cells]." Nan Fang Yi Ke Da Xue Xue Bao **28**(7): 1154-6.

22) Cheskis, B. J., J. G. Greger, et al. (2007). "Signaling by estrogens." J Cell Physiol **213**(3): 610-7.

23) Chong, Z. Z., J. Q. Kang, et al. (2004). "Essential cellular regulatory elements of oxidative stress in early and late phases of apoptosis in the central nervous system." Antioxid Redox Signal **6**(2): 277-87.

24) Chuang, S. M., G. Y. Liou, et al. (2000). "Activation of JNK, p38 and ERK mitogen-activated protein kinases by chromium(VI) is mediated through oxidative stress but does not affect cytotoxicity." Carcinogenesis **21**(8): 1491-500.

25) Ciani, C., S. B. Doty, et al. (2005). "Mapping bone interstitial fluid movement: displacement of ferritin tracer during histological processing." Bone **37**(3): 379-87.

26) Cursio, R., C. Miele, et al. (2008). "Liver HIF-1 alpha induction precedes apoptosis following normothermic ischemia-reperfusion in rats." Transplant Proc **40**(6): 2042-5.

27) de la Torre, J. C. (2008). "Pathophysiology of neuronal energy crisis in Alzheimer's disease." Neurodegener Dis **5**(3-4): 126-32.

28) Denault, J. B. and G. S. Salvesen (2008). "Apoptotic caspase activation and activity." Methods Mol Biol **414**: 191-220.

29) Donahue, S. W., C. R. Jacobs, et al. (2001). "Flow-induced calcium oscillations in rat osteoblasts are age, loading frequency, and shear stress dependent." Am J Physiol Cell Physiol **281**(5): C1635-41.

30) Emerton, K., B. Hu, et al. (2008). Spatial and temporal linkage of osteocyte apoptosis and bone resorption following estrogen withdrawal in mice. Transactions of the Orthopaedic Research Society, San Francisco.

31) Ernst, M. and G. A. Rodan (1991). "Estradiol regulation of insulin-like growth factor-I expression in osteoblastic cells: evidence for transcriptional control." Mol Endocrinol **5**(8): 1081-9.

32) Finkel, T. and N. J. Holbrook (2000). "Oxidants, oxidative stress and the biology of ageing." Nature **408**(6809): 239-47.

33) Fritton, J., K. Emerton, et al. (2008). "Growth hormone is protective against ovariectomy-induced bone loss during states of low circulating IGF-1." Journal Clinical Investigation **Accepted September 2008**.

34) Frost, H. (1960). "Presence of Microscopic Cracks In Vivo In Bone." Henry Ford Hospital Medical Bulletin **8**: 25-35.

35) Fuchs, R. K., R. J. Phipps, et al. (2008). "Recovery of Trabecular and Cortical Bone Turnover Following Discontinuation of Risedronate and Alendronate Therapy in Ovariectomized Rats." J Bone Miner Res.

36) Gao, Y., W. P. Qian, et al. (2004). "Estrogen prevents bone loss through transforming growth factor beta signaling in T cells." Proc Natl Acad Sci U S A **101**(47): 16618-23.

37) Garcia-Segura, L. M., A. Sanz, et al. (2006). "Cross-talk between IGF-I and estradiol in the brain: focus on neuroprotection." Neuroendocrinology **84**(4): 275-9.

38) Grassi, F., G. Tell, et al. (2007). "Oxidative stress causes bone loss in estrogen-deficient mice through enhanced bone marrow dendritic cell activation." Proc Natl Acad Sci U S A **104**(38): 15087-92.

39) Green, F. (1991). The Sigma-Aldrich Handbook of Stains, Dyes, and Indicators. Milwaukee, Aldrich Chemical Company.

40) Gu, G., T. A. Hentunen, et al. (2005). "Estrogen protects primary osteocytes against glucocorticoid-induced apoptosis." Apoptosis **10**(3): 583-95.

41) Gu, G., M. Mulari, et al. (2005). "Death of osteocytes turns off the inhibition of osteoclasts and triggers local bone resorption." Biochem Biophys Res Commun **335**(4): 1095-101.

42) Hall, P. A., P. J. Coates, et al. (1994). "Regulation of cell number in the mammalian gastrointestinal tract: the importance of apoptosis." J Cell Sci **107 (Pt 12)**: 3569-77.

43) Hamada, Y., S. Kitazawa, et al. (2007). "Histomorphometric analysis of diabetic osteopenia in streptozotocin-induced diabetic mice: a possible role of oxidative stress." Bone **40**(5): 1408-14.

44) Harman, D. (1956). "Aging: a theory based on free radical and radiation chemistry." J Gerontol **11**(3): 298-300.

45) Hedgecock, N. L., T. Hadi, et al. (2007). "Quantitative regional associations between remodeling, modeling, and osteocyte apoptosis and density in rabbit tibial midshafts." Bone **40**(3): 627-37.

46) Heino, T. J., T. A. Hentunen, et al. (2002). "Osteocytes inhibit osteoclastic bone resorption through transforming growth factor-beta: enhancement by estrogen." J Cell Biochem **85**(1): 185-97.

47) Heino, T. J., T. A. Hentunen, et al. (2004). "Conditioned medium from osteocytes stimulates the proliferation of bone marrow mesenchymal stem cells and their differentiation into osteoblasts." Exp Cell Res **294**(2): 458-68.

48) Herman, B. (2008). Osteocytes Activation of Bone Remodeling. Orthopaedics. New York, Mount Sinai of Medicine. **Doctorate of Philosophy of Biological Sciences**.

49) Hirano, T., C. H. Turner, et al. (2000). "Does suppression of bone turnover impair mechanical properties by allowing microdamage accumulation?" Bone **27**: 13-20.

50) Ichiseki, T., A. Kaneuji, et al. (2005). "DNA oxidation injury in bone early after steroid administration is involved in the pathogenesis of steroid-induced osteonecrosis." Rheumatology (Oxford) **44**(4): 456-60.

51) Ito, H., M. Koefoed, et al. (2005). "Remodeling of cortical bone allografts mediated by adherent rAAV-RANKL and VEGF gene therapy." Nat Med **11**(3): 291-7.

52) Iwata, A., J. M. Harlan, et al. (2002). "The caspase inhibitor z-VAD is more effective than CD18 adhesion blockade in reducing muscle ischemia-reperfusion injury: implication for clinical trials." Blood **100**(6): 2077-80.

53) Jacewicz, M., M. Kiessling, et al. (1986). "Selective gene expression in focal cerebral ischemia." J Cereb Blood Flow Metab **6**(3): 263-72.

54) Jee, W. (2001). Integrated Bone Tissue Physiology: Anatomy and Physiology. Bone Mechanics. New York, CRC Press LLC. **1:** 1-56.

55) Johnell, O., J. A. Kanis, et al. (2004). "Mortality after osteoporotic fractures." Osteoporos Int **15**(1): 38-42.

56) Kameda, T., H. Mano, et al. (1997). "Estrogen inhibits bone resorption by directly inducing apoptosis of the bone-resorbing osteoclasts." J Exp Med **186**(4): 489-95.

57) Kousteni, S., T. Bellido, et al. (2001). "Nongenotropic, sex-nonspecific signaling through the estrogen or androgen receptors: dissociation from transcriptional activity." Cell **104**(5): 719-30.

58) Kousteni, S., J. R. Chen, et al. (2002). "Reversal of bone loss in mice by nongenotropic signaling of sex steroids." Science **298**(5594): 843-6.

59) Kousteni, S., L. Han, et al. (2003). "Kinase-mediated regulation of common transcription factors accounts for the bone-protective effects of sex steroids." J Clin Invest **111**(11): 1651-64.

60) Krum, S. A., G. A. Miranda-Carboni, et al. (2008). "Estrogen protects bone by inducing Fas ligand in osteoblasts to regulate osteoclast survival." Embo J **27**(3): 535-45.

61) Kwan Tat, S., M. Padrines, et al. (2004). "IL-6, RANKL, TNF-alpha/IL-1: interrelations in bone resorption pathophysiology." Cytokine Growth Factor Rev **15**(1): 49-60.

62) Laudier, D., M. B. Schaffler, et al. (2007). "Novel procedure for high-fidelity tendon histology." J Orthop Res **25**(3): 390-5.

63) Lean, J. M., J. T. Davies, et al. (2003). "A crucial role for thiol antioxidants in estrogen-deficiency bone loss." J Clin Invest **112**(6): 915-23.

64) Lee, M. Y., S. C. Jung, et al. (2008). "Estradiol-17beta protects against hypoxia-induced hepatocyte injury through ER-mediated upregulation of Bcl-2 as well as ER-independent antioxidant effects." Cell Res **18**(4): 491-9.

65) Li, C. Y., K. J. Jepsen, et al. (2006). "Mice lacking cathepsin K maintain bone remodeling but develop bone fragility despite high bone mass." J Bone Miner Res **21**(6): 865-75.

66) Li, C. Y., M. B. Schaffler, et al. (2005). "Genetic background influences cortical bone response to ovariectomy." J Bone Miner Res **20**(12): 2150-8.

67) Li, H., F. Colbourne, et al. (2000). "Caspase inhibitors reduce neuronal injury after focal but not global cerebral ischemia in rats." Stroke **31**(1): 176-82.

68) Lindberg, M. K., Z. Weihua, et al. (2002). "Estrogen receptor specificity for the effects of estrogen in ovariectomized mice." J Endocrinol **174**(2): 167-78.

69) Liu, H., H. Wang, et al. (2004). "Glutathione metabolism during aging and in Alzheimer disease." Ann N Y Acad Sci **1019**: 346-9.

70) Majeska, R. (2001). Cell Biology of Bone. Bone Mechanics. New York, CRC Press LLC. **1:** 2.1-2.23.

71) Mann, V., C. Huber, et al. (2007). "The antioxidant effect of estrogen and Selective Estrogen Receptor Modulators in the inhibition of osteocyte apoptosis in vitro." Bone **40**(3): 674-84.

72) Martin, R. B. (2000). "Toward a unifying theory of bone remodeling." Bone **26**(1): 1-6.

73) Martin, T. J. and N. A. Sims (2005). "Osteoclast-derived activity in the coupling of bone formation to resorption." Trends Mol Med **11**(2): 76-81.

74) Mashiba, T., T. Hirano, et al. (2000). "Suppressed bone turnover by bisphosphonates increases microdamage accumulation and reduces some biomechanical properties in dog rib." J Bone Miner Res **15**(4): 613-20.

75) McMillan, J., R. C. Kinney, et al. (2006). "Osteoinductivity of demineralized bone matrix in immunocompromised mice and rats is decreased by ovariectomy and restored by estrogen replacement." Bone.

76) McNamara, L. M., A. G. Ederveen, et al. (2006). "Strength of cancellous bone trabecular tissue from normal, ovariectomized and drug-treated rats over the course of ageing." Bone **39**(2): 392-400.

77) Mendez-Davila, C., C. Garcia-Moreno, et al. (2004). "Effects of 17beta-estradiol, tamoxifen and raloxifene on the protein and mRNA expression of interleukin-6, transforming growth factor-beta1 and insulin-like growth factor-1 in primary human osteoblast cultures." J Endocrinol Invest **27**(10): 904-12.

78) Mohamed, M. K. and A. A. Abdel-Rahman (2000). "Effect of long-term ovariectomy and estrogen replacement on the expression of estrogen receptor gene in female rats." Eur J Endocrinol **142**(3): 307-14.

79) Mori, S., R. Harruff, et al. (1997). "Trabecular bone volume and microdamage accumulation in the femoral heads of women with and without femoral neck fractures." Bone **21**(6): 521-6.

80) Nagata, S. (1999). "Fas ligand-induced apoptosis." Annu Rev Genet **33**: 29-55.

81) Nakamura, T., Y. Imai, et al. (2007). "Estrogen prevents bone loss via estrogen receptor alpha and induction of Fas ligand in osteoclasts." Cell **130**(5): 811-23.

82) Nazarian, A., E. Cory, et al. (2008). "Shortcomings of DXA to assess changes in bone tissue density and microstructure induced by metabolic bone diseases in rat models." Osteoporos Int.

83) Nilsen, J. and R. Diaz Brinton (2003). "Mechanism of estrogen-mediated neuroprotection: regulation of mitochondrial calcium and Bcl-2 expression." Proc Natl Acad Sci U S A **100**(5): 2842-7.

84) Nishida, T., S. Kondo, et al. (2008). "CCN family 2/connective tissue growth factor (CCN2/CTGF) regulates the expression of Vegf through Hif-1alpha expression in a chondrocytic cell line, HCS-2/8, under hypoxic condition." Bone.

85) Noble, B. S., H. Stevens, et al. (1997). "Identification of apoptotic changes in osteocytes in normal and pathological human bone." Bone **20**(3): 273-82.

86) Ominsky, M. S., X. Li, et al. (2008). "RANKL inhibition with osteoprotegerin increases bone strength by improving cortical and trabecular bone architecture in ovariectomized rats." J Bone Miner Res **23**(5): 672-82.

87) Oshima, S., S. Onodera, et al. (2006). "Macrophage migration inhibitory factor-deficient mice are resistant to ovariectomy-induced bone loss." FEBS Lett **580**(5): 1251-6.

88) Ott, S. (2002). Histomorphometric Analysis of Bone Remodeling. Principles of bone Biology, Academic Press. **1:** 303-316.

89) Pacifici, R. (1996). "Estrogen, cytokines, and pathogenesis of postmenopausal osteoporosis." J Bone Miner Res **11**(8): 1043-51.

90) Pacifici, R. (1998). "Cytokines, estrogen, and postmenopausal osteoporosis--the second decade." Endocrinology **139**(6): 2659-61.

91) Pacifici, R. (2007). "T cells and post menopausal osteoporosis in murine models." Arthritis Res Ther **9**(2): 102.

92) Pajamaki, I., H. Sievanen, et al. (2008). "Skeletal effects of estrogen and mechanical loading are structurally distinct." Bone **43**(4): 748-57.

93) Pantschenko, A. G., W. Zhang, et al. (2005). "Effect of osteoblast-targeted expression of bcl-2 in bone: differential response in male and female mice." J Bone Miner Res **20**(8): 1414-29.

94) Parfitt, A. M. (1994). "Osteonal and hemi-osteonal remodeling: the spatial and temporal framework for signal traffic in adult human bone." J Cell Biochem **55**(3): 273-86.

95) Parfitt, A. M. (1996). "Hormonal influences on bone remodeling and bone loss: applicatin to the management of primary hyperparathyroidism." Ann Intern Med **125**(5): 413-5.

96) Patil, K. and S. C. Sharma (2004). "Broad spectrum caspase inhibitor rescues retinal ganglion cells after ischemia." Neuroreport **15**(6): 981-4.

97) Plotkin, L. I., J. I. Aguirre, et al. (2005). "Bisphosphonates and estrogens inhibit osteocyte apoptosis via distinct molecular mechanisms downstream of extracellular signal-regulated kinase activation." J Biol Chem **280**(8): 7317-25.

98) Plotkin, L. I., S. C. Manolagas, et al. (2006). "Dissociation of the pro-apoptotic effects of bisphosphonates on osteoclasts from their anti-apoptotic effects on osteoblasts/osteocytes with novel analogs." Bone **39**(3): 443-52.

99) Poole, K. E., R. L. van Bezooijen, et al. (2005). "Sclerostin is a delayed secreted product of osteocytes that inhibits bone formation." Faseb J **19**(13): 1842-4.

100) Price, C., B. C. Herman, et al. (2005). "Genetic variation in bone growth patterns defines adult mouse bone fragility." J Bone Miner Res **20**(11): 1983-91.

101) Qui, S., T. Boyce, et al. (1997). "Osteocyte loss and microdamage in aging human compact bone." Trans Orthop Res Soc **22**: 88.

102) Rickard, D., S. H. R. Turner, et al. (2002). Estrogens and Progestins. Principles of Bone Biology, Academic Press
1: 655-67.

103) Rikans, L. E. and K. R. Hornbrook (1997). "Lipid peroxidation, antioxidant protection and aging." Biochim Biophys Acta **1362**(2-3): 116-27.

104) Rivera, F., G. Costa, et al. (2008). "Reduction of ischemic brain damage and increase of glutathione by a liposomal preparation of quercetin in permanent focal ischemia in rats." Neurotox Res **13**(2): 105-14.

105) Rogakou, E. P., W. Nieves-Neira, et al. (2000). "Initiation of DNA fragmentation during apoptosis induces phosphorylation of H2AX histone at serine 139." J Biol Chem **275**(13): 9390-5.

106) Russo, R., F. Cavaliere, et al. (2008). "17Beta-estradiol prevents retinal ganglion cell loss induced by acute rise of intraocular pressure in rat." Prog Brain Res **173**: 583-90.

107) Sawada, H., M. Ibi, et al. (2000). "Mechanisms of antiapoptotic effects of estrogens in nigral dopaminergic neurons." Faseb J **14**(9): 1202-14.

108) Scheidegger, K. J., B. Cenni, et al. (2000). "Estradiol decreases IGF-1 and IGF-1 receptor expression in rat aortic smooth muscle cells. Mechanisms for its atheroprotective effects." J Biol Chem **275**(49): 38921-8.

109) Services, U. D. o. H. a. H. (2004). Surgeon General's Report on Bone Health and Osteoporosis, U.S. Department of Health and Human Services, Office of the Surgeon General.

110) Shevde, N. K., A. C. Bendixen, et al. (2000). "Estrogens suppress RANK ligand-induced osteoclast differentiation via a stromal cell independent mechanism involving c-Jun repression." Proc Natl Acad Sci U S A **97**(14): 7829-34.

111) Shimizu, H., M. Sakamoto, et al. (1990). "Bone resorption by isolated osteoclasts in living versus devitalized bone: differences in mode and extent and the effects of human recombinant tissue inhibitor of metalloproteinases." J Bone Miner Res **5**(4): 411-8.

112) Slee, E. A., H. Zhu, et al. (1996). "Benzyloxycarbonyl-Val-Ala-Asp (OMe) fluoromethylketone (Z-VAD.FMK) inhibits apoptosis by blocking the processing of CPP32." Biochem J **315 (Pt 1)**: 21-4.

113) Srinivas, V., X. Zhu, et al. (1998). "Hypoxia-inducible factor 1alpha (HIF-1alpha) is a non-heme iron protein. Implications for oxygen sensing." J Biol Chem **273**(29): 18019-22.

114) Strasser, A., L. O'Connor, et al. (2000). "Apoptosis signaling." Annu Rev Biochem **69**: 217-45.

115) Stroka, D. M., T. Burkhardt, et al. (2001). "HIF-1 is expressed in normoxic tissue and displays an organ-specific regulation under systemic hypoxia." Faseb J **15**(13): 2445-53.

116) Sudoh, N., K. Toba, et al. (2001). "Estrogen prevents oxidative stress-induced endothelial cell apoptosis in rats." Circulation **103**(5): 724-9.

117) Syed, F. A., U. I. Modder, et al. (2005). "Skeletal effects of estrogen are mediated by opposing actions of classical and nonclassical estrogen receptor pathways." J Bone Miner Res **20**(11): 1992-2001.

118) Tam, N. N., S. Ghatak, et al. (2003). "Sex hormone-induced alterations in the activities of antioxidant enzymes and lipid peroxidation status in the prostate of Noble rats." Prostate **55**(1): 1-8.

119) Tami, A. E., M. B. Schaffler, et al. (2003). "Probing the tissue to subcellular level structure underlying bone's molecular sieving function." Biorheology **40**(6): 577-90.

120) Tatsumi, S., K. Ishii, et al. (2007). "Targeted ablation of osteocytes induces osteoporosis with defective mechanotransduction." Cell Metab **5**(6): 464-75.

121) Teitelbaum, S. L. (2004). "Postmenopausal osteoporosis, T cells, and immune dysfunction." Proc Natl Acad Sci U S A **101**(48): 16711-2.

122) Thi, M. M., T. Kojima, et al. (2003). "Fluid shear stress remodels expression and function of junctional proteins in cultured bone cells." Am J Physiol Cell Physiol **284**(2): C389-403.

123) Tomkinson, A., E. F. Gevers, et al. (1998). "The role of estrogen in the control of rat osteocyte apoptosis." J Bone Miner Res **13**(8): 1243-50.

124) Tomkinson, A., J. Reeve, et al. (1997). "The death of osteocytes via apoptosis accompanies estrogen withdrawal in human bone." J Clin Endocrinol Metab **82**(9): 3128-35.

125) Tyner, S. D., S. Venkatachalam, et al. (2002). "p53 mutant mice that display early ageing-associated phenotypes." Nature **415**(6867): 45-53.

126) Verborgt, O., G. J. Gibson, et al. (2000). "Loss of osteocyte integrity in association with microdamage and bone remodeling after fatigue in vivo." J Bone Miner Res **15**(1): 60-7.

127) Verborgt, O., N. A. Tatton, et al. (2002). "Spatial distribution of Bax and Bcl-2 in osteocytes after bone fatigue: complementary roles in bone remodeling regulation?" J Bone Miner Res **17**(5): 907-14.

128) Waarsing, J. H., J. S. Day, et al. (2006). "Bone loss dynamics result in trabecular alignment in aging and ovariectomized rats." J Orthop Res **24**(5): 926-35.

129) Wang, H., H. Liu, et al. (2003). "Gender difference in glutathione metabolism during aging in mice." Exp Gerontol **38**(5): 507-17.

130) Wang, L., C. Ciani, et al. (2004). "Delineating bone's interstitial fluid pathway in vivo." Bone **34**(3): 499-509.

131) Wang, L., Y. Wang, et al. (2005). "In situ measurement of solute transport in the bone lacunar-canalicular system." Proc Natl Acad Sci U S A **102**(33): 11911-6.

132) Wang, L., Y. Wang, et al. (2005). Genetic Variations in the bone lacunar-canalicular system: potential influence on communication among osteocytes. 52nd Annual Meeting of the Orthopaedic Research Society, Paper No: 0192.

133) Weinbaum, S., S. C. Cowin, et al. (1994). "A model for the excitation of osteocytes by mechanical loading-induced bone fluid shear stresses." J Biomech **27**(3): 339-60.

134) Weinstein, R. S., R. W. Nicholas, et al. (2000). "Apoptosis of osteocytes in glucocorticoid-induced osteonecrosis of the hip." J Clin Endocrinol Metab **85**(8): 2907-12.

135) Windahl, S. H., M. K. Lagerquist, et al. (2007). "Identification of Target Cells for the Genomic Effects of Estrogens in Bone." Endocrinology.

136) Wiren, K. M., A. R. Toombs, et al. (2006). "Osteoblast and osteocyte apoptosis associated with androgen action in bone: requirement of increased Bax/Bcl-2 ratio." Bone **38**(5): 637-51.

137) Yang, L., S. Sugama, et al. (2004). "A novel systemically active caspase inhibitor attenuates the toxicities of MPTP, malonate, and 3NP in vivo." Neurobiol Dis **17**(2): 250-9.

138) Zaman, G., H. L. Jessop, et al. (2006). "Osteocytes use estrogen receptor alpha to respond to strain but their ERalpha content is regulated by estrogen." J Bone Miner Res **21**(8): 1297-306.

139) Zhang, X., L. Wang, et al. (2006). In situ measurement of solute transport in the bone lacunar-canalicular sytem in aging mice. 53rd Annual Meeting of the Orthopaedic Research Society, Paper No: 0313.